DISS. ETH NO. 21873

Regulation of adipogenesis and energy metabolism through the cross-talk between adipose tissue, gastrointestinal wall and the brain: Evidence from adipokines and incretin hormones

A thesis submitted to attain the degree of

DOCTOR OF SCIENCES of ETH ZURICH

(Dr. sc. ETH Zurich)

presented by

TENAGNE DELESSA CHALLA

M.Sc. in Nutrition Sciences

The Hebrew University of Jerusalem

born on 20.05.1981

Citizen of Ethiopia

accepted on the recommendation of

Prof. Dr. Christian Wolfrum

Prof. Dr. Wolfgang Langhans

Prof. Dr. Michael Detmar

Prof. Dr. med. Gottfried Rudofsky

2014

Table of Contents

Abbreviations

AC	adenylate cyclase
AGRP	agouti-related protein
ASC	adipose-derived stem cell
ARC	arcuate nucleus
BAT	brown adipose tissue
BDNF	brain-derived neurotrophic factor
Cpq	Carboxypeptidase Q
C/ebp β	CCAAT/enhancer binding proteins beta
C/ebp δ	CCAAT/enhancer binding proteins delta
CNS	central nervous system
CT	computed Tomography
CVD	cardiovascular disease
CX	cortex
Dexa	dexamethasone
DPPIV	dipeptidyl-peptidase-4
EE	energy expenditure
FBS	fetal bovine serum
FFA	free fatty acids
FPLC	Fast Protein Liquid Chromatography
GH	growth hormone
GIP	glucose-dependent insulinotropic polypeptide
GIPr	glucose-dependent insulinotropic polypeptide receptor
GLP-1	glucagon-like peptide-1
GLP-1R	glucagon-like peptide-1 receptor
Got2	aspartate aminotransferase, mitochondrial
HFD	high fat diet
HIP	hippocampus
HYP	hypothalamus
IBMX	3-isobutyl-1-methylxanthine
IFG	impaired fasting glucose
IGF-1	insulin-like growth factor 1
IGT	impaired glucose tolerance

IL-6	interleukin-6
Il1rl1	interleukin-1 receptor-like 1
IPGTT	intraperitoneal glucose tolerance test
ITT	insulin tolerance test
MESC	mesenchymal stem cells
NPY	neuropeptide Y
OGTT	oral glucose tolerance test
PKA	cAMP-dependent protein kinase
PMCH	promelanin-concentrating hormone
POMC	pro-opiomelanocortin
PPARγ	peroxisome proliferator-activated receptor gamma
RER	respiratory exchange ratio
SA	subcutaneous adipocyte
SAT	subcutaneous adipose tissue
SE	subcutaneous adipose tissue explants
siRNA	small interfering RNA
Slc27a1	long-chain fatty acid transport protein 1
SVF	stromal vascular fraction
TAC	transverse aortic constriction
TG	triglyceride
TNF-α	tumor necrosis factor alpha
T2D	type II diabetes mellitus
VA	visceral adipocyte
VAT	visceral adipose tissue
VE	visceral adipose tissue explants
Vim	vimentin
VLDL	very low-density lipoprotein
VTA	ventral tegmental area
WAT	white adipose tissue

General Abstract

Adipose tissue is a dynamic endocrine organ that stores energy and secretes adipokines to maintain energy homeostasis. The excessive accumulation of adipose tissue and dysregulation of adipokines secretion results in the development of obesity and obesity related metabolic disorders such as Type II diabetes and insulin resistance. The increasing incidence of these metabolic diseases has reached pandemic levels due to a lack of insight into the precise molecular mechanisms underlying the regulation of energy metabolism. A deeper understanding of the communication pathways linking the white adipose tissue, intestinal wall and the brain might represent potential and promising intervention points to treat different metabolic disorders. In this thesis, we investigated the cross-talk between white adipose tissue, the gastrointestinal wall and the brain on the regulation of energy metabolism both *in vitro* as well as in *in vivo* studies. The main aim of this thesis was to identify and investigate the potential signal transduction between central nervous system (CNS), gut and adipose tissue via adipokines and incretin hormones to maintain energy homeostasis.

In Chapter 2, we investigated the signal transduction between gastrointestinal wall and adipose tissue to control high-energy intake. The incretin hormone, glucagon-like peptide-1 (GLP-1) is secreted by the gastrointestinal wall upon nutrient intake which then enhances insulin secretion. Using *in vitro* cell culture and *in vivo* mouse models, we found that the GLP-1 or its analog liraglutide induced adipogenesis by directly activating its receptor/ GLP-1R. This finding indicates that adipose tissue and intestinal wall interacts through GLP-1 to store energy in lipid droplets by promoting adipocyte development thereby enhancing insulin sensitivity. This concept might contribute to improved whole body energy metabolism. Another incretin hormone, glucose-dependent insulinotropic polypeptide (GIP), is released from K-cells and stimulates insulin secretion. GIP and GIP receptor (GIPr) are highly expressed in the CNS including the hypothalamus, but its role on central energy metabolism is still not well understood.

In Chapter 3, we studied CNS-GIPr effect on energy metabolism by generating CNS specific GIPr knockout mice. Our results demonstrate that CNS-specific hGIPr deletion protects high fat diet (HFD) induced obesity, insulin resistance and hepatic steatosis,

thereby improving insulin sensitivity and glucose tolerance. This effect could in part be explained through increased physical activity and suppressed food intake. To elucidate the molecular mechanism underlying central GIP effect in the regulation of whole body energy metabolism further investigation will be required.

Adipose tissue produces adipokines to communicate with the brain about whole body long term energy balance. There are a lot of known adipokines differentially secreted from the different adipose depots. In this respect, a study was conducted (Chapter 4) to identify new adipokines and to investigate the paracrine and autocrine effects of these adipokines on adipocyte development. By using the Fast Protein Liquid Chromatography (FPLC) technique, we were able to fractionate adipocytes or adipose tissue explants secretion and could demonstrate how they exert both induction and inhibition effects on adipocyte formation. Based on the effects of these fractions we used a proteomic approach to identify the factors which positively or negatively affected adipocyte formation. Among the secreted factors, we identified Slc27a1, Vim, Cp and Ecm1 as factors that promote pre-adipocyte differentiation, whereas Got2, Cpq, Il1rl1, SPARC, Ces1d, Fbln2, Lgals3bp and Tf were factors which decreased adipogenesis. Our findings demonstrate that adipocytes and adipose tissue secrete several paracrine, autocrine and endocrine factors, which could potentially affect whole body energy metabolism.

In conclusion, the studies from this thesis demonstrate that interactions exist between adipose tissue, the intestinal wall and the brain in the regulation of energy homeostasis. The CNS - GIPr regulation of energy metabolism provides evidence for the existence of potential therapeutic targets to tackle the epidemic of obesity and type II diabetes. Moreover, the identification of novel adipokines from adipocytes or adipose tissue explants with paracrine or autocrine effects on adipocyte development suggests the possibility to employ these factors to modulate energy homoeostasis which may be used in the future for pharmacological approaches towards the treatment of obesity and associated metabolic disorders.

Zusammenfassung

Fettgewebe ist ein dynamisches endokrines Organ, das Energie speichert und Adipokines absondert um Energiehomöostase aufrecht zu erhalten. Die übermäßige Ansammlung von Fettgewebe und Dysregulation der Sekretion von Adpokinen führt zur Entwicklung von Adipositas und Stoffwechselerkrankungen im Zusammenhang Typ-2-Diabetes und Insulinresistenz. Die zunehmende Häufigkeit dieser Stoffwechselerkrankungen haben in den letzten Jahren das Ausmaß einer Pandemie erreicht. Der Grund dafür ist der mangelnde Einblick in die molekularen Mechanismen, die der Regulation des Energiestoffwechsels zu Grunde liegen. Ein weiterführendes Verständnis für die Kommunikationswege und die Verknüpfung des weißen Fettgewebes, der Darmwand und des Gehirns könnten potenziell vielversprechende Ansatzpunkte sein, verschiedene Stoffwechselstörungen zu behandeln. Die Interaktion zwischen weißem Fettgewebe, der Magen-Darm- Wand und dem Gehirn und die daraus resultierende Regulierung des Energiestoffwechsels wurde in der vorliegenden Arbeit sowohl in vitro als auch in vivo-Studien untersucht. Das Hauptziel dieser Arbeit war es, die Signalübertragung zwischen Zentralnervensystem, Darm und Fettgewebe über Adipokine und Inkretin Hormone, zu charakterisieren. In Kapitel 2, untersuchten wir die Signalübertragung zwischen Darmwand und Fettgewebe um Hochenergieaufnahme zu kontrollieren. Das Inkretin GLP-1, was durch die Magen-Darm-Wand bei der Nahrungsaufnahme ausgeschüttet wird, verbessert die Insulin Sekretion. Verwendung von in vitro -Zellkultur -und in -vivo- Mausmodell zeigten, dass GLP-1 oder dessen Analog Liraglutide Adipogenese durch direkte Aktivierung von seinem Rezeptor (GLP-1R) induziert. Dieses Ergebnis zeigt, dass Fettgewebe und Darmwand über GLP-1 kommunizieren um Energie in Lipid Tröpfchen zu lagern. Dies geschieht durch die Neubildung von Adipozyten wodurch sich die Insulinempfindlichkeit sich verbessert. Dieses Konzept könnte dazu beitragen, im ganzen Körper den Energiestoffwechsel zu verbessern. Ein weiteres Inkretin Hormon, Glukose-abhängiges Insulinotropic Polypeptide (GIP), wird von K-Zellen freigesetzt und stimuliert die Insulin-Sekretion. GIP und GIP-Rezeptor (GIPr) sind im ZNS einschließlich des Hypothalamus exprimiert, aber die Rolle diese Hormons auf den zentralen Energiestoffwechsel ist noch nicht ausreichend untersucht. In Kapitel 3, untersuchten wir ZNS - GIPR Wirkung auf den Energiestoffwechsel durch die Generierung von ZNS- spezifischen GIPR Knockout-Mäusen. Die Ergebnisse zeigten, dass CNS-spezifische hGIPr Entfernung vor

den schlechten Einflüssen fettreicher Diät (HFD) un der daraus bedingten Adipositas schützt. Dies führt zu einer Verbesserung der hepatischen Steatose, wodurch sich die Insulin Sensitiviät und Glukose-Toleranz verbessern. Dieser Effekt tritt teilweise durch erhöhte körperliche Aktivität und unterdrückte Nahrungsaufnahme auf. Um die diesen Effekten zu Grunde liegenden molekularen Mechanismen zu studierenwerden weitere untersuchungen benötigt.

Fettgewebe produziert Adipokine, mit dem Gehirn über die langfristige Energiebilanz kommunizieren. Es gibt eine Menge bekannter Adipokine die differentiell aus verschiedenem Fettdepot abgesondert werden. Eine Studie wurde durchgeführt (Kapitel 4) um neue Adipokine zu identifizieren und die parakrine und autokrine Funktion dieser Adipokine auf die Adipozyten Entwicklung zu untersuchen. Durch die Verwendung von FPLC wurden Fraktionen aus Adipozyten oder Fettgewebesexplantaten identifiziert die sowohl eine Induktions- und eine Hemmwirkung auf die Bildung von Adipozyten haben. Basierend auf der Aktivität dieser Fraktionen haben wir in einem proteomischen Ansatz versucht die Adipokine zu identifzieren die die Adipozyten Bildung positiv oder negativ beeinflussen. Die Ergebnisse zeigten, dass die sezernierten Faktoren Slc27a1, Vim, Cp und Ecm1 die Präadipozyten Differenzierung fördern, während GOT2 , Cpq , Il1rl1 , SPARC , Ces1d , Fbln2 , Lgals3bp und Tf die Adipogenese verringert. Unsere Ergebnisse zeigen, dass Adipozyten und Fettgewebe mehrere parakrine, autokrine und endokrine Faktoren absondern welche den Ganzkörper-Energiestoffwechsel regulieren können.

Zusammenfassend haben die Untersuchungen dieser Arbeit gezeigt, daß es Wechselwirkungen zwischen dem Fettgewebe, der Darmwand und dem Gehirn in der Regulation des Energie Homöostase gibt. Die ZNS - GIPr-Regulation des Energiestoffwechsels deutet auf mögliche neue therapeutische Ziele zur Bekämpfung der Epidemie der Adipositas und Typ-II-Diabetes hin. Die Identifizierung neuer Adipokine aus Adipozyten oder Fettgewebe mit Auswirkungen auf die Adipozyten Entwicklung legt die Möglichkeit nahe, diese Faktoren als pharmakologische Tools zur Behandlung von Adipositas und den damit assoziierten Stoffwechselstörungen zu verwenden.

Chapter 1

1. General Introduction

1.1. Obesity and the progression of metabolic disorders

Obesity, the excessive accumulation of adipose tissue, is strongly associated with a number of chronic diseases: hyperlipidaemia, type II diabetes (T2D), insulin resistance, some types of cancer and cardiovascular disease (CVD) (1-6). On the other hand, lipodystrophy also results in insulin resistance, T2D and abnormal lipid metabolism (7). Obesity is a multifactorial disorder and its onset and progression have been related to genetic background, environmental factors, lifestyle, underlying illness and socioeconomic status. It is a major public health problem in developed countries, and surprisingly affects developing countries (8). According to the World Health Organization (WHO) more than 1.4 billion adults are overweight in 2008 (60). Approximately 65% of the world population lives in countries where overweight and obesity kills more people than being underweight (60). More than 40 million children under the age of five were overweight in 2010 (9).

According to the WHO, a person with a body-mass index (BMI) < 18.5 is categorized as underweight, 18.5-25 is considered as a normal body weight, ≥ 25 is overweight and ≥ 30 is considered as obese (61). However, BMI should be considered as a rough guide only, as it may not correspond to the same degree of body fat for people from different ethnic backgrounds (10). For example, Asians generally have a higher percentage of body fat than white people of the same age, sex, and BMI (61). Moreover, Asians and black subjects developed T2D and CVD at a higher rate, at an earlier age, and at lower ranges of BMI than their Caucasian counterparts (10). Therefore, BMI is not a golden standard to assess obesity in different ethnic backgrounds. Because of an increased prevalence of obesity, T2D has become a global epidemic, with more than 300 million individuals worldwide predicted to be affected by the year 2025 (11,12). Hence, there is a great interest to find effective prevention strategies and therapies for obesity associated T2D by understanding the molecular and cellular biology of adipose tissue development.

The exact association between obesity and each of the above mentioned chronic diseases is poorly understood, but cumulative data support the role of fat mass and especially, body fat distribution in the development of obesity related risk factors (2,3,5,13,14). Therefore, studies have focused on the importance of different depots where fat is accumulated, for example visceral obesity is known to be a stronger risk factor for insulin resistance and T2D (12) than subcutaneous fat. Interestingly, a reduction in body fat content reduces the risk of these chronic diseases (15) demonstrating the major role of fat mass in the development of obesity related metabolic disorders.

T2D is characterized by hyperglycemia or insulin resistance resulting from defects in insulin secretion, insulin action, or both (12). For T2D diagnosis and prevention, clinical studies have focused on people with impaired glucose tolerance (IGT) and impaired fasting glucose (IFG) (16). Both IGT and IFG are associated with metabolic disorder/metabolic syndrome (syndrome X) (17). Metabolic syndrome is a cluster of diseases such as CVD, T2D, and hyper-insulinaemia, dyslipidaemia, hypertension as well as visceral obesity (12). The chronic hyperglycemia in T2D is associated with failure of several organs, especially the eyes, kidneys, nerves, heart, and blood vessels (2,3,5,13,14). Thus, understanding the underlining mechanism between excessive adipose tissue mass, obesity and T2D is important.

1.2. The development of adipose tissue and composition of adipocytes

Adipose tissue is a specialized connective tissue that functions as the major storage site for fat in the form of triglycerides (TG). Adipose tissue is found in mammals in two different forms: white adipose tissue (WAT) and brown adipose tissue (BAT) (18). Brown adipocytes contain multilocular lipid droplets and are rich in mitochondria. BAT is a thermogenic organ, which expresses uncoupling protein 1 and produces heat by uncoupling mitochondrial respiration from ATP synthesis (19,20). Therefore, BAT is essential for classical non-shivering thermogenesis and for the cold acclimation-recruited norepinephrine-induced thermogenesis (19). Interestingly, a finding in our laboratory showed the trans-differentiation between BAT and WAT (21).

White adipocytes mostly derive from the lateral plate mesoderm from stem cells that are negative for the myogenic factor Myf5 (22) although this concept has been recently challenged. WAT development begins with an accumulation of a dense mass of mesenchymal stem cells (MSCs) at various sites where angiogenesis occurs (23). MSCs develop into adipocytes near the capillary networks (23,24). Early fat cell (adipocyte) clusters then develop into WAT. Fat mass can range from 2 to 3% of body weight in extremely well-conditioned athletes or 60 - 70% of body weight in morbidly / super obese individuals (25). Normal values for fat mass are 9 - 18% in males and 14–28% in females. In obesity, fat mass exceeds 22% of body weight in males or 32% in females (26). Previously, it had been thought that adipose tissue development is completed in early life and that fat mass expansion in later life was due to enlargement of the size of white adipocytes. However, recent studies have shown the development of WAT at birth and continuous development throughout adult life. The number of adipocytes is relatively stable, and the turnover rate is approximately 10% per year in adult life (27). Thus, about half of the white adipocytes in humans are replaced every 8.3 years (27).

1.3. Distribution of fat depots in the body

WAT is distributed throughout the entire body and has the capacity to expand massively. Fat depots from different areas of the body display distinct structural and functional properties (62). WAT is divided into two major depots: subcutaneous (superficial) and visceral (deep) fat (Fig.1) (27,28). Visceral adipose tissue (VAT) includes; omental, mesenteric, retroperitoneal and gonadal fat depots. The epididymal, peritesticular, periovarian and periuterine, are well developed in rodents and their mass increases with age (28,29). The VAT surrounds the inner organs in the abdominal cavity and mediastinum, while the subcutaneous adipose tissue (SAT) forms a fat layer under the skin and contributes to the physical functions including temperature regulation and thermal isolation (27).

Adipocytes are the main components of WAT. The lipid droplet occupies the cytoplasm of adipocytes while the nucleus is located to the side of the cell. Due to the presence of a single large lipid droplet in the cytoplasm, a fat cell or adipocyte is referred to as a unicellular adipocyte (28). The lipid droplet is a large component of the adipocyte (>95% of the mass of the adipocyte). Changes in the amount of lipid stored within the

adipocyte affect fat cell size (ranging from 25 to 250 μm). The volume of an adipocyte is a determinant of cell's functionality, with larger adipocytes generally exhibiting higher metabolic activity and secreting more chemoattractants for immune cells (30).

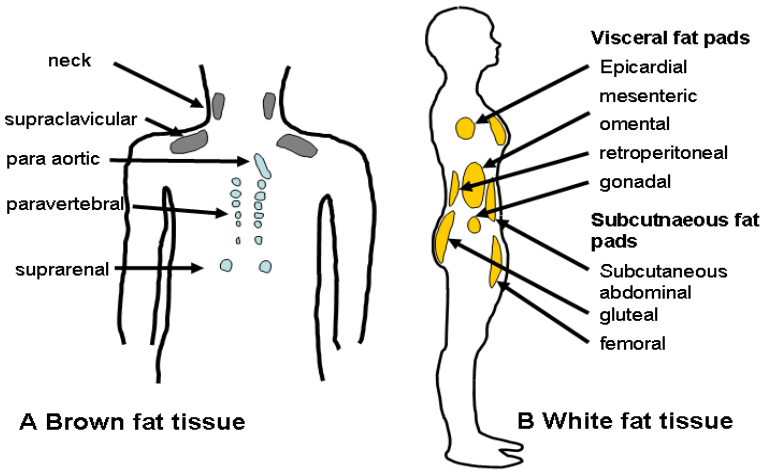

Figure 1. **Brown (A) and white (B) adipose tissue distribution (62).**

1.4. Proliferation and differentiation of adipocytes (Adipogenesis)

White adipose tissue plays a major role for maintaining energy metabolism of the organism by storing excess energy derived from high caloric intake and mobilizing this energy during times of energy deprivation. The main function of adipocytes is to store energy in the form of TG in lipid droplets during energy consumption and the release of free fatty acids (FA) if energy intake is less than energy expenditure (31,32). The formation of adipocytes from precursor stem cells is very complex and highly regulated. MSCs can differentiate into a variety of cell types including adipocytes, osteoblasts, chondrocytes and myocytes (33). Several signals are involve in the determination of MSCs fate into the formation of adipocytes (34). For instance, the bone morphogenetic proteins (BMPs) and insulin-like growth factor 1 (IGF-1) are involved in this process (33,35,36). The process by which MSCs are committed to pre-adipocytes, then proliferate, differentiate and convert into adipocytes, is known as adipogenesis (36).

Adipogenesis has two important stages: commitment and differentiation. Commitment is the process by which the MSCs respond to one of the above-mentioned signals and

are committed to become pre-adipocytes (36). Differentiation is the process by which pre-adipocytes differentiate into mature adipocytes under the appropriate stimulatory conditions (37). Pre-adipocytes are believed to be present throughout life (26), showing the dynamic nature of adipose tissue and how it can be remodeled throughout adult life. Adipose tissue growth involves cellular hypertrophy (increase in size) and hyperplasia (increase in number) (26,32,37). Both adipocyte hypertrophy and hyperplasia occur in association with high caloric intake during normal growth and in the development of obesity (26).

Development of adipocytes has been studied *in vitro* by using both primary pre-adipocytes isolated from the stromal-vascular fraction (SVF) of adipose tissue and established cell lines of murine origin, such as the pluripotent fibroblasts (C3H10T1/2, Balb/c 3T3, and CHE/18 fibroblast) and the uni-potent cell line (3T3-L1, 3T3-F442A, 1246, Ob1771, TA1 and 30A5) (38,39). In this PhD thesis we have used the primary subcutaneous and visceral pre-adipocytes and 3T3-L1 cell lines. Notably, the 3T3-L1 cell line is one of the best characterized, reliable and widely used cell lines to study adipogenesis (35). In addition, we have used a mouse model tracking adipogenesis *in vivo*.

1.5. Molecular regulation of adipogenesis

Adipogenesis is highly regulated; environmentally, nutritionally, genetically and hormonally. In cell culture, a cascade of transcription factors is activated in pre-adipocytes when confluent cells are treated with adipogenic differentiation cocktails, leading to the formation of adipocytes (36). Immediately after induction of pre-adipocytes by adipogenic induction cocktails, the expression of c-fos, c-jun, junB, c-myc and CCAAT/enhancer binding proteins (C/ebp) β and δ is observed (31). The early transcription factor, C/EBPβ is primarily activated by dexamethasone (Dexa), while C/EBPδ is responsive to 3-isobutyl-1-methylxanthine (IBMX) (31). Glucocorticoid enhances C/EBPδ expression and promotes C/EBPβ acetylation leading to potentiated C/EBP β and δ dependent adipogenic differentiation (63).

The activity of C/EBP β and δ activates the expression of late phase adipogenic differentiation markers, peroxisome proliferator-activated receptor γ (PPARγ) (40) and C/EBPα, in the transcriptional cascade of adipogenesis (31). Activated PPARγ and

C/EBPα synergistically regulate each other's expression and induce pre-adipocytes to differentiate into adipocytes (36).

Subsequently, PPARγ and C/EBPα cooperate to induce the expression of adipocyte specific genes such as fatty acid-binding protein 4 (FABP4), glucose transporter type 4 (GLUT4), adiponectin, phosphoenolpyruvate carboxykinase (PEPCK), cluster of differentiation 36 (CD36), lipoprotein lipase (LPL), perilipin 1 (PLIN1), and leptin (31). On the other hand, C/EBPζ, can act as an anti-adipogenic factor that can form heterodimers with other C/EBPs preventing them from binding to DNA (36). Both C/EBPs and PPARγ are regulated by insulin/AKT (protein kinase B) signaling pathways to promote differentiation (63). Similarly krueppel-like factor 5 (KLF5) acts in concert with C/EBPδ to induce the expression of PPARγ2 and PPARγ and promote lipid accumulation (36). In contrast, krueppel-like factor 2 (KLF2) and sirtuin proteins function as negative regulators of adipogenesis by inhibiting PPARγ expression (63). Moreover, the Wnt and hedgehog pathways also act as anti-adipogenic elements (33). Understanding the molecular mechanisms regulating pre-adipocyte proliferation and differentiation into adipocytes will provide new targets for action against obesity and obesity related diseases.

1.6. Failure of adipogenesis and its consequence

Adipose tissue mass is determined by the balance of adipogenesis. The metabolic consequences of obesity depend on whether expansion of adipose tissue is achieved by an increase in adipocyte number or adipocyte size (32). Increased adipocyte number or adipogenesis *per se* does not contribute to obesity. This is because obesity represents an excess of stored calories, which results from an imbalance between energy intake and energy expenditure (34). Moreover, the recruitment of a new and smaller size adipocyte increases insulin sensitivity by increasing the capacity to store lipids in the newly formed adipocytes (Fig. 2) (32). This is in part due to the action of PPARγ to enhance GLUT4 and adiponectin expression, which enhances insulin sensitivity.
If such balance is impaired, the risk of developing obesity and insulin resistance is high (32,37).

In the case of increased adipocyte size, as a consequence of a failure of differentiation, the lipid storage capacity is limited, so the lipid is stored in non-adipose tissue (Fig. 2) (34). At this stage, non-adipose tissues are highly exposed to an excessive infiltration of TG and fatty acids (Fig. 2). TG accumulation in non-adipose tissues may play an important role in the development of insulin resistance by impairing insulin secretion from pancreatic β-cell and decreasing glucose uptake by skeletal muscle in obese subjects (34). Moreover, increased delivery of fatty acids to the liver leads to higher glucose production (Fig. 2). Also elevated hepatic very low-density lipoprotein (VLDL)-TG output and reduced glucose clearance by the liver, result in conditions associated with insulin resistance, such as glucose intolerance, hyperlipidemia and hyperinsulinemia (32,34,37,41). At this level pharmacological intervention is usually necessary. For instance, thiazolidinedione (TZDs), a PPARγ ligand, might act by stimulating new adipocyte formation, promoting appropriate lipid storage in adipocytes and diverting excess lipid storage from non-adipose tissue (7). Therefore, having balanced adipogenesis, lipogenesis and lipolysis with normal energy intake and energy expenditure is important to treat the metabolic consequences of excessive adipose tissue mass.

In summary, one reason why adipocyte hypertrophy has been linked to the development of T2D could be that enlarged adipocytes may not be able to effectively store dietary fatty acids due to defects in the ability of adipose tissue to respond rapidly to the dynamic situation after food intake by switching between fatty acid uptake and release. Consequently, lipid overflow, ectopic fat deposition and insulin resistance may develop. Another explanation for the observation that adipocyte hypertrophy is associated with insulin resistance and the development of T2D relates to the secretory function of adipocytes, as will be discussed below.

1.7. Adipose tissue as an endocrine organ

Beyond the traditional role of WAT as an energy storage organ, the metabolic role of this tissue is very complex.

Following the discovery of leptin in 1994 (42), the scientific perspective on WAT has radically changed. Leptin, an important hormone in energy homeostasis, gave WAT a new role as an endocrine organ (43). Adipocytes are now known to express and secrete

many active molecules or hormones termed adipokines (44). The secreted adipokines may act at local (autocrine /paracrine) or systemic (endocrine) level (45). The majority of these adipocyte-derived factors are categorized as: a) factors directly affecting metabolism; b) pro-inflammatory factors and acute phase reactants; c) extracellular matrix components and; d) pro-mitogenic and pro-angiogenic factors (Fig. 3) (46)

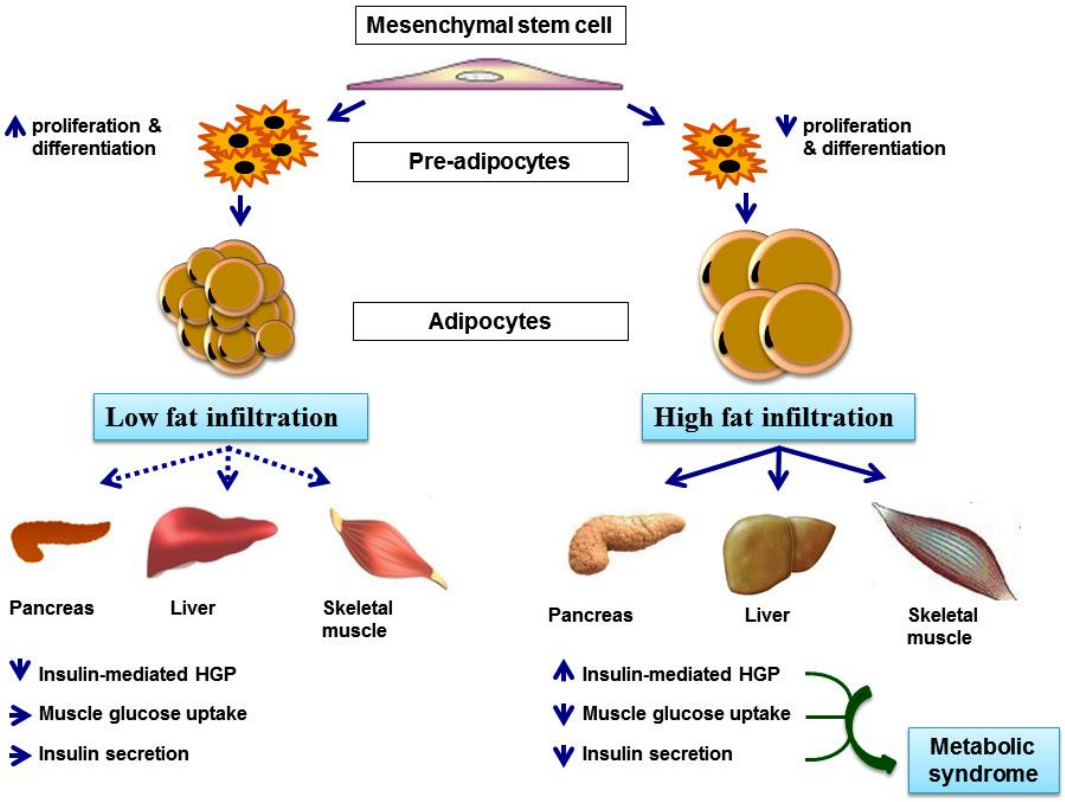

Figure 2. **Ectopic fat deposition and insulin resistance due to the failure of adipogenesis. HGP: hepatic glucose production.**

Besides its ability to regulate its own metabolic activity via autocrine and/or paracrine pathways, adipose tissue signals to other tissues to regulate their metabolism by the aforementioned adipokines (43). On the other hand, adipocytes contain many types of receptors for hormones, neurotransmitters and other signaling molecules to respond to afferent signals (47). Therefore, adipocytes are intimately involved in metabolic homeostasis by secreting and responding to hormones and cytokines that regulate energy intake and expenditure. Studies have reported that obesity and its associated metabolic disorders, particularly insulin resistance, T2D and CVD are influenced to a great extent by the impaired secretion of adipokines (45). Normalization of the

adipokines secretion profile is associated with weight loss and correlates well with the normalization of metabolic parameters, indicating that adipokines play an important role as molecular messengers and regulators of whole body energy balance (46).

Varieties of adipokines that may link obesity to insulin resistance are overexpressed in enlarged human and rodent adipocytes (48). It is well studied that chronic low-grade inflammation is a hallmark of obesity, insulin resistance and T2D (37,48). In line with this, studies have shown the presence of macrophages in obese adipose tissue and insulin resistant subjects (48), leading to increased expression and/or secretion of inflammatory molecules, including tumor necrosis factor-α (TNF-α), interleukin (IL-6), plasminogen activator inhibitor-1 (PAI-1) and monocyte chemotactic protein-1 (MCP-1) (32,37,41,49).

Contrary to the pro-inflammatory adipokines expression, the insulin-sensitizing factor, adiponectin is down regulated in obese, insulin resistant and T2D subjects (34). Supporting this result, large adipocytes from cultured human cells seem to express more pro-inflammatory adipokines compared to smaller adipocytes, which secrete more anti-inflammatory adipokines (46). In agreement with these finding, weight-loss resulted in a reduced adipocyte size and increases in beneficial anti-inflammatory adipokines secretion; adiponectin and IL-10 (46).

For example, when obese rats are treated with troglitazone the number of smaller adipocytes increases whereas the number of large adipocytes decreases, resulting in decreased expression level of TNF-α (48) and increased secretion of adiponectin, indicating an interaction between adipokines. Hence, the down regulation of adiponectin expression in obese subjects is partly due to the overexpression of TNF-α, MCP-1 and IL-6 (43). Furthermore, TNF-α has been demonstrated to increase IL-6 production in 3T3-L1 adipocytes (48). Thus, TNF-α appears to play a pivotal role with respect to the production of several other adipokines (32,34,37,41,49).

1.8. Regulation of adipogenesis by adipokines

As discussed above, adipocytes and adipose tissue are actively involved in metabolic processes such as angiogenesis (51), adipogenesis (52), glucose metabolism (53), lipid

metabolism (54) and hormone production (55). The growing interest in adipose tissue in relation to adipokine secretion has led to significant advances regarding the molecular basis for adipogenesis. The overall regulation of adipose tissue development involves complex interactions between endocrine, paracrine, and autocrine systems (34). Furthermore, the presence of adipokine receptor in adipocytes makes these cells available to the autocrine and paracrine effects of adipokines (37). For instance; leptin, adiponectin, TNF α, IL-6, visfatin, and resistin influence adipocyte growth through central and peripheral mechanisms (32,34,37,48).

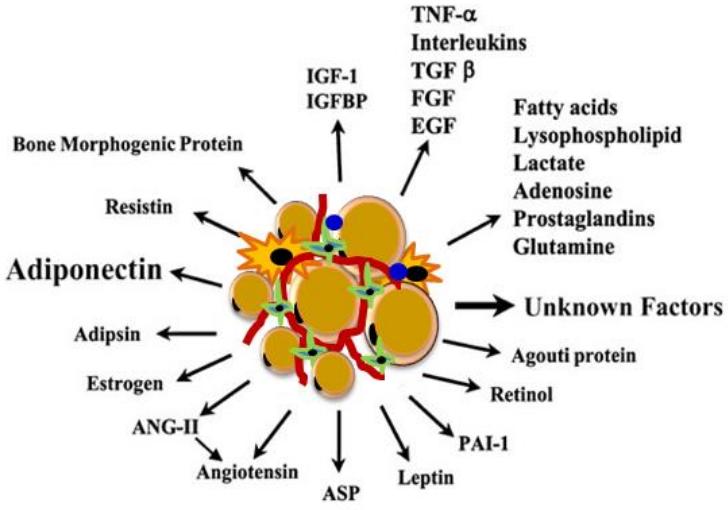

Figure 3. **Secreted adipokines from adipose tissue (Adapted from (50)).**

Different adipose depots have distinct patterns of gene expression and adipokine secretion as well as adipogenic capacity (56). For instance, subcutaneous adipose tissue secretes more leptin and adiponectin, but less IL-6 and free fatty acids (56). In addition, subcutaneous pre-adipocytes have a higher capacity of adipogenesis compared with visceral pre-adipocytes (48). This fact explains why subcutaneous and visceral fat depots secrete different adipokines and why their ability to respond to adipokines and other stimuli for adipogenesis is different.

The ever increasing adipokine secretion list from adipose tissue and adipocytes and their endocrine, paracrine, and autocrine effects on adipocyte development in addition to their broader effects on whole body energy homeostasis, create a big interest to identify new secreted adipokines and study their role on adipocyte development.

1.9. Regulation of energy metabolism by incretin hormones

As mentioned above, adipose tissue mass is determined by the volume and number of adipocytes, factors that are dependent upon a balance between pre-adipocyte differentiation and maturation of adipocytes to store energy (32). In addition to adipokines, incretin hormones also contribute to the regulation of adipocyte development thereby whole body energy metabolism. Glucose-dependent insulinotropic polypeptide (GIP) and glucagon-like peptide-1 (GLP-1) are the two major incretin hormones that potentiate glucose-stimulated insulin secretion during a meal and exert additional beneficial effects on β-cell proliferation and survival (57,58). The intestinal wall and adipose tissue communicates via GIP and GLP-1 to regulate adipocyte formation and adipose tissue function (40,59). The effect of GIP and GLP-1 on energy metabolism is discussed in details in chapter two and chapter three of this PhD thesis.

1.10. Hypothesis and aims of this PhD thesis study

Hypothesis

We hypothesized that, in addition to the known proteins released from adipose tissue and adipocytes, there are other secreted factors affecting adipose tissue plasticity. These factors might act locally and centrally and may be involved in the regulation of adipose tissue development, thereby positively or negatively affecting whole body energy metabolism. Besides adipokines, incretin hormones (GLP-1 and GIP) might play a major role in modulating adipose tissue development by integrating peripheral and central signals, thereby controlling energy homeostasis.

The specific hypotheses are that factors secreted from adipocytes or gut:

- Regulate adipocyte formation from pre-adipocytes to mature adipocytes and thereby controlling adipocyte size (hypertrophy) - this may be the underlying cause for the development of metabolic disorders.
- Alternatively, these factors might increase adipogenesis by increasing the recruitment of new precursor cells from adipose tissue and enhance the proliferation and differentiation of pre-adipocyte to adipocyte (hyperplasia) - this may improve insulin sensitivity and decrease the ectopic lipid storage in non-adipose tissue.
- GLP-1 and GIP secreted from the intestine might signal to adipose tissue and CNS, thereby influencing adipocyte development and energy metabolism.

Objectives

1) The overall objective of this project was to identify novel factor(s) secreted from white adipose tissue explant or adipocytes. This work is presented in chapter 4.
2) To investigate the cross talk between intestinal wall and adipose tissue, via GLP-1/GLP-1R that would regulate adipose tissue development *in vivo* and *in vitro.* This work is presented in Chapter 2.
3) To investigate the role of human GIPr in the brain on energy metabolism. Therefore, we generated CNS specific hGIPr knockout mice as presented in detail in Chapter 3.

By achieving these aims, we were able to identify and investigate novel biological factors secreted from adipocytes or adipose tissue explant, which will help us to

understand the direct or indirect feedback loop regulation of adipogenesis by novel identified adipokines. We were also able to get a better perspective on the cross talk between intestinal wall and adipose tissue in energy metabolism via the GLP-1/ GLP-1R signalling pathway. Moreover, we studied how GIPr centrally regulates whole body energy metabolism. Overall, the findings from this PhD thesis provide the basis for understanding the molecular mechanisms that underlie the adipogenic process and the CNS regulation of energy metabolism.

1.11. References

1. Matsuzawa, Y., Fujioka, S., Tokunaga, K., and Tarui, S. (1992) *Proc Soc Exp Biol Med* **200**, 197-201
2. Montague, C. T., and O'Rahilly, S. (2000) *Diabetes* **49**, 883-888
3. Anderson, J. W., Hamilton, C. C., and Brinkman-Kaplan, V. (1992) *Am J Gastroenterol* **87**, 6-15
4. Dowling, H. J., and Pi-Sunyer, F. X. (1993) *Diabetes* **42**, 537-543
5. Pi-Sunyer, F. X. (1993) *Ann Intern Med* **119**, 655-660
6. Bays, H. E., Gonzalez-Campoy, J. M., Bray, G. A., Kitabchi, A. E., Bergman, D. A., Schorr, A. B., Rodbard, H. W., and Henry, R. R. (2008) *Expert Rev Cardiovasc Ther* **6**, 343-368
7. Park, K. W., Halperin, D. S., and Tontonoz, P. (2008) *Cell Metab* **8**, 454-457
8. Popkin, B. M., and Doak, C. M. (1998) *Nutr Rev* **56**, 106-114
9. Han, J. C., Lawlor, D. A., and Kimm, S. Y. (2010) *Lancet* **375**, 1737-1748
10. Chiu, M., Austin, P. C., Manuel, D. G., Shah, B. R., and Tu, J. V. (2011) *Diabetes Care* **34**, 1741-1748
11. Wickelgren, I. (1998) *Science* **280**, 1364-1367
12. Zimmet, P., Alberti, K. G. M. M., and Shaw, J. (2001) *Nature* **414**, 782-787
13. Fox, K., Peters, D., Armstrong, N., Sharpe, P., and Bell, M. (1993) *Int J Obes Relat Metab Disord* **17**, 11-16
14. Gautier, J. F., Mourier, A., de Kerviler, E., Tarentola, A., Bigard, A. X., Villette, J. M., Guezennec, C. Y., and Cathelineau, G. (1998) *J Clin Endocrinol Metab* **83**, 1306-1311
15. Barzilai, N., and Gupta, G. (1999) *J Gerontol A Biol Sci Med Sci* **54**, B89-96; discussion B97-88
16. Tuomilehto, J., Lindstrom, J., Eriksson, J. G., Valle, T. T., Hamalainen, H., Ilanne-Parikka, P., Keinanen-Kiukaanniemi, S., Laakso, M., Louheranta, A., Rastas, M., Salminen, V., Uusitupa, M., and Finnish Diabetes Prevention Study, G. (2001) *The New England journal of medicine* **344**, 1343-1350
17. Groop, L. C. (1997) *Journal of internal medicine* **241**, 95-101
18. Cinti, S. (2009) *Am J Physiol Endocrinol Metab* **297**, E977-986
19. Cannon, B., and Nedergaard, J. (2004) *Physiol Rev* **84**, 277-359
20. Skala, J., Barnard, T., and Lindberg, O. (1970) *Comparative biochemistry and physiology* **33**, 509-528
21. Rosenwald, M., Perdikari, A., Rulicke, T., and Wolfrum, C. (2013) *Nat Cell Biol* **15**, 659-667
22. Billon, N., Iannarelli, P., Monteiro, M. C., Glavieux-Pardanaud, C., Richardson, W. D., Kessaris, N., Dani, C., and Dupin, E. (2007) *Development* **134**, 2283-2292
23. Ailhaud, G., Grimaldi, P., and Negrel, R. (1992) *Annu Rev Nutr* **12**, 207-233
24. Rosen, E. D., and Spiegelman, B. M. (2006) *Nature* **444**, 847-853
25. Rigamonti, A., Brennand, K., Lau, F., and Cowan, C. A. (2011) *PLoS One* **6**, e17637
26. Hausman, D. B., DiGirolamo, M., Bartness, T. J., Hausman, G. J., and Martin, R. J. (2001) *Obes Rev* **2**, 239-254
27. Spalding, K. L., Arner, E., Westermark, P. O., Bernard, S., Buchholz, B. A., Bergmann, O., Blomqvist, L., Hoffstedt, J., Naslund, E., Britton, T., Concha, H., Hassan, M., Ryden, M., Frisen, J., and Arner, P. (2008) *Nature* **453**, 783-787

28. Wronska, A., and Kmiec, Z. (2012) *Acta physiologica* **205**, 194-208
29. Bjorndal, B., Burri, L., Staalesen, V., Skorve, J., and Berge, R. K. (2011) *Journal of obesity* **2011**, 490650
30. Skurk, T., Alberti-Huber, C., Herder, C., and Hauner, H. (2007) *J Clin Endocrinol Metab* **92**, 1023-1033
31. Ntambi, J. M., and Young-Cheul, K. (2000) *J Nutr* **130**, 3122S-3126S
32. Vazquez-Vela, M. E., Torres, N., and Tovar, A. R. (2008) *Arch Med Res* **39**, 715-728
33. Lowe, C. E., O'Rahilly, S., and Rochford, J. J. (2011) *J Cell Sci* **124**, 2681-2686
34. Heilbronn, L., Smith, S. R., and Ravussin, E. (2004) *Int J Obes Relat Metab Disord* **28 Suppl 4**, S12-21
35. Qiu, Z., Wei, Y., Chen, N., Jiang, M., Wu, J., and Liao, K. (2001) *J Biol Chem* **276**, 11988-11995
36. Romao, J. M., Jin, W., Dodson, M. V., Hausman, G. J., Moore, S. S., and Guan, L. L. (2011) *Exp Biol Med (Maywood)* **236**, 997-1004
37. Karastergiou, K., and Mohamed-Ali, V. (2010) *Mol Cell Endocrinol* **318**, 69-78
38. Gospodarowicz, D., Greene, G., and Moran, J. (1975) *Biochem Biophys Res Commun* **65**, 779-787
39. Ntambi, J. M., and Young-Cheul, K. (2000) *The Journal of nutrition* **130**, 3122S-3126S
40. Challa, T. D., Beaton, N., Arnold, M., Rudofsky, G., Langhans, W., and Wolfrum, C. (2012) *J Biol Chem* **287**, 6421-6430
41. Gastaldelli, A., Natali, A., Vettor, R., and Corradini, S. G. (2010) *Dig Liver Dis* **42**, 310-319
42. Zhang, Y., Proenca, R., Maffei, M., Barone, M., Leopold, L., and Friedman, J. M. (1994) *Nature* **372**, 425-432
43. MacDougald, O. A., and Burant, C. F. (2007) *Cell Metab* **6**, 159-161
44. Mohamed-Ali, V., Pinkney, J. H., and Coppack, S. W. (1998) *International journal of obesity and related metabolic disorders : journal of the International Association for the Study of Obesity* **22**, 1145-1158
45. Kershaw, E. E., and Flier, J. S. (2004) *The Journal of clinical endocrinology and metabolism* **89**, 2548-2556
46. Deng, Y., and Scherer, P. E. (2010) *Annals of the New York Academy of Sciences* **1212**, E1-E19
47. Ouchi, N., Higuchi, A., Ohashi, K., Oshima, Y., Gokce, N., Shibata, R., Akasaki, Y., Shimono, A., and Walsh, K. (2010) *Science* **329**, 454-457
48. Goossens, G. H. (2008) *Physiol Behav* **94**, 206-218
49. Trayhurn, P., and Beattie, J. H. (2001) *Proc Nutr Soc* **60**, 329-339
50. Ravussin, E. (2002) *The pharmacogenomics journal* **2**, 4-7
51. Cao, Y. (2010) *Nat Rev Drug Discov* **9**, 107-115
52. Wolfrum, C., Shih, D. Q., Kuwajima, S., Norris, A. W., Kahn, C. R., and Stoffel, M. (2003) *J Clin Invest* **112**, 345-356
53. Horowitz, J. F., Coppack, S. W., and Klein, S. (2001) *Am J Clin Nutr* **73**, 517-522
54. Yu, Y. H., and Ginsberg, H. N. (2005) *Circ Res* **96**, 1042-1052
55. Havel, P. J. (2004) *Diabetes* **53 Suppl 1**, S143-151
56. Feng, B., Zhang, T., and Xu, H. (2013) *Ann N Y Acad Sci* **1281**, 160-177
57. Brown, J. C., Pederson, R. A., Jorpes, E., and Mutt, V. (1969) *Canadian journal of physiology and pharmacology* **47**, 113-114

58. Miyawaki, K., Yamada, Y., Yano, H., Niwa, H., Ban, N., Ihara, Y., Kubota, A., Fujimoto, S., Kajikawa, M., Kuroe, A., Tsuda, K., Hashimoto, H., Yamashita, T., Jomori, T., Tashiro, F., Miyazaki, J., and Seino, Y. (1999) *Proc Natl Acad Sci U S A* **96**, 14843-14847
59. Yabe, D., and Seino, Y. (2011) *Progress in biophysics and molecular biology* **107**, 248-256
60. WHO (2008a) Waist Circumference and Waist-Hip Ratio Report of a WHO Expert Consultation GENEVA, 8-11 DECEMBER 2008
61. WHO (2008b) Waist Circumference and Waist-Hip Ratio Report of a WHO Expert Consultation GENEVA, 8-11 DECEMBER 2008
62. Awada, R., Parimisetty, A., d'Hellencourt, C.L. Influence of Obesity on Neurodegenerative Diseases. http://dx.doi.org/10.5772/53671
63. Liu, G.-S., Chan, E.C., Higuchi, M., Gregory J. (2012) Dusting and Fan Jiang. Redox mechanisms in regulation of adipocyte differentiation: Beyond a General Stress Response. Cells **4**, 976-993

Chapter 2

2. Regulation of adipocyte formation by GLP-1/GLP-1R signaling

Tenagne Delessa Challa[1], Nigel Beaton[1], Myrtha Arnold[1], Gottfried Rudofsky[2], Wolfgang Langhans[1] and Christian Wolfrum[1]

[1]Swiss Federal Institute of Technology, ETH Zürich, Institute of Food Nutrition and Health, Schorenstrasse 16, 8603 Schwerzenbach, Switzerland
[2]Department of Medicine I and Clinical Chemistry, University of Heidelberg, Im Neuenheimer Feld 410, 69120 Heidelberg, Germany

Published in the Journal of Biological Chemistry. Vol. 287, No. 9, pp. 6421–6430, Feb. 24, 2012.

Background: Nutrient intake directly affects adipose tissue function and growth.

Results: The gut peptide GLP-1 controls adipogenesis via its receptor through regulation of cell proliferation and apoptosis.

Conclusion: GLP-1 is a signaling molecule from the intestine relating nutritional status to the adipose tissue.

Significance: GLP-1 is used in treatment of Type II diabetes, and regulation of adipose tissue mass might be one influencing factor.

2.1. Summary

Increased nutrient intake leads to excessive adipose tissue accumulation, obesity, and the development of associated metabolic disorders. How the intestine signals to adipose tissue to adapt to increased nutrient intake, however, is still not completely understood. We show here, that the gut peptide GLP-1 or its long-lasting analog liraglutide, function as intestinally derived signals to induce adipocyte formation, both in vitro and in vivo. GLP-1 and liraglutide activate the GLP-1R, thereby promoting pre-adipocyte proliferation and inhibition of apoptosis. This is achieved at least partly through activation of ERK, PKC, and AKT signaling pathways. In contrast, loss of GLP-1R expression causes reduction in adipogenesis, through induction of apoptosis in pre-adipocytes, by inhibition of the above mentioned pathways. Because GLP-1 and liraglutide are used for the treatment of Type II diabetes, these findings implicate GLP-1 as a regulator of adipogenesis, which could be an alternate pathway leading to improved lipid homeostasis and controlled downstream insulin signaling.

2.2. Introduction

Adipose tissue is a key component of the metabolic syndrome, often associated with the development of Type II diabetes mellitus, atherosclerosis, and hyperlipidemia (1–4). The growth of adipose tissue involves cellular hypertrophy (cell size increase) and hyperplasia (cell number increase) (5). Hypertrophy is the result of excess lipid accumulation in existing adipocytes due to high energy intake (2). Obesity in adults is characterized by adipocyte hypertrophy, linked to down-regulation of adiponectin secretion, leading to the development of insulin resistance and Type II diabetes (T2D) (6). In contrast, hyperplasia results from the recruitment of new adipocytes from precursor cells in adipose tissue and involves proliferation (2) and differentiation of preadipocytes (7, 8). Interestingly, it was reported that hyperplasia in both visceral and subcutaneous adipose tissue might be protective against lipid, as well as glucose/insulin abnormalities in obesity (9). Adipocytes play an important role in energy homeostasis by storing energy in lipid droplets (10, 11). Furthermore, adipose tissue functions as an endocrine organ, secreting adipocytokines that regulate energy metabolism in fat and other tissues (12, 13).

Glucagon-like peptide-1 (GLP-1), an incretin hormone, produced by post-translational processing of proglucagon gene (14, 15) in enteroendocrine L-cells in response to food intake, is secreted as one of the gut hormones (15, 16) and collected in the intestinal lymph duct. Plasma levels of GLP-1 rise rapidly within minutes after food intake (17). The major physiological roles of this endocrine hormone include: 1) the stimulation of glucose-dependent insulin secretion from pancreatic β-cells, 2) stimulation of insulin biosynthesis and insulin sensitivity, 3) enhancement of pancreatic β-cell proliferation and protection against apoptosis, 4) inhibition of glucagon secretion and gastric emptying, and 5) inhibition of food intake (14, 18–21). As a result GLP-1 facilitates the rapid clearance and storage of blood glucose (16). For instance, subcutaneous administration of native GLP-1 to patients with Type II diabetes mellitus lowers fasting and postprandial levels of glucose and HbA1c effectively, and reduces weight gain (22).

Given the rapid inactivation of endogenous GLP-1 (half-life of less than 2 min) by the enzyme dipeptidyl-peptidase-4 (DPPIV), alternative therapeutic approaches have been developed using GLP-1 analogues which are resistant to DPP-IV mediated degradation (14). One of the FDA-approved GLP-1R agonists is liraglutide which is used to treat

T2D (23). Liraglutide has a 97% homology with human GLP-1 including a lysine to arginine mutation at position 34 and a palmitoyl side-chain at lysine 26 (24).

Because of the above mentioned reasons, GLP-1 and GLP-1 analogs are currently among the most promising therapeutic options for the pharmacotherapy of T2D and obesity because these substances do not lose their eating-inhibitory and beneficial metabolic effects with chronic treatment and because they are still effective in obese patients, which show reduced GLP-1 levels. Although the cause of this association between obesity and GLP-1 is unknown (25), it might be a contributing factor toward the development of obesity as GLP-1secretion is improved after weight loss (14, 25, 26).

The intracellular effect of GLP-1 is mediated via activation of its specific receptor (GLP-1R). GLP-1R belongs to the class B family of 7-transmembrane-spanning, heterotrimeric G-protein-coupled receptors (21). GLP-1R is expressed in many tissues, including pancreas, lung, heart, kidney, intestine, stomach, adipose tissue, muscle, as well as the central and peripheral nervous systems (17,19). Upon its activation, GLP-1R couples with Gαs and activates adenylate cyclase (AC) to stimulate cAMP production (27), leading to the activation of second messenger pathways, such as cAMP-dependent protein kinase (PKA) and cAMP-regulated guanine nucleotide exchange factors of the Epac family (21). Here, we show that GLP-1 or its analogue liraglutide stimulate pre-adipocyte differentiation via GLP-1R, both in vitro and in vivo. Suppression of Glp-1R expression reduces proliferation and differentiation while inducing apoptosis of pre-adipocytes. This mechanism is the basis for a cross talk between the intestine and adipocyte precursor cells leading to an induction of adipogenesis in response to nutrient intake.

2.3. Experimental procedures

Materials

Glucagon-Like Peptide (7-36) GLP-1 was obtained from Bachem. Bodipy493/503, Hoechst, Syto60 were purchased from Invitrogen. Dexamethasone, 3-isobutyl-1-methylxanthine (IBMX) and insulin were from Sigma-Aldrich.

Differentiation of pre-adipocytes

The 3T3-L1 fibroblasts as well as primary pre-adipocytes were grown and differentiated as described previously (7). High throughput image analysis to calculate adipogenesis was performed as described before (7, 28). In short, SVF cells and 3T3-L1 pre-adipocytes were cultured on collagen coated black 96-well plates with clear bottoms. Fluorescent images were taken with an Operetta high throughput imaging system (Perkin Elmer). Images were analyzed using either Cell Profiler or Harmony software (Perkin Elmer).

Lentiviral knockdown

For propagation and downstream purification of a short hairpin RNA (shRNA) clones, sequence-verified shRNA lentiviral plasmids (pLKO.1-puro) targeting mouse GLP-1R were obtained as frozen bacterial glycerol stocks (Sigma–Aldrich). Five different lentiviral vector plasmids constructs of mission shRNA clones were used. PLKO.1 plasmids were used to generate lentiviral particles in the packaging HEK293T cell line. 60-70% confluent pre-adipocytes were infected with GLP-1R shRNA lentivirus or a scrambled shRNA control in complete medium (10% FBS and 1% penicillin streptomycin) in the presence of polybrene (8µg/ml). The next day the medium was changed to complete medium, which was subsequently changed every 48 hours for a total of 6 days.

RNA isolation and quantitative real-time RT-PCR

Total RNA was extracted using TRIzol reagent according to the manufacturer's protocol. 1.0 µg of total RNA was converted into first-strand cDNA using the SuperScript III First-Strand kit (Invitrogen). Real-time PCR quantification was

performed using platinum SYBR Green and gene specific primer sets (Table 1, Appendix 2).

Western blot analysis

For whole cell lysate preparation, differentiated cells were lysed in hypotonic buffer containing 10 mM KCL, 1.5 mM $MgCl_2$, 0.2% Tween 20, 10 mM HEPES, pH 7.9 and 2% (v/v) protease inhibitors (Roche) for 5 min on ice. Hypertonic buffer containing 0.5 % (v/v) of 150 mM NaCl, 20 mM HEPES pH 7.9, 25 % glycerol, 0.2 mM EDTA, 1.5 mM $MgCl_2$, 1.2 mM NaCl and 2% (v/v) protease inhibitors was added and the sample was incubated for 30 min by overhead rotation at 4^{o}C. Cell lysates were centrifuged at 16000 rpm for 20 min, and protein concentrations were measured. Equal amounts of lysate proteins were resolved by SDS-PAGE (10–15%) gel and transferred onto a nitrocellulose membrane (Perkin Elmer). The following primary antibodies were used: ant-PKC (PKCβII), anti-GLP-1R, (Abcam); anti-C/EBPβ, anti-C/EBPδ, anti-PPARγ, anti-FABP4, anti-Phospho-PKC (βII ser660), anti-ERK1/2, anti-phospho-ERK1/2 (Thr202/ Tyr204), anti-phospho-Akt (Ser473), anti-Akt, anti-phospho-Bad (Ser136), anti-Cleaved Caspase-3 (Cell Signaling). Loading controls were measured with a mouse anti-γ-Tubulin (Sigma-Aldrich).

Cell proliferation and apoptosis

Cell proliferation was determined by measuring 5-ethynyl-2'-deoxyuridine (EdU) incorporation. By using the fluorescent Alexa Fluor® 488 azide from the Click-iT® EDU Alexa Fluor® 488 assay kit (Invitrogen). An ELISA apoptosis detection kit (Enzo) targeting denatured DNA with a monoclonal antibody to single stranded DNA (ssDNA) was used to evaluate apoptosis in adipocytes cells. The assay was carried out according to the manufacturer's instructions.

Animal studies

The Canton of Zurich Veterinary Office approved all animal studies. Male 10 to 12-week-old C57BL/6 mice were obtained from Charles River. They were housed in a pathogen-free animal facility on 12 h dark/light cycle. In vivo differentiation was performed as described, previously (28). In short, male mice were sacrificed and fat tissues (subcutaneous and visceral) were minced and incubated with collagenase type II

in KRB buffer for 1 h at 37°C. SVF cells were pelleted by centrifugation and filtered with a 40 µm mesh. For in vivo adipogenesis, 10^6 cells were resuspended in 100 µl of Matrigel (BD) and injected into the subcutaneous subscapular region of acceptor mice. To induce adipogenesis mice were fed a high fat diet (HFD) for 6 weeks. To assess the influence of liraglutide (Bachem), animals were injected for the last 17 days of the study with the long lasting GLP-1 analogue, liraglutide at 100 µg/kg twice daily. Mice were sacrificed and Matrigel pads were excised, adipose tissue was fixed in 5% paraformaldehyde, paraffin embedded and cut into 10 µm sections. The cut tissues were stained with hematoxylin/eosin. The amount of adipocytes present in a tissue section was quantified using Cell Profiler (28).

Statistical analysis

All data are expressed as mean ± SEM. The significance of differences between groups was determined using a two-tailed Student's t test.

2.4. Results

GLP-1 regulates adipogenesis

To determine the effects of GLP-1 on adipogenic differentiation, cultured 3T3-L1 cells, as well as primary pre-adipocytes were treated with or without GLP-1 or its synthetic analog liraglutide at different concentrations (Fig. 1, A-C; Supplemental Fig. 1, A-D). Interestingly, cells treated with GLP-1 or liraglutide demonstrated a significantly higher degree of differentiation than control cells. Furthermore, we observed a dose-dependent increase in the number of differentiated adipocytes after GLP-1 or liraglutide treatment in 3T3-L1 cells, as well as an increase in differentiation in primary pre-adipocytes. To further examine liraglutide effects on adipogenesis in vivo, we implanted pre-adipocytes in a matrigel pad into the subscapular region of acceptor mice which were fed a HFD, in addition to treatment with liraglutide. Interestingly, 100 µg/kg twice daily IP injection of liraglutide into mice for 17 days induced pre-adipocyte differentiation significantly (Fig. 1D), even though the same mice showed a trend towards reduced weight gain and blood glucose levels (Supplemental Fig. 1, E and F, Appendix 2). Taken together these results demonstrate that nutrient intake leads to an increased circulation of GLP-1 which can regulate the process of adipogenesis.

The effects of GLP-1 on adipogenesis are mediated through GLP-1R

Based on our findings that GLP-1 promotes adipogenesis, we next examined the role of GLP-1R during differentiation. In agreement with previous results (29), we found GLP-1R to be expressed both in undifferentiated and differentiated 3T3-L1 cells. Interestingly, the expression of Glp-1R mRNA and protein was markedly increased during late phase adipocyte differentiation (Fig. 2, A and B). This expression pattern was similar to the late phase adipogenic differentiation marker Pparγ and different from the early adipocyte differentiation markers c-Jun, C/ebpβ and C/ebpδ. To further analyze the functionality of the GLP-1R, 3T3-L1 cells were treated with or without GLP-1 or liraglutide at different concentrations. As shown in Supplemental Fig. S2A, appendix 2, cAMP levels increased in response to GLP-1 or liraglutide treatment and reached a maximum at 1 nM, comparable to isoproterenol, indicating the presence of a functional GLP-1R in 3T3-L1 cells.

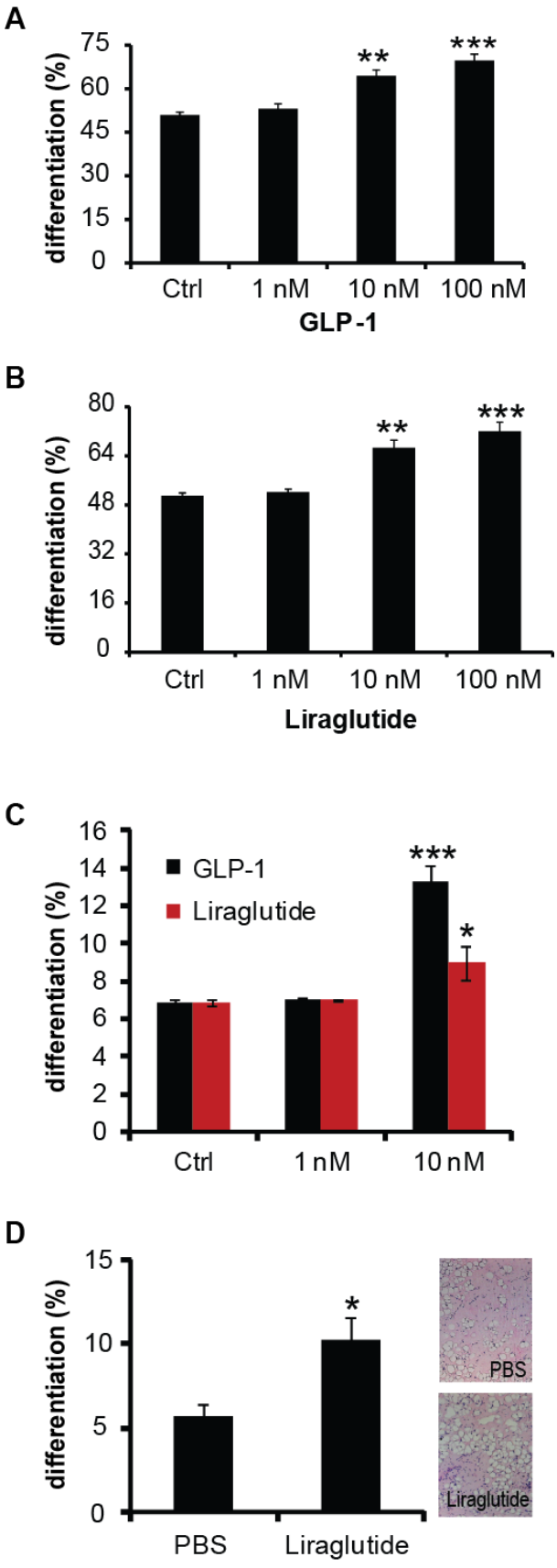

Fig. 1. GLP-1 regulates adipocyte differentiation. A,B) 3T3-L1 pre-adipocytes were treated with indicated concentrations of GLP-1 or liraglutide during induction of adipogenesis. Differentiation was quantified using image based analysis (n=12). **C**) Primary pre-adipocytes were treated with indicated concentrations of GLP-1 or liraglutide during induction of adipogenesis. Differentiation was quantified as described above (n=4). **D**) In vivo pre-adipocyte differentiation in mice injected with 100 µg/kg liraglutide or PBS for 17 days (n=12). Adipogenesis was quantified using image based analysis of adipocyte formation. All values are shown as mean ± SEM (*<0.05,**p<0.01, ***p<0.001).

To study the potential role of GLP-1R during adipocyte differentiation, 3T3-L1 cells were infected with lentivirus containing shRNA against GLP-1R or a scrambled shRNA control. GLP-1R knockdown was confirmed by RT-PCR analyses (Fig. 2C). Reduction of GLP-1R expression decreased differentiation compared to the scrambled control in the presence of GLP-1 (Fig. 2D, Supplemental Fig. 2B, Appendix 2). To study the potential molecular mechanisms underlying GLP-l mediated activation of adipogenesis we focused on the major adipogenic differentiation markers.

Knockdown of GLP-1R in the presence of GLP-1 significantly inhibited the expression of Pparγ as well as that of its target A-Fabp genes (Fig. 2, E and F; Supplemental Fig. 2C, Appendix 2).

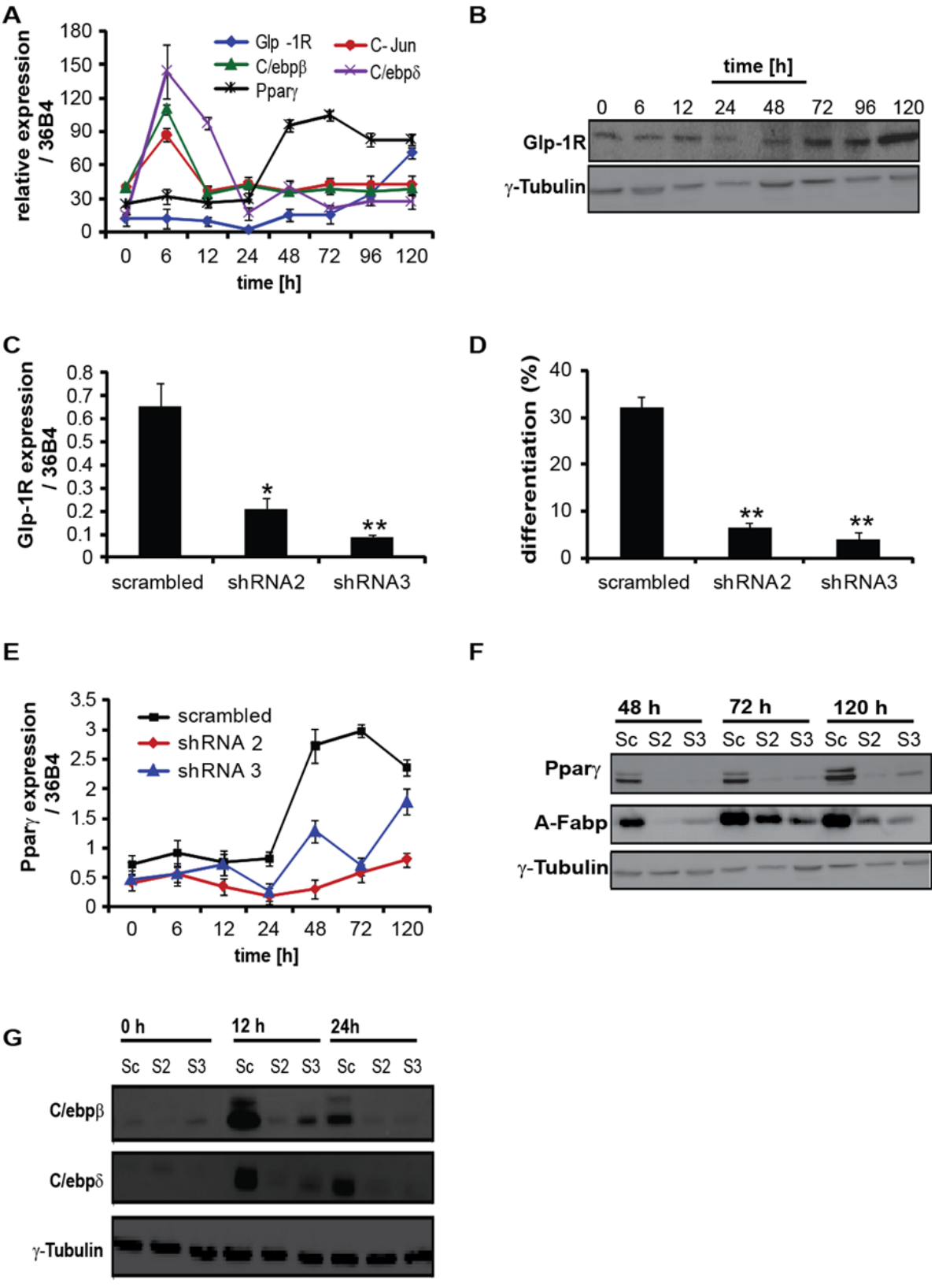

Fig. 2. GLP-1 regulates adipogenesis via GLP-1R. A and **B**) Expression of Glp-1R mRNA and protein in 3T3-L1 cells was measured at different time points during adipogenesis (n=8). **C**) 3T3-L1 pre-adipocytes were infected with GLP-1R shRNA expressing lentivirus (shRNA2 and shRNA3) or scrambled shRNA control. Glp-1R expression was analyzed by qPCR (n=4). **D**) Quantitative analysis of adipocyte differentiation using high-throughput image analysis in cells infected with GLP-1R shRNA expressing lentivirus or scrambled shRNA control (n=12) and treated with GLP-1. **E** and **G**) Analysis of Pparγ, A-Fabp, C/ebpβ/δ mRNA and protein expression in 3T3-L1 pre-adipocytes infected with GLP-1R shRNA expressing lentivirus (shRNA2 and shRNA3) or scrambled shRNA and treated with GLP-1 (n=4). Cells were analyzed at indicated time points post induction of differentiation. γ-Tubulin was used as a loading control. The graphs represents mean ± SEM (**p<0.01, ***p<0.001).

Furthermore, GLP-1R knockdown in the presence of GLP-1 led to the down-regulation of C/ebpβ and C/ebpδ expression (Fig. 2G; Supplemental Fig. 2, D and E, Appendix 2). Taken together these results indicate that GLP-1 mediates its adipogenic effect via GLP-1R through regulation of early events of differentiation, as evidenced by the down-regulation of C/ebpβ/δ, as well as the reduced expression of Pparγ and its target genes.

GLP-1/GLP-1R regulate cell proliferation and adipogenesis in pre-adipocytes

Given the fact that GLP-1 and GLP-1R regulate early adipogenic events we next examined, whether this effect is due to changes in proliferation or apoptosis of pre-adipocytes. To this end, we treated 3T3-L1 cells with GLP-1 or its synthetic analog liraglutide and analyzed the degree of proliferation during the first 24 hours of adipogenesis. As seen in Fig. 3, A and B, GLP-1 and liraglutide incubation led to a significant increase in the number of proliferating cells as evidenced by EDU incorporation. In addition, we examined cell proliferation in GLP-1R knockdown cells, to evaluate whether GLP-1 acts via its receptor to regulate cell proliferation. To this end, 3T3-L1 pre-adipocytes were infected with shRNA against GLP-1R or a scrambled control. Differentiation was induced after confluence and cells were treated with 10 nM of GLP-1 (Fig. 3C). We could show that knockdown of GLP-1R led to a significant decrease of EDU positive cells compared with the scrambled control.

Because adipose tissue mass is determined by the volume and number of adipocytes, factors that are dependent upon a balance between pre-adipocyte proliferation, differentiation and cell loss by apoptosis, we quantified the effect of GLP-1 and its receptor on the regulation of apoptosis in 3T3-L1 cells. We observed a significant

decrease in cell death of induced 3T3-L1 pre-adipocytes treated with GLP-1 or liraglutide (Fig. 3, D and E). In contrast, 3T3-L1 cells infected with GLP-1R shRNA and treated with GLP-1 showed significant induction of cell apoptosis compared with that of scrambled control (Fig. 3F). Thus, knockdown of GLP-1R induces apoptosis in pre-adipocytes during adipogenesis, which cannot be rescued by GLP-1.

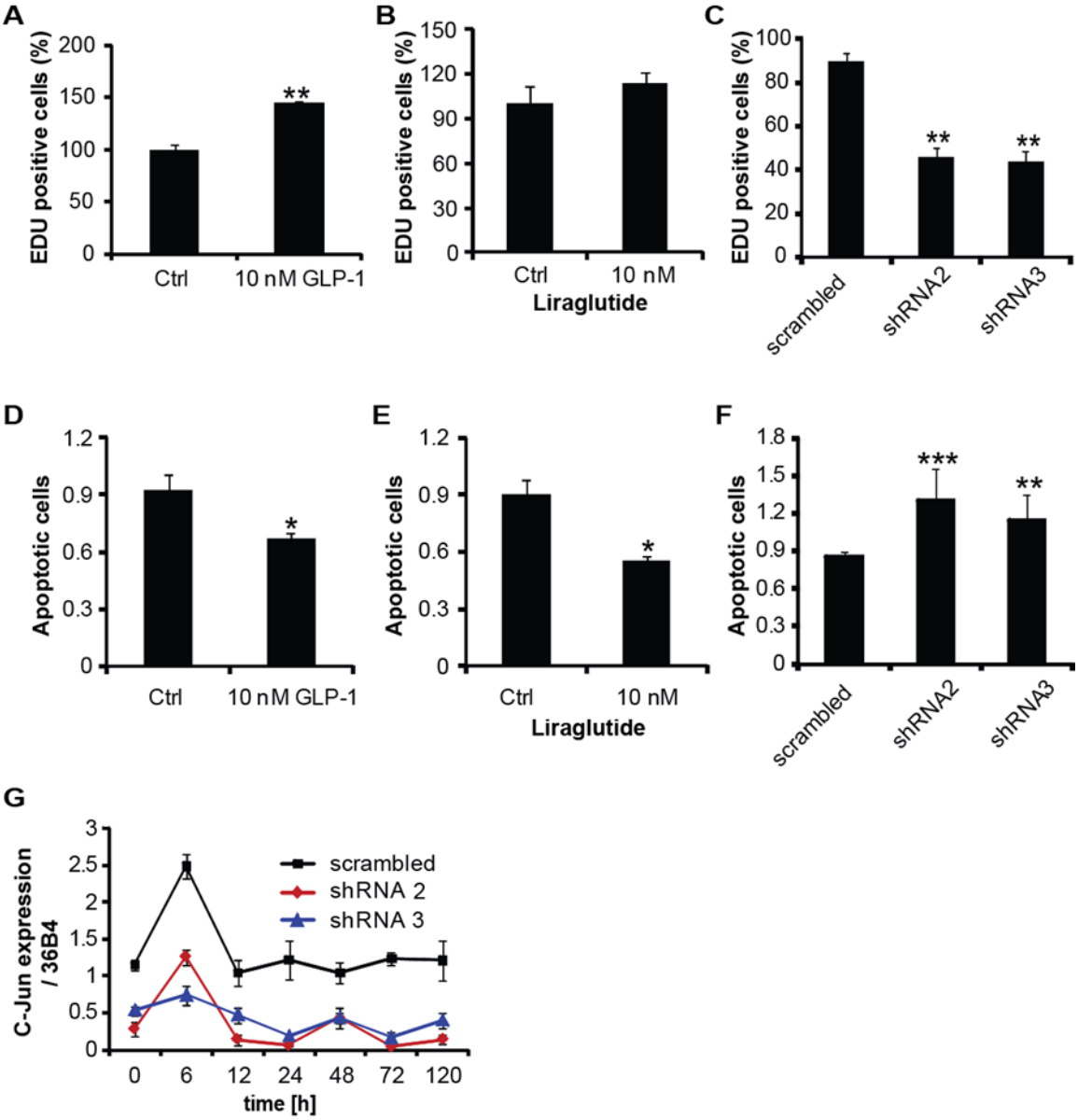

Fig. 3. Regulation cell proliferation and apoptosis by GLP-1/GLP-1R. A and **B**) The effect of GLP-1 and liraglutide on cell proliferation was measured by EDU incorporation into 3T3-L1 pre-adipocytes (n=8). **C**) 3T3-L1 pre-adipocytes were infected with GLP-1R shRNA expressing lentivirus (shRNA2 and shRNA3) or scrambled shRNA control and treated with 10 nM GLP-1 during induction of cell differentiation. EDU incorporation as a marker for cell proliferation was quantified 24 h post induction (n=8). **D** and **E**) The effect of GLP-1 and liraglutide on cell apoptosis

measured by TUNNEL (n=4). **F**) 3T3-L1 pre-adipocytes were infected with GLP-1R shRNA expressing lentivirus (shRNA2 and shRNA3) or scrambled shRNA control and treated with 10 nM GLP-1 during induction of cell differentiation. Apoptosis was quantified by TUNNEL, 24 h post induction (n=4). **G**) Analysis of c-Jun mRNA expression in 3T3-L1 pre-adipocytes infected with GLP-1R shRNA expressing lentivirus (shRNA2 and shRNA3) or scrambled shRNA (n=4) and treated with 10 nM GLP-1 during induction of cell differentiation. The graphs represents mean ± SEM (**p<0.01, ***p<0.001).

Because c-Jun is involved in many cellular processes including cell proliferation, apoptosis, differentiation and cell transformation, we studied the effects of GLP-1 and its receptor on the expression of c-Jun during adipogenic differentiation of 3T3-L1 cells. c-Jun was found to be expressed throughout differentiation in the scrambled control group, with a sharp increase during early differentiation (6h) (Fig. 3G). The c-Jun mRNA levels were significantly down-regulated upon GLP-1R knockdown and GLP-1 was unable to reverse down-regulation of c-Jun expression.

Taken together, our result indicated that GLP-1 regulates adipogenesis by affecting the early clonal expansion phase through regulation of c-Jun expression, as well as by shifting the balance of proliferation and apoptosis.

Effects of GLP-1/GLP-1R are mediated by PKC signaling

To identify the signaling pathways mediating the effects of GLP-1 and its receptor we studied the expression of the key signaling molecules and their posttranslational modifications by Western blot analysis.

One important signaling cascade regulating proliferation and apoptosis are the extracellular signal-regulated kinases (ERK) 1 and 2 pathways. We observed GLP-1 induced Erk1/2 phosphorylation during early phases of differentiation, with maximal phosphorylation attained at 24 hours post-induction (Fig. 4A). In contrast, GLP-1 induced Erk1/2 phosphorylation levels decreased in response to GLP-1R knockdown at 0, 12 and 24 hours, respectively (Fig. 4A). Total Erk1/2 protein levels were not affected by either GLP-1 or GLP-1R knockdown. Another important pathway that regulates apoptosis/proliferation is the protein kinase C beta pathway (PKCβ), which regulates its own expression through the (MAPK)–ERK-dependent signaling pathway. We could

show increased phosphorylation of PkcβII by GLP-1 and a reduced phosphorylation by GLP-1 in the absence of GLP-1R, with no changes in total protein levels (Fig. 4A).

Lastly, the AKT signaling cascade is considered important for adipogenesis, as it appears to induce or activate Pparγ and C/ebpα expression during adipocyte differentiation. Therefore, we measured the phosphorylation states of AKT, after knockdown of GLP-1R. Consistent with Erk and PkcβII, GLP-1 treatment increased Akt phosphorylation levels in scrambled control during 3T3-L1 cell differentiation at 0, 12 and 24 hours post-induction (Fig. 4A). Similarly, GLP-1R knockdown decreased GLP-1 mediated induction of p-Akt levels (Fig. 4A). Taken together these results identify three possible pathways that could explain the alterations in adipogenesis upon GLP-1R activation or knockdown.

Bcl-xL/Bcl-2-associated death promoter homolog (BAD) is pro-apoptotic member of the Bcl-2 family; its pro-apoptotic activity is regulated by phosphorylation at several sites. ERK1/2 activation mediates the Ser-112 phosphorylation of BAD, through p90RSK activation, allowing the association of BAD with the scaffold protein 14-3-3, leading to its inactivation and inhibition of β-cell apoptosis (21). Consistent with these findings we could show that the decrease in Erk1/2 and Akt phosphorylation resulted in reduced pBAD levels in response to GLP-1R knockdown compared to scrambled control cells (Fig. 4A).

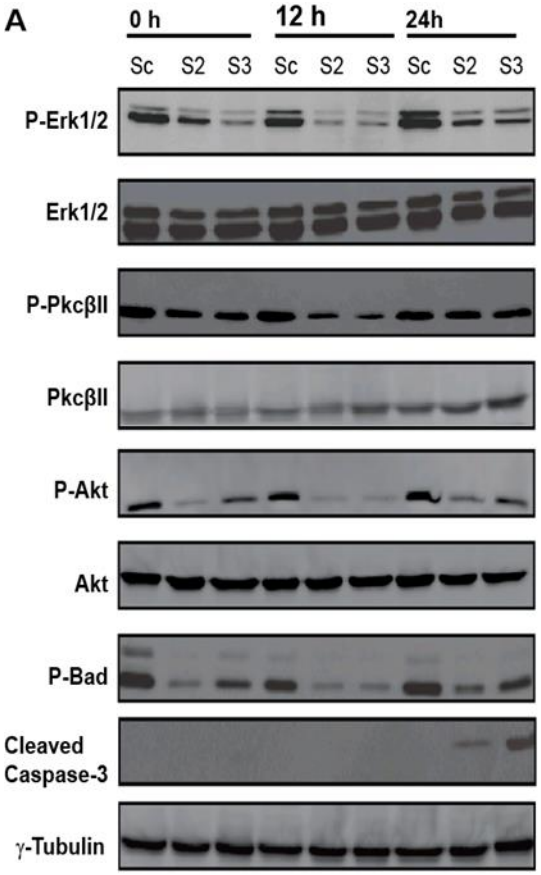
A
0 h
12 h
24h
Sc S2 S3 Sc S2 S3 Sc S2 S3
P-Erk1/2
Erk1/2
P-PkcβII
PkcβII
P-Akt
Akt
P-Bad
Cleaved Caspase-3
γ-Tubulin

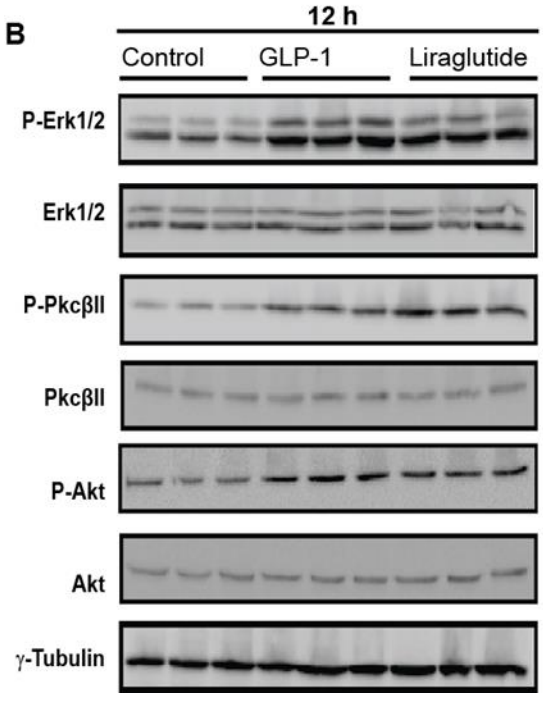
B
12 h
Control
GLP-1
Liraglutide
P-Erk1/2
Erk1/2
P-PkcβII
PkcβII
P-Akt
Akt
γ-Tubulin

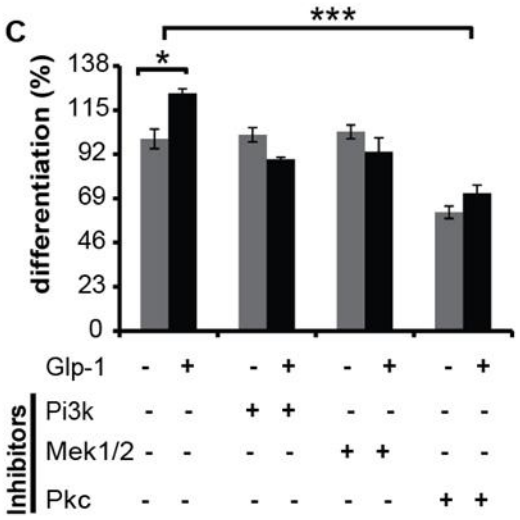
C
differentiation (%)
138
115
92
69
46
23
0
*
***
Glp-1 - + - + - + - +
Inhibitors
Pi3k - - + + - - - -
Mek1/2 - - - - + + - -
Pkc - - - - - - + +

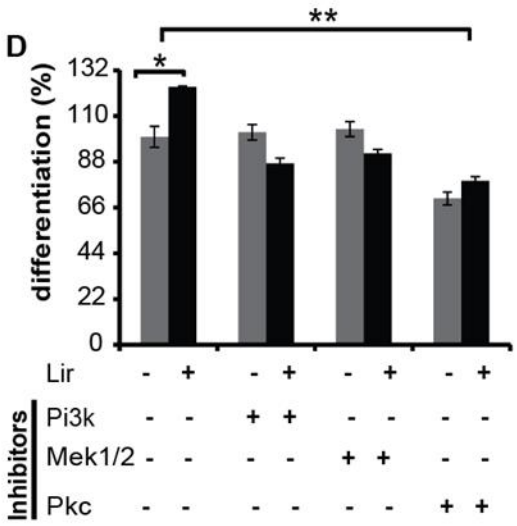
D
differentiation (%)
132
110
88
66
44
22
0
*
**
Lir - + - + - + - +
Inhibitors
Pi3k - - + + - - - -
Mek1/2 - - - - + + - -
Pkc - - - - - - + +

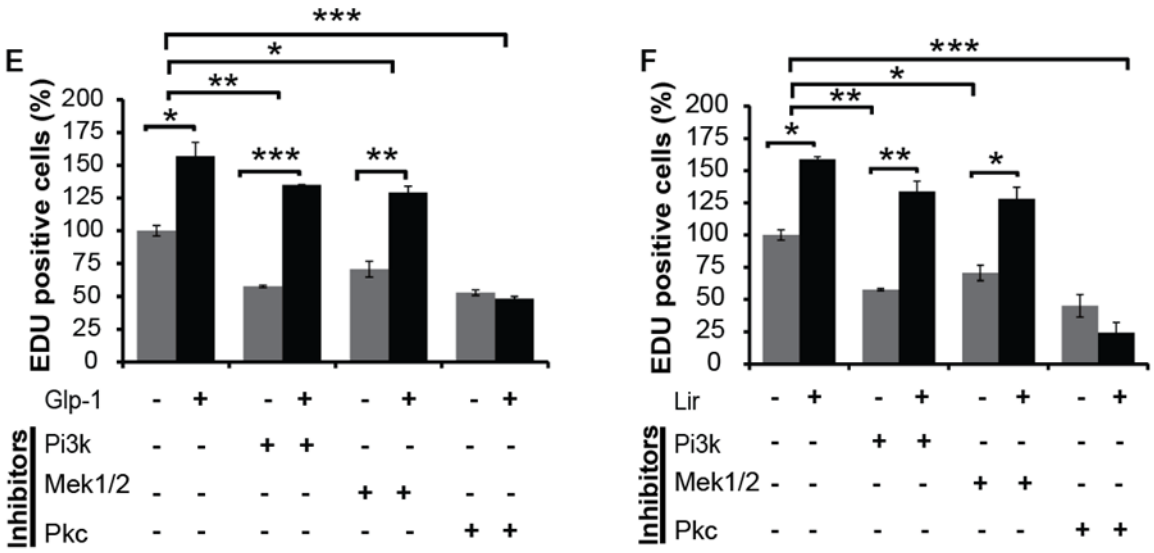

Fig. 4. Signaling pathways of GLP-1/GLP-R regulating pre-adipocyte proliferation and differentiation. **A**) Analysis of p-Erk1/2, Erk1/2, p-Pkc, Pkc, p-Akt, Akt, p-Bad and cleaved Caspase-3 protein expression in 3T3-L1 pre-adipocytes infected with GLP-1R shRNA expressing lentivirus (shRNA2 and shRNA3) or scrambled shRNA (n=4) and treated with 10 nM GLP-1 during induction of cell differentiation. **B**) Analysis of p-Erk1/2, Erk1/2, p-Pkc, Pkc, p-Akt and Akt protein expression in 3T3-L1 pre-adipocytes (n=3) treated with or without 10 nM GLP-1or liraglutide during induction of cell differentiation. Cells were analyzed at indicated time points post induction of differentiation. γ-Tubulin was used as a loading control. **C** and **D**) Analysis of pre-adipocyte differentiation in 3T3L-1 cells induced in serum free medium in the presence or absence of either PI3k inhibitor LY294002 (10 μM), Mek1/2 inhibitor PD-98059 (20 μM) or PKC inhibitor (1nM). In addition cells were treated with 10 nM GLP-1 or liraglutide. Quantitative analysis of adipocyte differentiation was achieved, using high-throughput image analysis (n=4). **E** and **F**) Analysis of pre-adipocyte proliferation in 3T3L-1 cells induced in serum free medium in the presence or absence of either PI3K inhibitor LY294002 (10 μM), MEK1/2 inhibitor PD-98059 (20 μM) or PKC inhibitor (1 nM). In addition cells were treated with 10 nM GLP-1 or liraglutide. Quantitative analysis of adipocyte proliferation was measured by nuclear EDU incorporation (n=4). The graphs represents mean ± SEM (*< 0.05, **p<0.01, ***p<0.001).

Caspase-3 activation plays a pivotal role in the signal transduction pathways of cell apoptosis. Therefore, we further investigated the role of GLP-1R knockdown in caspase-3 regulation. In contrast to decreased pBAD levels during adipogenesis, cleaved caspase-3 levels were significantly increased in GLP-1R knockdown cells in the presence of GLP-1 at 24 hours post- induction (Fig. 4A). The increase in cleaved caspase-3, a key executioner and marker of apoptosis, protein levels at 24 hours fits with the reduction of cell proliferation and induction of apoptosis at 24 hours after induction

of adipogenesis. This indicates that GLP-1 and its receptor are directly involved in the regulation of adipogenesis via activation of proliferation and survival pathways.
To study whether GLP-1 directly regulates the signaling pathways downstream of GLP-1R, 3T3-L1 pre-adipocytes were treated with or without GLP-1 or liraglutide. In accordance with our previous findings, GLP-1 and liraglutide increased Erk1/2, PkcβII, and Akt phosphorylation during differentiation (Fig. 4B) while total Erk1/2, Pkc and Akt protein levels did not change (Fig. 4B). Taken together, this data indicates that GLP-1 and liraglutide activate GLP-1R and mediate cell proliferation and differentiation by regulating the ERK1/2, PKC and AKT signaling pathways.

To determine which signaling pathways are essential for GLP-1/liraglutide mediated adipogenic actions, we used specific pathway inhibitors. Following serum starvation, 3T3-L1 pre-adipocytes were incubated in the presence or absence of GLP-1or liraglutide and treated with different kinase inhibitors or kinases alone for 24 hours in induction medium. The result showed that GLP-1/liraglutide effects were reduced in cells, where PI3K or MEK1/2 was inhibited. Inhibition of PKC led to complete ablation of GLP-1 or liraglutide mediated induction of adipogenesis (Fig. 4, C and D). These data are supported by cell proliferation analysis, as we could show that inhibition of either PI3K or MEK1/2 significantly blunted the proliferative effect of GLP-1 or liraglutide. Similar to the differentiation results we observed a complete ablation of GLP-1 or liraglutide mediated proliferation if PKC was inhibited (Fig. 4, E and F). Taken together these data demonstrate that GLP-1, or its synthetic analogue liraglutide, regulate cell proliferation through different mechanisms involving PI3K, MEK1/2 and PKC signaling to modulate adipogenesis.

2.5. Discussion

It is well known that obesity and the excessive growth of adipose tissue are linked with lymphatic disease (30-32). Furthermore, abnormal subtle lymph leakage from Prox1$^{+/-}$ mice is known to induce adipogenesis (33). However, so far it is unclear which factors contribute to the adipogenic effects of lymph. One prominent member of the gut hormones secreted from the intestinal wall is GLP-1, which is secreted after food intake and which we show here to regulate adipogenesis via its receptor.

We have demonstrated that injection of liraglutide into mice fed a HFD induces in vivo adipocyte differentiation. Liraglutide has been reported to enhance glucose-dependent insulin secretion and inhibit postprandial glucagon secretion (34). Clinical studies have found liraglutide to enhance β-cell function and prevent insulin resistance (35). Other groups have demonstrated the beneficial effects of liraglutide, independent of weight loss, since liraglutide at low concentrations improved cardiac function and increased the survival of the mice without reducing their weight, (36). Interestingly, we observed a stimulation of in vivo adipogenesis, albeit reduced glucose level and reduced weight gain as reported, previously (36). This suggests that even though these mice lose their adipogenic insulin stimulus, liraglutide itself is still able to activate adipogenesis. Moreover, it has been shown that GLP-1 secretion is reduced in obesity (14) and that GLP-1 secretion improves after weight loss (26). Based on our findings it can be speculated that GLP-1 receptor activation acts locally at the tissue level to maintain adipogenesis and mass at an equilibrium set point.

Suppressed adipogenesis, accompanied by an increase in adipocytes size, is linked to increased insulin resistance (7). In contrast, up-regulation of adipocyte differentiation results in increased glucose disposal (37) and high adiponectin secretion (38), both of which are known to enhance insulin sensitivity and prevent excess lipid storage in the liver, heart or muscle (39). Based on our studies we suggest that in response to food intake, GLP-1 increases the differentiation of adipocyte precursors into mature adipocytes, which may further contribute to enhanced whole body insulin sensitivity (3) by decelerating ectopic lipid accumulation and weight gain.

We show that GLP-1 and liraglutide mediate their effect on adipogenesis by regulating cell proliferation and apoptosis of pre-adipocytes. Consistent with these results, others have also reported that GLP-1 and liraglutide regulate islet growth and act as differentiation factors of the endocrine pancreas (40). Our data, however, is inconsistent with previous findings showing that GLP-1 prevents human bone marrow-derived mesenchymal stem cell (hMSCs) differentiation into adipocytes (41). Given the fact that hMSCs are not committed adipocyte precursors, this discrepancy might be due to cell line differences.

In agreement with previous data (29), we found that 3T3-L1 cells express GLP-1R. The expression of Glp-1R correlated with Pparγ, a late phase marker of adipocyte differentiation, suggesting that GLP-1R might be a direct target gene of PPARγ and also play a role in mature adipocyte function. Furthermore, we confirmed the function of GLP-1R as a GPCR by measuring an elevation in cAMP levels after GLP-1 or liraglutide treatment. We also show that knockdown of GLP-1R markedly decreases 3T3-L1 pre-adipocyte differentiation. Consistent with this finding, a previous study indicated that male *Glp-1r*$^{-/-}$mice are protected from HF diet-induced weight gain (42). Others have reported that *Glp-1r*$^{-/-}$ mice exhibit glucose intolerance, due to diminish insulin levels, albeit having normal body weight and feeding behavior (43). This could be due to impaired adipogenesis in *Glp-1r*$^{-/-}$ mice, leading to a decreased glucose uptake and reduced insulin sensitivity. To directly analyze the effect in vivo it would be necessary to knock out GLP-1R in pre-adipocytes, however, unfortunately so far no markers exists that would allow such an experiment.

In line with the suppressed Pparγ expression, we observe here a reduced expression of C/ebpβ and C/ebpδ upon GLP-1R knockdown. These actions of GLP-1 and GLP-1R on early adipogenic regulation events seem to be mediated through cellular proliferation. This is consistent with previous results demonstrating that GLP-1 promotes cellular proliferation of hMSC cells and significantly reduces cell apoptosis (41). These findings, combined with our results, strengthen the notion that GLP-1 or liraglutide regulate adipogenesis via suppression of apoptosis and stimulation of proliferation.

GLP-1, via GLP-1R activates ERK1/2 in β-cells by Gαs/cAMP/PKA and β-arrestin dependent pathways controlling cell proliferation and apoptosis (21). We observe here,

that GLP-1R silencing markedly reduced Erk1/2 phosphorylation, compared to control cells. These findings confirmed the observed decrease in cell proliferation and increase in apoptosis upon GLP-1R knockdown, suggesting that activation of ERK1/2 might be required for the proliferative effect of GLP-1 via its receptor (44).
In addition to ERK signaling, the PKC family plays important roles in various biological functions such as proliferation, differentiation, cell migration and apoptosis (45). Studies have suggested that the PKC pathway is involved in the regulation of adipogenesis (46). In agreement with our findings, increased PkcβII expression has been associated with increased cell proliferation and suppression of apoptosis, which was reported in distal colon crypt cells (47).

Previous studies reported that interference with the IRS-1 and AKT associated signaling pathways represses adipogenesis (48). Activation of these pathways induces Pparγ and C/ebpα expression during 3T3-L1 adipocyte differentiation and inactivation of the AKT signal can induce apoptosis (49, 50). In line with these findings we observed decreased pAkt levels upon GLP-1R knockdown. Activation of the AKT pathway is also known to regulate BAD activity as a survival response (51). Here we show that GLP-1R silencing suppresses BAD phosphorylation, while increasing cleaved-caspase-3 and caspase-3 activity, which could explain the induction of apoptosis. Thus, our data suggests that the reduced adipogenic differentiation of 3T3-L1 cells with a GLP-1R knockdown is partly due to a decrease Erk1/2, PkcβII and Akt phosphorylation.

To further confirm the mechanism behind the regulation of adipogenesis by GLP-1R, we investigated the effects of different kinase inhibitors. Consistent with our data, it has been shown that inhibiting the PKC pathway with pharmacological inhibitors, such as Ro318220 and Go6976, inhibits adipocyte differentiation (52). At low doses inhibition of PKC signaling significantly decreased both GLP-1 and liraglutide mediated induction of both cell proliferation and differentiation. These results further confirm that the PKC pathway is involved in mediating liraglutide and GLP-1 signals that regulate pre-adipocyte proliferation, apoptosis and differentiation.

In conclusion, our data show the cross-talk between the intestinal wall and adipose tissue through GLP-1. GLP-1 directly activates adipogenesis through GLP-1R. The underlying signaling pathway involves activation of PKC, ERK and AKT, which leads to altered proliferation, apoptosis and differentiation. Our findings suggest that GLP-1 and its receptor might contribute to nutrient induced adipocyte development and thereby might influence whole body energy metabolism.

2.6. References

1. Bays, H. E., Gonzalez-Campoy, J. M., Bray, G. A., Kitabchi, A. E., Bergman, D. A., Schorr, A. B., Rodbard, H. W., and Henry, R. R. (2008) *Expert Rev Cardiovasc Ther* **6**, 343-368
2. Hausman, D. B., DiGirolamo, M., Bartness, T. J., Hausman, G. J., and Martin, R. J. (2001) *Obes Rev* **2**, 239-254
3. Kahn, B. B., and Flier, J. S. (2000) *J Clin Invest* **106**, 473-481
4. Kaplan, N. M. (1998) *J Hypertens Suppl* **16**, S35-37
5. Jo, J., Gavrilova, O., Pack, S., Jou, W., Mullen, S., Sumner, A. E., Cushman, S. W., and Periwal, V. (2009) *PLoS Comput Biol* **5**, e1000324
6. Kadowaki, T., and Yamauchi, T. (2005) *Endocr Rev* **26**, 439-451
7. Meissburger, B., Stachorski, L., Roder, E., Rudofsky, G., and Wolfrum, C. (2011) *Diabetologia* **54**, 1468-1479
8. Wolfrum, C., Shih, D. Q., Kuwajima, S., Norris, A. W., Kahn, C. R., and Stoffel, M. (2003) *J Clin Invest* **112**, 345-356
9. Hoffstedt, J., Arner, E., Wahrenberg, H., Andersson, D. P., Qvisth, V., Lofgren, P., Ryden, M., Thorne, A., Wiren, M., Palmer, M., Thorell, A., Toft, E., and Arner, P. (2010) *Diabetologia* **53**, 2496-2503
10. Cornelius, P., MacDougald, O. A., and Lane, M. D. (1994) *Annu Rev Nutr* **14**, 99-129
11. Hwang, C. S., Loftus, T. M., Mandrup, S., and Lane, M. D. (1997) *Annu Rev Cell Dev Biol* **13**, 231-259
12. Korner, A., Bluher, S., Kapellen, T., Garten, A., Klammt, J., Kratzsch, J., and Kiess, W. (2005) *Hormones (Athens)* **4**, 189-199
13. Takeda, S., Elefteriou, F., Levasseur, R., Liu, X., Zhao, L., Parker, K. L., Armstrong, D., Ducy, P., and Karsenty, G. (2002) *Cell* **111**, 305-317
14. Holst, J. J. (2007) *Physiol Rev* **87**, 1409-1439
15. Lovshin, J. A., and Drucker, D. J. (2009) *Nat Rev Endocrinol* **5**, 262-269
16. Hayes, M. R., Kanoski, S. E., Alhadeff, A. L., and Grill, H. J. (2011) *Obesity (Silver Spring)* **19**, 1342-1349
17. Drucker, D. J. (2006) *Cell Metab* **3**, 153-165
18. Huang, Y., Wilkinson, G. F., and Willars, G. B. (2010) *Br J Pharmacol* **159**, 237-251
19. Li, Y., Tweedie, D., Mattson, M. P., Holloway, H. W., and Greig, N. H. (2010) *J Neurochem* **113**, 1621-1631
20. Montrose-Rafizadeh, C., Yang, H., Wang, Y., Roth, J., Montrose, M. H., and Adams, L. G. (1997) *J Cell Physiol* **172**, 275-283
21. Quoyer, J., Longuet, C., Broca, C., Linck, N., Costes, S., Varin, E., Bockaert, J., Bertrand, G., and Dalle, S. (2010) *J Biol Chem* **285**, 1989-2002
22. Zander, M., Madsbad, S., Madsen, J. L., and Holst, J. J. (2002) *Lancet* **359**, 824-830
23. Drucker, D. J., Dritselis, A., and Kirkpatrick, P. (2010) *Nat Rev Drug Discov* **9**, 267-268
24. Knudsen, L. B., Nielsen, P. F., Huusfeldt, P. O., Johansen, N. L., Madsen, K., Pedersen, F. Z., Thogersen, H., Wilken, M., and Agerso, H. (2000) *J Med Chem* **43**, 1664-1669
25. Rask, E., Olsson, T., Soderberg, S., Johnson, O., Seckl, J., Holst, J. J., and Ahren, B. (2001) *Diabetes Care* **24**, 1640-1645

26. Verdich, C., Toubro, S., Buemann, B., Lysgard Madsen, J., Juul Holst, J., and Astrup, A. (2001) *Int J Obes Relat Metab Disord* **25**, 1206-1214
27. Buteau, J. (2008) *Diabetes Metab* **34 Suppl 2**, S73-77
28. Meissburger, B., Ukropec, J., Roeder, E., Beaton, N., Geiger, M., Teupser, D., Civan, B., Langhans, W., Nawroth, P. P., Gasperikova, D., Rudofsky, G., and Wolfrum, C. (2011) *EMBO Mol Med*, Epub online
29. Egan, J. M., Montrose-Rafizadeh, C., Wang, Y., Bernier, M., and Roth, J. (1994) *Endocrinology* **135**, 2070-2075
30. Lo, Y. F., Cheung, Y. C., Hsueh, S., and Ho, K. C. (2009) *Chang Gung Med J* **32**, 51-58
31. Tong, J., Tschop, M. H., Aulinger, B. A., Davis, H. W., Yang, Q., Liu, J., Gaylinn, B. D., Thorner, M. O., D'Alessio, D., and Tso, P. (2010) *Am J Physiol Gastrointest Liver Physiol* **298**, G474-480
32. von der Weid, P. Y., and Rainey, K. J. (2010) *Aliment Pharmacol Ther* **32**, 697-711
33. Harvey, N. L., Srinivasan, R. S., Dillard, M. E., Johnson, N. C., Witte, M. H., Boyd, K., Sleeman, M. W., and Oliver, G. (2005) *Nat Genet* **37**, 1072-1081
34. Bregenholt, S., Moldrup, A., Blume, N., Karlsen, A. E., Nissen Friedrichsen, B., Tornhave, D., Knudsen, L. B., and Petersen, J. S. (2005) *Biochem Biophys Res Commun* **330**, 577-584
35. Mari, A., Degn, K., Brock, B., Rungby, J., Ferrannini, E., and Schmitz, O. (2007) *Diabetes Care* **30**, 2032-2033
36. Noyan-Ashraf, M. H., Momen, M. A., Ban, K., Sadi, A. M., Zhou, Y. Q., Riazi, A. M., Baggio, L. L., Henkelman, R. M., Husain, M., and Drucker, D. J. (2009) *Diabetes* **58**, 975-983
37. Dubuisson, O., Dhurandhar, E. J., Krishnapuram, R., Kirk-Ballard, H., Gupta, A. K., Hegde, V., Floyd, E., Gimble, J. M., and Dhurandhar, N. V. (2011) *Endocrinology*
38. Lee, N. K., and Karsenty, G. (2008) *Trends Endocrinol Metab* **19**, 161-166
39. Berg, A. H., and Scherer, P. E. (2005) *Circ Res* **96**, 939-949
40. Egan, J. M., Bulotta, A., Hui, H., and Perfetti, R. (2003) *Diabetes Metab Res Rev* **19**, 115-123
41. Sanz, C., Vazquez, P., Blazquez, C., Barrio, P. A., Alvarez Mdel, M., and Blazquez, E. (2010) *Am J Physiol Endocrinol Metab* **298**, E634-643
42. Hansotia, T., Maida, A., Flock, G., Yamada, Y., Tsukiyama, K., Seino, Y., and Drucker, D. J. (2007) *J Clin Invest* **117**, 143-152
43. Thorens, B. (1992) *Proc Natl Acad Sci U S A* **89**, 8641-8645
44. Bost, F., Aouadi, M., Caron, L., and Binetruy, B. (2005) *Biochimie* **87**, 51-56
45. Clemens, M. J., Trayner, I., and Menaya, J. (1992) *J Cell Sci* **103 (Pt 4)**, 881-887
46. Lacasa, D., Agli, B., and Giudicelli, Y. (1995) *Biochem Biophys Res Commun* **217**, 123-130
47. Davidson, L. A., Brown, R. E., Chang, W. C., Morris, J. S., Wang, N., Carroll, R. J., Turner, N. D., Lupton, J. R., and Chapkin, R. S. (2000) *Carcinogenesis* **21**, 1513-1519
48. Baudry, A., Yang, Z. Z., and Hemmings, B. A. (2006) *J Cell Sci* **119**, 889-897
49. Kim, J. E., and Chen, J. (2004) *Diabetes* **53**, 2748-2756
50. Kortum, R. L., Costanzo, D. L., Haferbier, J., Schreiner, S. J., Razidlo, G. L., Wu, M. H., Volle, D. J., Mori, T., Sakaue, H., Chaika, N. V., Chaika, O. V., and Lewis, R. E. (2005) *Mol Cell Biol* **25**, 7592-7604

51. Friedrichsen, B. N., Neubauer, N., Lee, Y. C., Gram, V. K., Blume, N., Petersen, J. S., Nielsen, J. H., and Moldrup, A. (2006) *J Endocrinol* **188**, 481-492
52. Zhou, Y., Wang, D., Li, F., Shi, J., and Song, J. (2006) *Int J Biochem Cell Biol* **38**, 2151-2163

Chapter 3

3. CNS-specific GIP receptor ablation protects from diet induced obesity and insulin resistance

Tenagne Delessa Challa[1], Leon Gabriel Straub[1], Peleg-Raibstein Daria[1], Myrtha Arnold[1], Eugenia McAllister[1], Wolfgang Langhans[1] and Christian Wolfrum[1]

[1]Swiss Federal Institute of Technology, ETH Zürich, Institute of Food Nutrition and Health, Schorenstrasse 16, 8603 Schwerzenbach, Switzerland

3.1. Abstract

The glucose-dependent insulinotropic polypeptide receptor (GIPr) is involved in the regulation of diet-induced obesity and insulin resistance, but which organs mediate these effects remains unknown. To investigate the role of GIPr on energy metabolism contribution to central *versus* peripheral interactions, we generated humanized conditional knockout GIPr (hGIPr) mice with targeted specific deletion of hGIPr in the central nervous system. Here we demonstrate that selective deletion of hGIPr in the nervous system protects mice from high fat diet-induced obesity, insulin resistance and hepatic steatosis. The failure to increase body weight is mediated, in part, by increased physical activity and suppressed food intake leading to decreased body fat mass storage and reduced hepatic lipid accumulation. The improvement of insulin sensitivity is correlated with an up-regulation of brain-derived neurotrophic factor (BDNF), adiponectin and glucagon-like peptide-1 (GLP-1) secretion and down-regulation of insulin-like growth factor 1 (IGF-1) and insulin release. The changes in these signaling pathways might be involved in improved glucose tolerance and the protection from the development of insulin resistance. Taken together these findings implicate that the CNS-GIPr axis could represent an alternative pharmacological target to regulate excessive adipose accumulation by decreasing energy intake.

Key words: GIPr, CNS, obesity, insulin resistance

3.2. Introduction

Obesity has become a public health problem and understanding the biology of fat may translate into potential therapeutic intervention for the epidemic of obesity and type II diabetes (T2D). Adipose tissue is recognized as an organ that not only stores energy, but also acts as a multifunctional endocrine tissue (1). Adipocytes produce hormones (adipokines) that regulate systemic processes, including food intake and nutrient metabolism, insulin sensitivity and inflammation (2). Adipocytes also express numerous receptors that allow it to respond to afferent signals, such as hormones and signals from the central nervous system (CNS) (4), intestinal wall (5), skeletal muscle and liver (6) to regulate energy metabolism. Therefore, adipocytes are intimately involved in metabolic homeostasis by secreting and responding to hormones and cytokines that regulate energy intake and expenditure (3).

Several years ago glucose-lowering elements from gut extracts were purified and subsequently named as incretin (7). Incretins are the hormonal components that stimulated insulin secretion in a glucose-dependent manner (8,9). They are released after ingestion of glucose or other nutrients to stimulate insulin secretion from pancreatic β-cells (8). Thus, incretin hormones play a major role in the signal transduction from the gut to pancreatic β-cells to regulate energy metabolism. It has been estimated that incretins account for 50–65% of the total insulin response, depending on the oral nutrient load (8,9). The two gastrointestinal peptide hormones identified to act as physiological incretins, are gastric inhibitory polypeptide (GIP) and glucagon-like peptide-1 (GLP-1) (10). Gastric inhibitory polypeptide (GIP) was originally found to inhibit gastric acid secretion and gastrointestinal motility in dogs (11). A subsequent study discovered that GIP stimulates glucose-dependent insulin secretion (12) and was then renamed as glucose-dependent insulinotropic polypeptide (13).

GIP, a 42 amino acid hormone, is produced by enteroendocrine K-cells of the upper small intestine (duodenum and jejunum) (14). The GIP sequence is highly conserved among species with human, mouse, rat, porcine, and bovine and which exhibit more than 90% amino acid sequence homology (15). In addition to its insulinotropic effect, GIP also increases secretion of GLP-1 from intestine L-cells; thus glucose stimulates

GLP-1 release via GIP (10). GIP exerts its effects by binding to its specific receptor, named the GIP receptor (GIPR) (16). Mouse and human GIP receptor share about 79.5 % sequence identity (16). A previous study has suggested that alternative mRNA splicing results in the production of GIP receptor variants of differing lengths in human, rat and mouse pancreatic islets, adipose tissue and intestine (17). The GIP receptor is expressed in multiple organs and tissues: including the pancreas, adipose tissue, stomach, small intestine, thymus, brain, adrenal cortex, pituitary, lung, heart, kidney, thyroid, bone and several regions in the CNS (18-21).

GIPR belongs to the G-protein coupled receptor family. Activation of GIPR by GIP activates adenylate cyclase, MAPK and increase levels of intracellular cAMP in pancreatic β cells, thereby enhancing glucose-dependent insulin secretion (10). Furthermore, activation of GIP receptor stimulates growth, proliferation, differentiation and survival of pancreatic β-cells (18,19). In addition to, its insulinotropic actions in maintaining glucose homeostasis (10), GIP is also involved in fat metabolism in adipocytes to enhance lipid storage, stimulate lipoprotein lipase activity and modulate fatty acid synthesis (7). Interestingly a high fat diet (HFD) increases K cell hyperplasia then enhances GIP gene expression and increase circulating GIP concentration (19). Increased secretion of GIP in obese and Type II diabetes (T2D) humans and animal model has also been reported (19). Surprisingly the insulinotropic effect of GIP is selectively impaired despite increased GIP secretion in T2D, while the effect of GLP-1 is preserved (10). These findings suggest that GIP is more involved in the pathogenesis of T2D, although GLP-1 is used T2D treatment.

Similarly, wild type mice fed a HFD, develop insulin resistance and GIP hyper-secretion (22). On the other hand, normal and obese/diabetic *ob/ob* global *Gipr* knockout mice are protected from HFD-induced obesity and insulin resistance (19,22). However, the mechanism that accounts for the effect of GIP receptor deficiency as a means to control body weight gain is unclear. Since tissue-specific GIP receptor knockout mice are not available it remains unclear which organ plays a major role in the diet-induced regulation of body weight by GIPR.

The key peripheral metabolic organ, the gastrointestinal tract, pancreas, liver, muscle, and adipose tissue communicate with the brain to maintain energy balance (23). The

hypothalamus, particularly the arcuate nucleus (ARC), is a major site for integrating nutritionally relevant information originating from all peripheral organs and mediated through circulating hormones and metabolites and/or neural pathways mainly from the brainstem (23). The primary centers in the brain involved in the control of appetite are the hypothalamic-pituitary axis and the brain stem. Interestingly, the GIP peptide was reported to be expressed in the brainstem and synthetized in a subset of neurons in the brain (20,21). Therefore, the brain represents a possible site of GIP receptor function because the hypothalamus and pituitary gland are known to regulate energy metabolism, including feeding behavior, physical activity, and energy expenditure (23). Moreover, recently the presence of GIP ligand along with the expression of its receptor in several parts of the brain including cortex, hippocampus and hypothalamus has been reported (20,21). Although, GIP and GIPR are detected in the brain, no study to date has looked at the potential role that GIP and its receptor could play in the CNS to regulate energy metabolism. The purpose of this study was therefore to investigate the role of GIP receptor in the brain on the regulation of energy metabolism. Our study approach was to examine the effect of selective deletion of GIPR in the mouse nervous system.

3.3. Material and methods

Animals

All experimental protocols were approved by the Canton of Zurich Veterinary Office. Mice were single- or group-housed in a pathogen-free animal facility on 12 h dark/light cycle in a temperature controlled room, with free access to food and water. The mice were placed on either 60% high fat diets or chow diet food based on the experimental design.

Generating CNS-hGIP receptor knockout mice

Human gastric inhibitory polypeptide receptor (hGIPr) floxed mice were obtained from Boehringer Ingelheim. The hGIPr-floxed mice were generated by replacing mouse *GIPr* from exon 3 to 14 with human *GIPr*. The mice were maintained on a C57BL/6 (Charles River) background for more than six generations. They were further backcrossed in our laboratory with C57BL/6 and crossbred with Nestin-cre transgenic mice for this study.

To generate central nervous system specific human GIP receptor knockout ($hGIPr^{d/d}$) mice, nestin-cre transgenic (Nes-Cre) mice were first crossed with hGIPr-floxed ($hGIPr^{loxP/loxP}$) ($hGIPr^{P/P}$) mice to generate intermediate F1 ($hGIPr^{p/+}$, $NesCre^{+}$) mice. The F1 mice were then backcrossed with hGIPr-floxed ($hGIPr^{P/P}$) mice to generate homozygous humanized GIPr ($hGIPr^{P/P}$, NesCre-), hGIPr knockout ($hGIPr^{d/d}$, $NesCre^{+}$), heterozygous humanized hGIPr ($hGIPr^{P/+}$, $NesCre^{+}$) and heterozygous humanized hGIPr ($hGIPr^{P/+}$, $NesCre^{-}$) mice. To derive the desired wild type control mice: WT, $NesCre^{+}$ and WT, $NesCre^{-}$ mice, the F2 generation $hGIPr^{P/+}$, $NesCre^{+}$ and $hGIPr^{p/+,}$ $NesCre^{-}$ mice were crossed. The genotype of each mouse was determined by PCR with the respective primers (Table 1, Appendix 3) and genomic DNA was extracted from tail tips. All the PCR master mix (reaction buffers) was obtained from Invitrogen.

High fat diet feeding study

Eight week old male mice were fed a HFD containing 60% kilocalories from fat. Individual mouse body weights and fasted blood glucose levels were monitored every week over a period of 12 weeks during HFD feeding study. Body composition (fat and lean mass) was determined by Aloka LaTheta Computed Tomography (CT) scanner using LaTheta software (Zinsser Analytic, UK). For metabolic measurements mice were

adapted to individual metabolic chambers under controlled temperature and light with free access to food and water for at least 3 days. Oxygen consumption, carbon dioxide production, food intake, water consumption, locomotor activity and energy expenditure were performed using metabolic cages (TSE Phenomaster, Systems). The data were determined every 5 min for 5 consecutive days. Recorded data was normalized for body weight. For each animal, the accumulated metabolic activities in each light and dark cycle in 3 days were calculated separately and averaged. The ingested food intake each hour in the dark and light cycle was compared.

At the end of the experiment mice were fasted for 6 h and anesthetized and blood was collected into tubes with EDTA. Plasma was collected after centrifugation and stored at -80°C. Different brain parts, fat tissue and liver were collected for RNA and proteins extraction and stored at -80°C. Fat tissue and liver samples were also fixed in 4% paraformaldehyde for histological analysis.

Western blot analysis

After overnight fasting, 20 week old male hGIPr$^{P/P}$, hGIPr$^{d/d}$ and their wild type (WT, NesCre^{+} and WT, NesCre^{-}) littermates mice were sacrificed and the hypothalamus, hippocampus, ventral tegmental area and cortex were dissected on ice followed by snap-freezing in liquid nitrogen. The frozen tissues were stored at -80°C until use. For total protein extraction the tissue were homogenized by douncing in cold whole cell extraction buffer containing 150 mM NaCl, 50 mM Tris pH 7.4, 5 mM EDTA, 0.1% SDS, 2% (v/v) protease inhibitors (Roche) and 1% (v/v)phosphatase inhibitor cocktail (Thermo Scientific). The homogenate was centrifuged at 16000 rpm for 10 min at 4°C. Forty micrograms of total protein from each sample was loaded to 12% SDS-PAGE gel for electrophoresis. Afterwards, the proteins were transferred onto a nitrocellulose membrane (Perkin Elmer) and blocked in 5% milk then incubated with anti-hGLPr (Abgent), anti-POMC (Novus Biologicals) primary antibodies. The signal was developed by image Quant LAS4000 mini (GE health care). Loading controls were measured with mouse anti-γ-Tubulin (Sigma-Aldrich).

RNA isolation and quantitative real-time RT-PCR

Total RNA was extracted using TRIzol reagent according to the manufacturer's protocol. One µg of total RNA was converted into first-strand cDNA using high capacity cDNA reverse transcription kit (Invitrogen). Real-time PCR quantification was performed using a fast SYBR Green master mix and gene specific primer sets (Table 2, Appendix 3).

Biochemical analysis

Blood sample was taken from 6 h fasted tail vein of conscious mice. Plasma was collected after centrifugation and stored at -80°C. Plasma insulin levels were determined with the ultra-sensitive Mouse Insulin ELISA kit (Crystal Chem). Plasma triglyceride was measured with the Trig/GB Kit against the C.f.a.s. standard (Roche) and total cholesterol levels and free fatty acids were measured with the NEAFA-HR kit (Wako). Total GIP, leptin, GLP-1 and adiponectin were measured using ELISA kits from (Meso scale discovery). IGF-1 levels were determined using an ELISA kit from R and D systems. All analyses were carried out according to instructions supplied by the manufacturers.

Glucose and insulin tolerance tests

Mice fed a HFD for 8-10 weeks were fasted for 6 h and a 1.5 g/kg body weight of glucose was injected intraperitoneally (ip) for glucose tolerance test (IPGTT). Oral glucose tolerance test (OGTT) was assessed with 1.5 g/kg oral glucose challenge through a gavage tube into 6 h fasted mice. Insulin tolerance test (ITT) was assessed using 0.75 U/kg body weight ip insulin injections into 6 h fasted animals. For IPGTT, OGTT, and ITT fasted blood glucose levels was measured before glucose or insulin challenge at baseline (0), and after glucose or insulin administration at 15, 30, 60, 90 and 120 min with a glucometer.

Histological analysis of tissue sections

Tissue for histology was fixed in 4% paraformaldehyde embedded in paraffin and cut into 5µm sections using a microtome, mounted on slides, and stained with hematoxylin and eosin. Paraformaldehyde-fixed liver tissues were stained with Oil Red O solution

for 10 min at room temperature followed by a light counter stain with hematoxylin. Stained slides were viewed under a microscope.

Statistical analysis

Differences between groups were examined for statistical significance using a two tailed Student's t test and declared significant if $p \leq 0.05$.

3.4. Result

CNS-specific human GIPr knockout mice generation

GIP receptor expressed in many tissues, including in the brain. The effect of GIPR on energy homeostasis contribution to central *versus* peripheral interactions has however not been studied well. To investigate the role of GIPR in the central nervous system we generated humanized conditional knockout (hGIPr$^{loxP/loxP}$) or hGIPr$^{P/P}$ mice. The humanized mice were generated by replacing exons 3 to 14 of mice GIPR by human under chicken-β-actin promoter. With targeted deletion of hGIPr in the CNS, we created compound mutant mice (hGIPr$^{P/P}$, NesCre+) or hGIPr$^{d/d}$ (hGIPr$^{deleted/deleted}$) mice as described in the material and methods section. Genotype analysis of hGIPr$^{P/P}$ control mice and hGIPr$^{d/d}$ or hGIPr knockout mice showed that the hGIPrLoxP allele was efficiently deleted in the nervous system of hGIPr$^{d/d}$ mice (data not shown). Analysis of gene expression demonstrated that hGIPr was detected in brown (BAT), subcutaneous (SAT) and visceral (VAT) adipose tissue, skeletal muscle, hippocampus (HIP), ventral tegmental area (VTA), hypothalamus (HYP) and cortex (CX) of the control mice or hGIPr$^{P/P}$ (Fig. 1A).

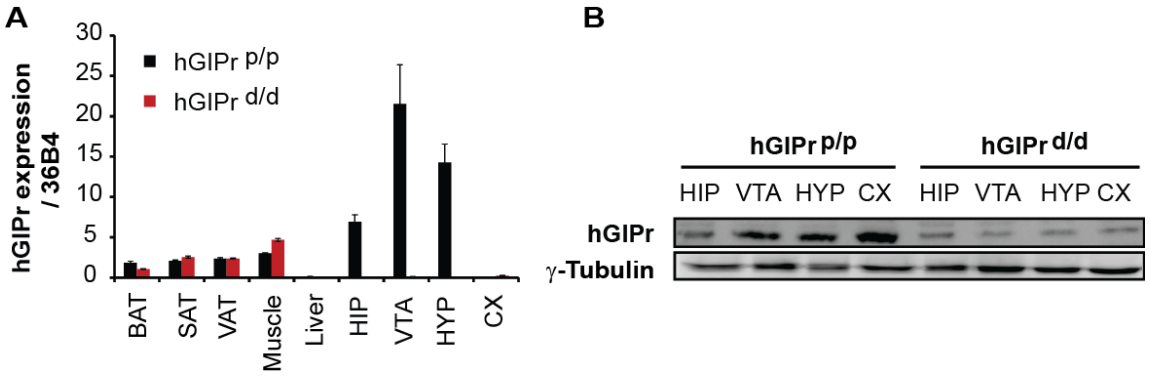

Figure 1. **Generation of CNS specific human GIP receptor knockout mice. A**) The relative expression of inserted human GIPr in the humanized mice strains in selected tissues (n = 4). **B**) Expression of hGIPr at the protein level was confirmed by Western blot analysis (n = 4). γ-tubulin was used as a loading control. Whole cell extracts were prepared from brown (BAT), subcutaneous (SAT) and visceral (VAT) adipose tissue, liver, skeletal muscle, hippocampus (HIP), ventral tegmental area (VTA), hypothalamus (HYP) and cortex (CX). hGIPr$^{P/P}$ = hGIPr-floxed (hGIPr$^{loxP/loxP}$) or homozygous humanized hGIPr (hGIPr$^{P/P}$, NesCre-) as control mice. hGIPr$^{d/d}$ = hGIPr knockout mice (hGIPr$^{d/d}$, NesCre^{+}) (hGIPr$^{d/d}$ = hGIPr $^{deleted/deleted}$) or homozygous humanized hGIPr (hGIPr$^{P/P}$,NesCre+), n = 4 to 5 per group.

Surprisingly the expression of hGIPr mRNA was highly up regulated in HIP, VTA and HYP but not detected CX. However, the expression of hGIPr was drastically decreased in the brain region (HIP, VTA, HYP and CX) and was detected in BAT, SAT, VAT and skeletal muscle of hGIPr$^{d/d}$ mice (Fig. 1A). The human GIPr was not detected in the liver of both hGIPr knockout and littermate control mice. The absence of hGIPr protein in hGIPr$^{d/d}$ mice was confirmed by Western blot analysis in HIP, VTA, HYP and CX (Fig. 1B).

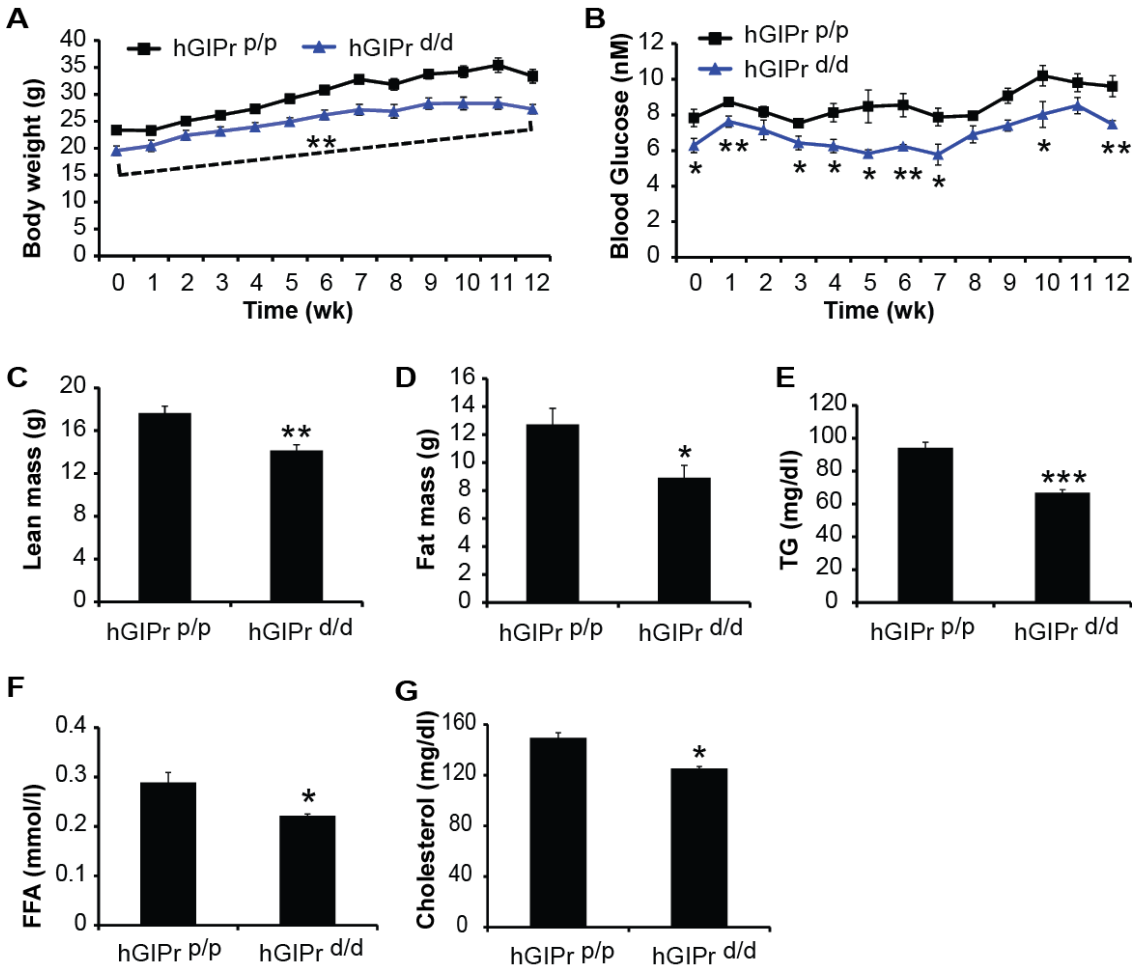

Figure 2. **hGIPr deletion in the CNS-prevents HFD-induced obesity. A** and **B**) Male mice were fed a HFD from age of 8 for 12 weeks, body weight and fasting blood glucose levels were monitored every week. **C** and **D**) Lean and fat body mass were measured by Aloka LaTheta laboratory-CT analyzed with LaTheta software after 11 weeks of HFD feeding. **E-G**) Plasma triglycerides (TG), free fatty acids (FFA) and cholesterol levels of 6 weeks HFD fed mice were analyzed. All values are shown as mean ± SEM (*<0.05, **p<0.01, ***p<0.001), n = 5 to 6 per group.

The data showed markedly reduced hGIPr protein in all regions of the CNS of hGIPr knockout mice that were examined in HIP, VTA, HYP and CX compared with the control $hGIPr^{P/P}$ littermate mice. These data indicate that $hGIPr^{d/d}$ mice exhibit a tissue-specific deletion in expression of hGIPr. Therefore, $hGIPr^{d/d}$ represents a model for the analysis of central nervous system specific hGIPr knockout mice.

CNS-hGIPr deletion protects against HFD-induced obesity

To investigate whether CNS GIPr is required for HFD-induced weight gain, $hGIPr^{P/P}$ and CNS-specific hGIPr deficient mice were fed a HFD for 12 weeks from age of 8 weeks old. The observed data showed that CNS specific hGIPr deficiency markedly reduced weight gain caused by a HFD compared with $hGIPr^{P/P}$ control mice (Fig. 2 A). Interestingly, the $hGIPr^{d/d}$ mice already showed decreased body weight compared with $hGIPr^{P/P}$ before starting the HFD feeding at age of 8 weeks as shown in Figure 2A. Fasting blood glucose level was correspondingly decreased during HFD-feeding study in $hGIPr^{d/d}$ mice compared with the control mice (Fig. 2B). Consistent with decreased body weight gain at age of 8 weeks before HFD started, the blood glucose levels were also significantly decreased in $hGIPr^{d/d}$ mice.

Measurement of lean and fat mass by Computed Tomography (CT) demonstrated the reduction of fat accumulation and lean mass in $hGIPr^{d/d}$ compared with $hGIPr^{P/P}$ mice (Fig. 2, C and D). Lean mass was unchanged after correction for body weight, whereas body fat mas decreased in $hGIPr^{d/d}$ after being normalized for body weight compared with the control mice (data not shown here). These data suggest that the defect in HFD induced weight gain observed in $hGIPr^{d/d}$ mice was due to a reduction in fat mass with modest contribution of lean mass. In line with these findings, plasma triglycerides (TG), free fatty acids (FFA) and cholesterol levels were decreased in hGIPr knockout mice compared with the control mice (Fig. 2, F-H).

Taken together, the resistance to weight gain in HFD-fed CNS-specific hGIPr knockout mice indicates GIP receptor in the CNS is required for the regulation of body weight gain induced by HFD feeding.

Human GIPr deficiency in the CNS increases insulin sensitivity

To determine the effect of CNS-hGIPr on glucose metabolism, we assessed IPGT OGTT and ITT of HFD fed mice. The fasting blood glucose levels were significantly decreased in hGIPr$^{d/d}$ compared with hGIPr$^{P/P}$ mice as clearly shown at zero time point or base line (Fig. 3, A-C). In IPGTT, hGIPr$^{d/d}$ mice had lower blood glucose levels at 15 min after i.p. glucose challenge (Fig. 3A). This difference was more pronounced in OGTT as blood glucose levels significantly decreased at 15 and 30 min after oral glucose load in hGIPr$^{d/ d}$ mice (Fig. 3B). It is well known that HFD-fed induced obesity contributes to the development of insulin resistance.

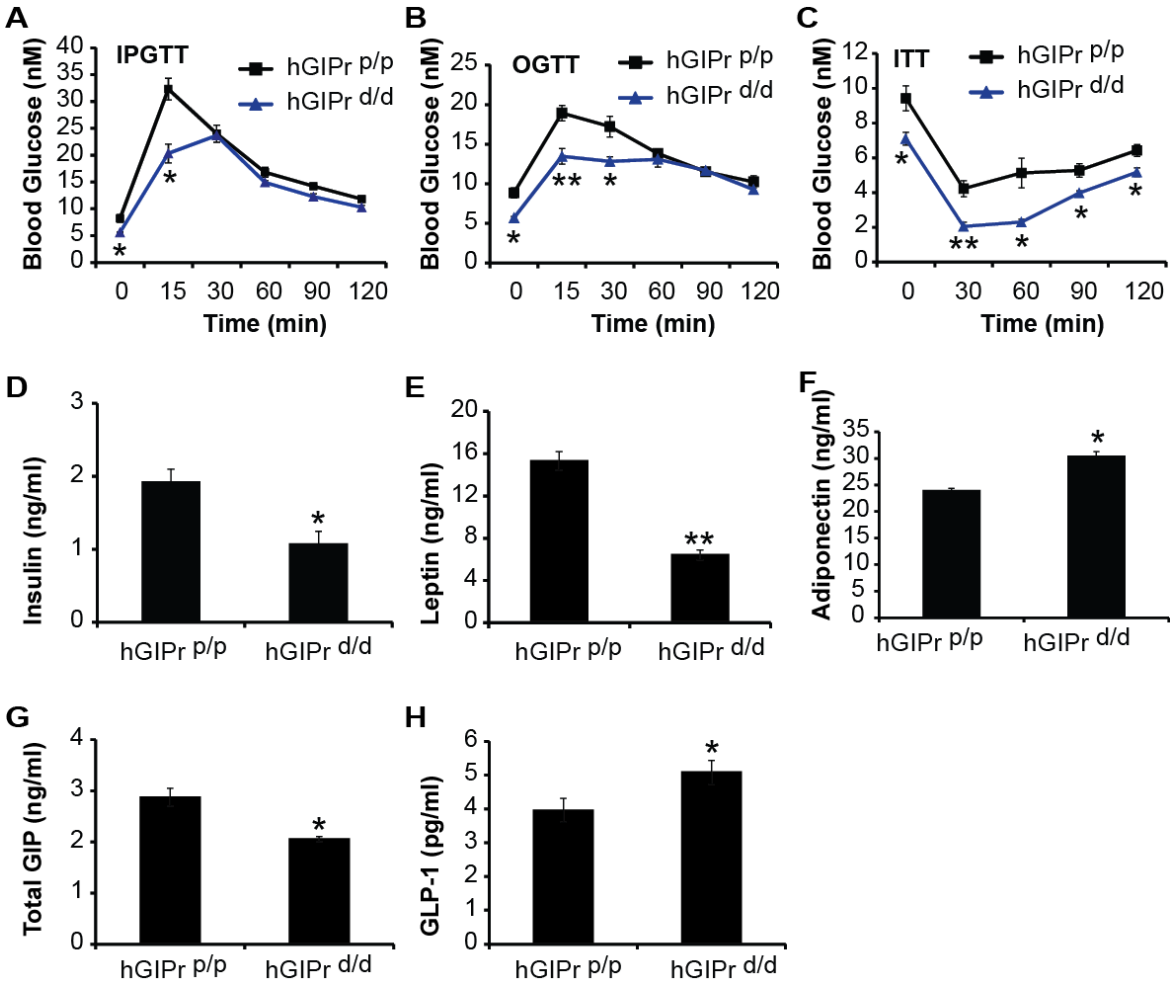

Figure 3. **Human GIPr deficiency in the CNS protects mice against the metabolic effects of a HFD feeding. A**) Mice fed a HFD for 8 to 10 weeks were fasted for 6 h and challenged with 1.5 g/kg body weight of intraperitoneal (i.p) glucose for glucose tolerant test (IPGTT). **B**) The same amount of glucose was given for oral glucose tolerance test (OGTT) in mice fasted for 6 h. **C**) Insulin tolerance test (ITT) was measured by i.p injection of insulin (0.75 U/kg body weight) in mice fasted for 6 h . Glucose and insulin tolerant test was performed by measuring blood glucose levels for

the indicated time points. **D-H**) Fasting plasma levels of insulin, leptin, adiponectin, total GIP and GLP-1 were assessed by ELISA. All values are shown as mean ± SEM (*<0.05, **p<0.01, ***p<0.001), n = 5 to 6 per group.

In agreement with this, hGIPr$^{P/P}$ control mice which were fed a HFD had higher base line of blood glucose levels and rapid disappearance of the effect of insulin in case of ITT, while hGIPr$^{d/d}$ mice remained more responsive to insulin (Fig. 3C). In line with this findings, fasting insulin levels were decreased in hGIPr$^{d/d}$ while elevated in control mice in agreement with a HFD-induced insulin resistance (Fig. 3D).

Similarly, the HFD-induced increase in plasma concentration of leptin was markedly reduced in HFD-fed hGIPr$^{d/d}$, while hGIPr$^{P/P}$ control mice had a 2-fold higher leptin levels (Fig. 3E). On the other hand, adiponectin levels were higher in HFD-fed hGIPr$^{d/d}$ compared with hGIPr$^{P/P}$ control mice, which confirms the insulin sensitivity of hGIPr knockout mice (Fig. 3F). To determine the cause of improved insulin sensitivity in HFD-fed hGIPr$^{d/d}$ mice we also measured the plasma total GIP and GLP-1(x-amide). In line with the increased fat mass, hGIPr$^{P/P}$ control mice had increased plasma total GIP, while GLP-1 levels decreased compared with hGIPr$^{d/d}$ mice (Fig. 3, G and H). These data together indicated that inhibition of the GIP signal in the CNS prevents diet induced obesity and insulin resistance.

Human GIPr deficient mice in the CNS protected from liver steatosis

Histological analysis of VAT and SAT showed larger adipocyte size in HFD fed hGIPr$^{P/P}$ control mice compared with hGIPr knockout mice (Fig. 4A), consistent with the increased body weight observed and suggesting that hGIPr$^{P/P}$ control mice developed hypertrophic fat storage. SAT of hGIPr knockout mice were much smaller than that of control mice. In case of BAT, the numbers of adipocytes was high and the size was also larger in hGIPr$^{P/P}$ mice compared with hGIPr knockout mice (Fig. 4A). Liver from hGIPr$^{P/P}$ mice showed markedly increased lipid accumulation following HFD feeding; however, hGIPr$^{d/d}$ mice exhibited no hepatic lipid accumulation after 12 weeks on HFD (Fig. 4, B and C). Slight differences in body length were observed between control and hGIPr deficient animals (Fig. 4, D and E).

The observed data demonstrate that the CNS-hGIPr knockout mice were protected from hypertrophic obesity and liver steatosis.

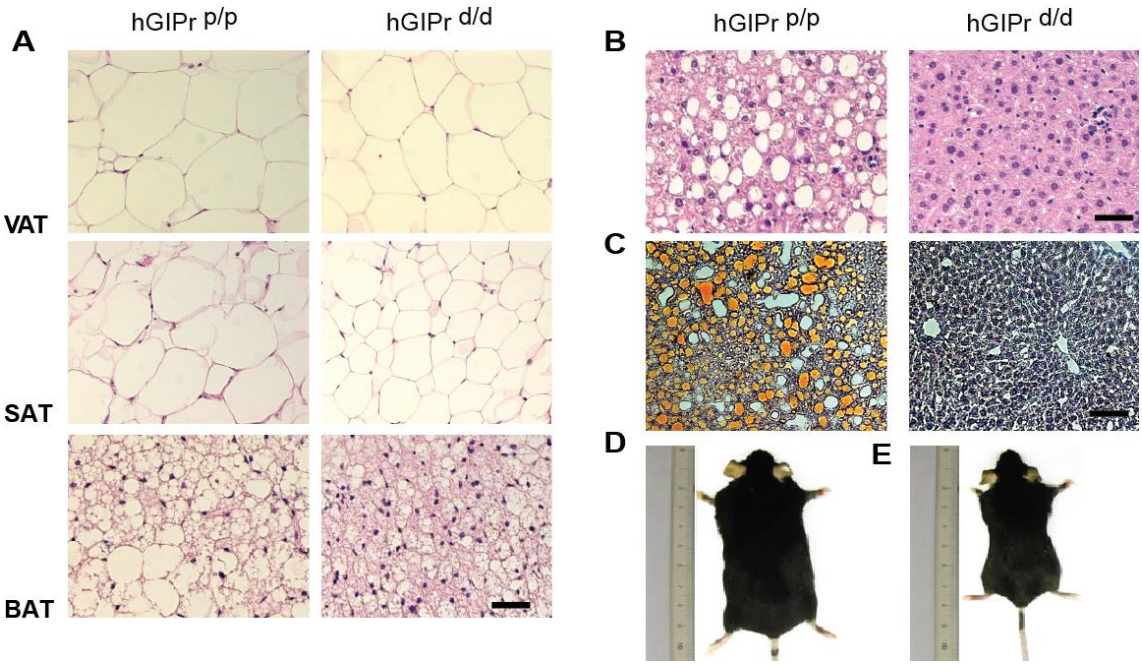

Figure 4. **Inhibition of GIP signaling prevents liver steatosis. A**) Histological analysis of Visceral (VAT), subcutaneous (SAT) and brown (BAT) adipose tissue from HFD fed hGIPr$^{P/P}$ and hGIPr$^{d/d}$ mice for 12 weeks. Sections were stained with hematoxylin and eosin (H and E). **B** and **C**) Histological analysis of liver from hGIPr$^{P/P}$ and hGIPr$^{d/d}$ mice on HFD for 12 weeks. **B**) Liver sections were stained with H and E. **C**) Liver sections were stained with Oil Red O. Representative gross appearance of hGIPr$^{P/P}$ (D) and hGIPr$^{d/d}$ (E) mice on HFD for 12 weeks (scale bars, 100 µm, n = 5 to 6 per group).

Human GIPr deficiency in the CNS reduces food intake

To determine the effects of CNS-specific hGIPr deficiency on energy balance, we evaluated energy expenditure of hGIPr$^{d/d}$ and hGIPr$^{P/P}$ mice fed a HFD for 12 weeks. The data showed that no difference in oxygen consumption (VO_2), carbon dioxide production (VCO_2) and respiratory exchange ratio (RER) (Fig. 5, A-C). However, hGIPr$^{P/P}$ mice showed significantly increased physical activity during the light phase and decreased during the dark phase (Fig. 5D). On the other hand, hGIPr$^{d/d}$ mice showed decreased physical activity during the light phase but significantly increased physical activity during the dark phase compared with hGIPr$^{P/P}$ mice (Fig. 5D). There was no difference in energy expenditure (EE) and water consumption between hGIPr$^{d/d}$ and

hGIPr$^{P/P}$ mice (Fig. 5, E and F). However, hGIPr$^{d/d}$ mice consumed less food than hGIPr$^{P/P}$ mice, (Fig. 5G). When food consumption was normalized to body weight the trend still showed less food intake in the hGIPr$^{d/d}$ mice (Fig. 5H). This decrease in food intake may contribute to the failure of HFD-fed hGIPr$^{d/d}$ mice to gain weight.

The effect of CNS hGIPr deficiency to cause increased physical activity and lower energy intake is likely to be a major determinant of central GIP signaling to regulate obesity and metabolic disorders, and may largely account for the resistance of HFD-induced obesity in hGIPr$^{d/d}$ mice.

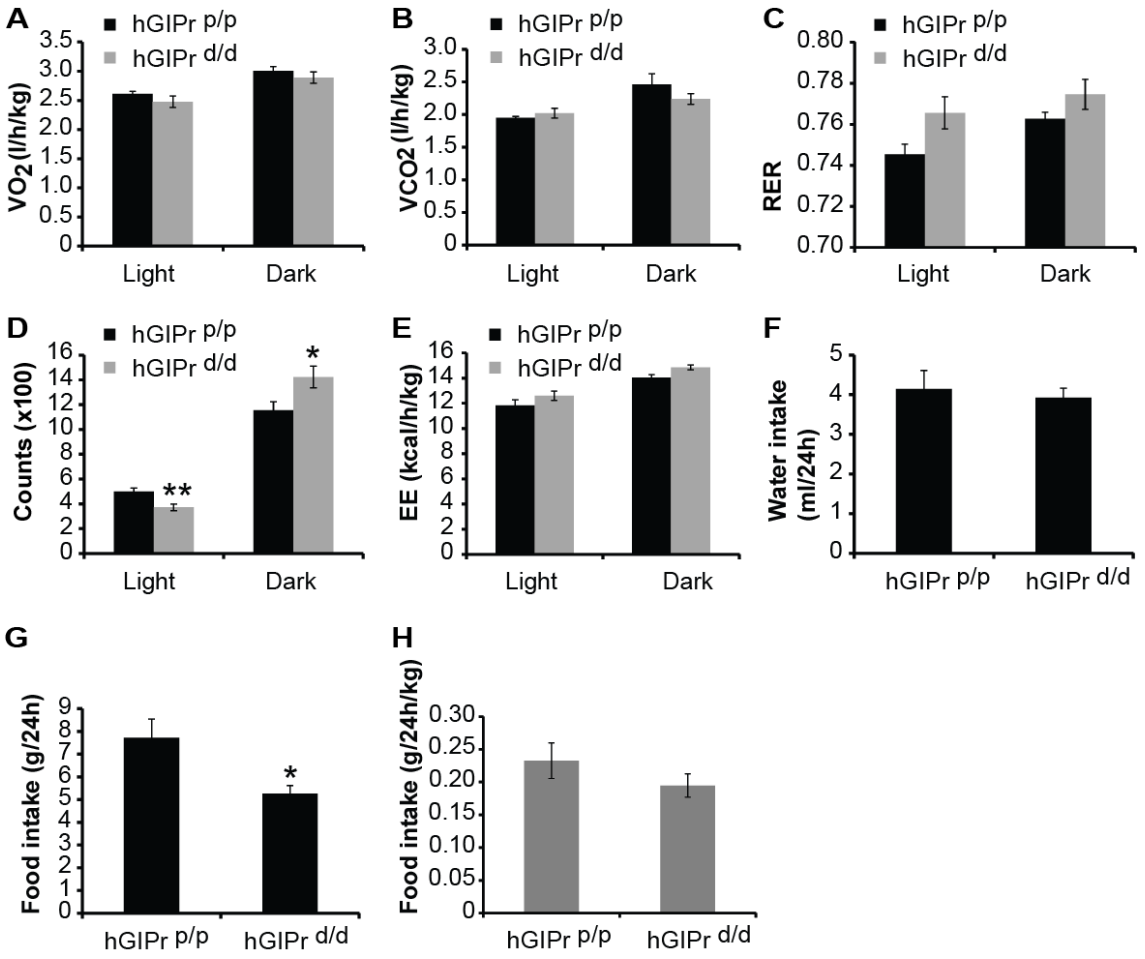

Figure 5. **Comparison of energy homeostasis of hGIPr$^{P/P}$ and hGIPr$^{d/d}$ mice. A-H**) A HFD fed mice for 12 weeks were examined to measure, (A) gas exchange (oxygen consumption (VO_2) and (B) carbon dioxide production (VCO_2)), (C) respiratory exchange ratio (RER) = [VCO_2]/ [VO_2], (D) physical activity (counts), (E) energy expenditure (EE), (F) water consumption and (G and H) food intake using metabolic cages for 3 days. All values are shown as mean ± SEM (*<0.05, **p<0.01), n = 5 to 6 per group.

Hypothalamic neuropeptides contribute to metabolic regulation by hGIPr

To investigate whether differences in food intake were associated with hypothalamic orexigenic and anorexigenic neuropeptides, their expression levels were examined. The expression of orexigenic neuropeptide Y (NPY), agouti-related protein (AGRP) and promelanin-concentrating hormone (PMCH), showed no difference between hGIPr$^{d/d}$ and hGIPr$^{P/P}$ mice (Fig. 6, A-C). However, the pro-opiomelanocortin (POMC) expression at mRNA levels were highly up-regulated and showed a modest increase at the protein level in hGIPr$^{d/d}$ mice as opposed to hGIPr$^{P/P}$ mice (Fig. 6, D and E).

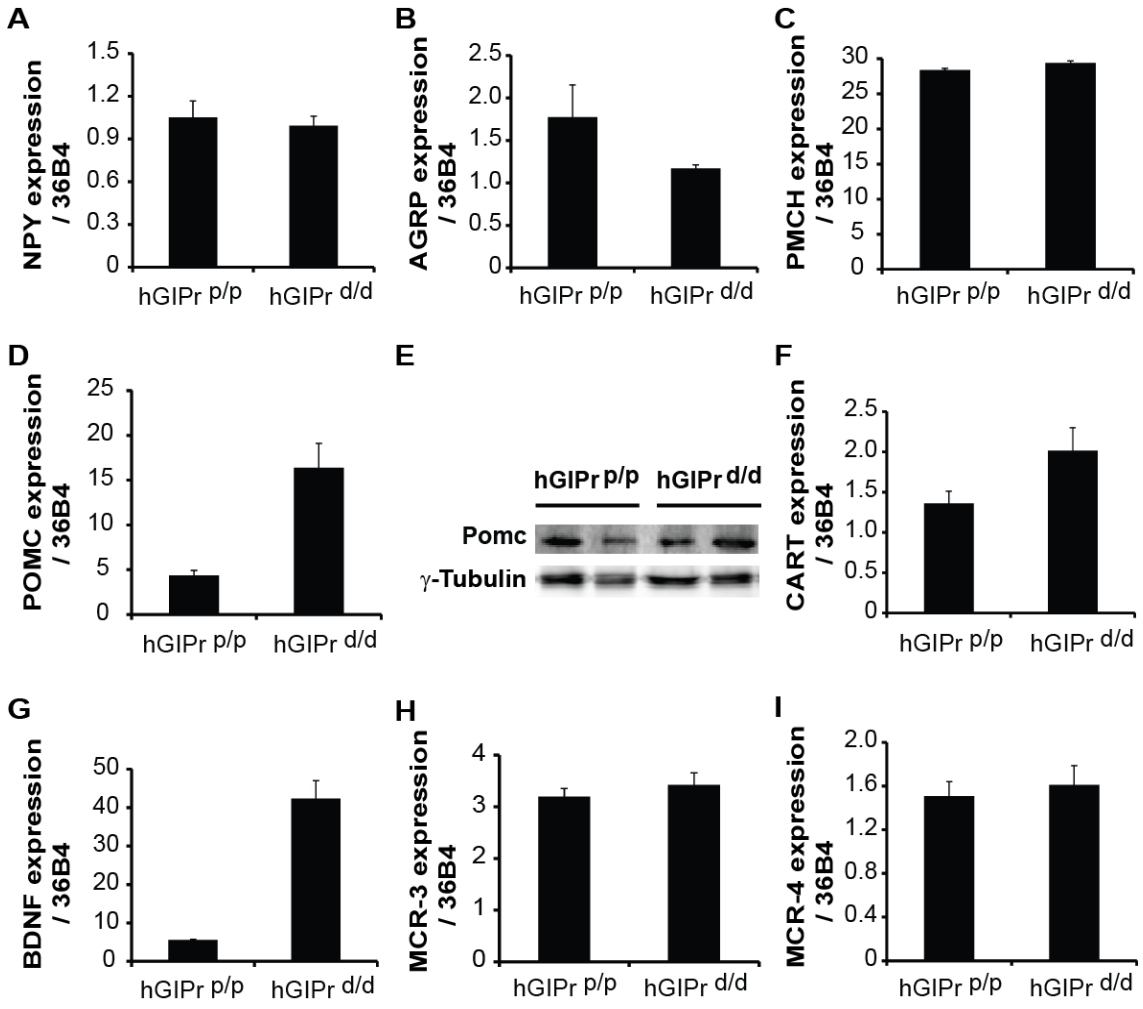

Figure 6. **Hypothalamic neuropeptides expression of hGIPr$^{P/P}$ and hGIPr$^{d/d}$ mice.** hGIPr$^{P/P}$ and hGIPr$^{d/d}$ mice were on HFD for 12 weeks and then fasted for 6 h. **A-D)** The expression of AgRP, NPY, PMCH and POMC mRNA in the hypothalamus was analyzed by qPCR (n = 4).**E**) Analysis of POMC at protein levels in the hypothalamus by Western blot (n = 4). γ-tubulin was used as a loading control. **F-I**) Expression of CART, BDNF, MCR-3 and 4 mRNA in the hypothalamus was analyzed by qPCR (n =

4). Neuropeptide Y (NPY), agouti-related protein (AGRP) and promelanin-concentrating hormone (PMCH), Cocaine- and amphetamine-regulated transcript (CART), Brain-derived neurotrophic factor (BDNF) and melanocortin receptor 3 and 4 (MCR-3 and MCR-4).

Cocaine- and amphetamine-regulated transcript (CART) expression levels also showed a trend toward being increased (Fig. 6F). Brain-derived neurotrophic factor (BDNF) levels were highly increased in hGIPr$^{d/d}$ mice, whereas melanocortin receptor 3 and 4 (MCR-3 and MCR-4) levels were indistinguishable between hGIPr$^{d/d}$ and hGIPr$^{P/P}$ mice (Fig. 6 H and I). Taken together the data indicate that defective GIP signaling in the CNS in association with increased levels of hypothalamic POMC, CART and BDNF, might account for decreased feeding behavior in hGIPr knockout mice.

GIP/IGF-1 signaling in development and food intake

To further investigate whether IGF-1 may be involved in the regulation of body development and insulin signaling pathway, IGF-1 levels were analyzed. IGF-1 expression levels in the liver and plasma were significantly decreased in hGIPr knockout mice as compared with hGIPr$^{P/P}$ control mice (Fig. 6, A and B). There was a slight difference in body length between these two mice strains (Fig. 6, C and D) partly confirming the reduction of IGF-1 levels in hGIPr knockout mice. In addition to regulation by GH, serum IGF-I levels were also affected by food intake.

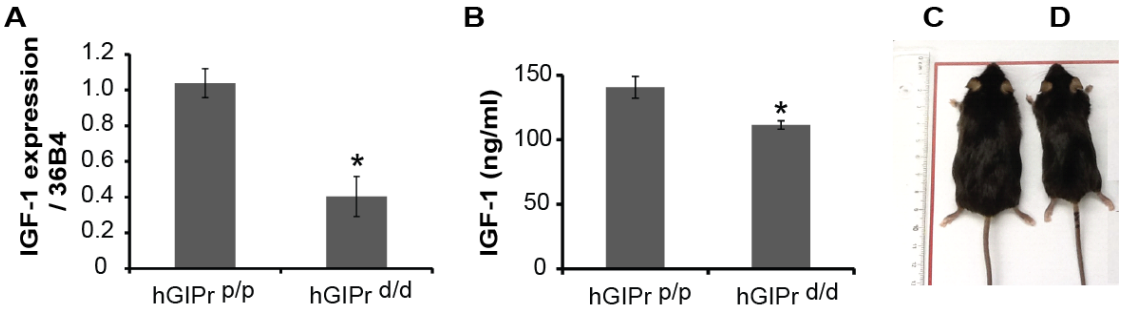

Figure 7. **Analysis of IGF-1 levels. A**) **hGIPr$^{P/P}$ and hGIPr$^{d/d}$ mice were on** a **HFD for 12 weeks and then fasted for 6 h**. The expression of IGF-1 mRNA in the liver was analyzed by qPCR (n = 4). **B**) hGIPr$^{P/P}$ and hGIPr$^{d/d}$ mice were on a HFD for 2 weeks and fasting plasma levels of IGF-1 was assessed by ELISA (n = 4). Representative gross appearance of hGIPr$^{P/P}$(**C**) and hGIPr$^{d/d}$ (**D**) mice on HFD for 12 weeks. All values are shown as mean ± SEM (*<0.05). Scale bars, 100 µm.

It is known that IGF-I signaling decrease nutrient-sensing pathway, therefore it is possible that decreased food intake in hGIPR knockout mice may be mediate via GIP/GH/IGF-1 signaling pathway which in turn controls mouse body weight.

3.5. Discussion

The mechanisms of obesity-induced insulin resistance and type II diabetes may involve the GIP/GIPr signaling pathway. Studies have reported that blockade of GIP action using GIP receptor antagonist (Pro3) GIP in mice reversed HFD induced obesity, insulin resistance, and associated metabolic disorders (19). Moreover, *Gipr*$^{-/-}$ mice are protected against the development of HFD-induced obesity and insulin resistance (22). However, studies on the tissue-specific function of GIP receptor are not available. Transgenic mice with over expression of human GIPr in adipose tissue do exhibit increased HFD-induced body weight gain (24). However, beta-cell targeted GIPr overexpression was shown not to prevent HFD-induced weight gain (24). In another study it was shown that double homozygous (*Gipr*$^{-/-}$, *Lep*^{ob}/*Lep*^{ob}) mice gained less weight and had lower adiposity than *Lep*^{ob}/*Lep*^{ob} mice (22); this demonstrates that GIP can regulate leptin signaling pathways to control weight gain.

To investigate the CNS involvement in the regulation of metabolic changes observed in the HFD-fed global GIPr knockout mice, we generated CNS-specific hGIPr knockout mice, by crossbreeding floxed humanized (hGIPr$^{p/p}$) mice with nestin-cre transgenic mice. In agreement with previous studies (22,25) we found that CNS-specific human GIPr knockout mice fed a HFD were protected from HFD induced weight gain. GIP and its receptor are present in several parts of the brain regions known to modulate neurogenesis in hippocampus (18-21) however; the central effect of GIPr on energy homeostasis has not been studied. The present study is the first to show the CNS specific GIP mediated regulation of body weight gain.

Interestingly, the hyperglycemia caused by feeding a HFD to hGIPr $^{p/p}$ control mice was significantly reduced in hGIPr$^{d/d}$ mice, in line with previously reported results in global GIPr knockout mice (22). The defects of glucose-stimulated insulin secretion and glucose intolerance due to the disruption of incretin receptor gene (GIP and GLP-1) have been reported (22,25). However, our findings show that with the loss of GIP/ GIPr function in the CNS, mice are still able to control fasting glucose levels, as evidenced by a dramatic reduction in fasting blood glucose levels. Moreover, this effect was accompanied by a reduction of fasting circulating triglycerides, free fatty acids and cholesterol. Previous studies have shown that HFD treatment increases intestinal K cell

hyperplasia and results in hyper-secretion of GIP that consequently GIP increase nutrient uptake and triglyceride accumulation in the adipocyte (19,22,24). However, blockade of GIP enhances uptake and rapid oxidation of fatty acids by muscle and liver. Based on our findings it is possible to speculate that central GIP/ GIPr inhibition modulates peripheral metabolic organ functions that are crucial for the regulation of energy homeostasis.

Here we show that, decreased body weight in hGIPr knockout mice is accompanied by lower amounts of fat mass and slight reduction of lean mass. In the same notion, *Gipr*$^{-/-}$ mice fed a HFD were reported to have significantly decreased visceral and subcutaneous fat mass compared with wild type mice (22). Moreover, mice immunized against GIP and fed a HFD had a lower total fat mass as assessed by dual energy x-ray absorption (26). Similarly, the GIP receptor antagonist (Pro3) GIP in HFD-induced obese mice, has been reported to reduce fat mass in subcutaneous but not in epididymal and perirenal fat (19,22,24). Interestingly, only in one study, *Gipr*$^{-/-}$ mice fed a HFD for 3 weeks have been reported to exhibit increased body fat mass when compared with regular diet-fed *Gipr*$^{-/-}$ mice (27). Consistent with our data, double knockout mice for receptors of GLP-1 and GIP (DIRKO) fed on a HFD have reduced body weight gain due to decreased fat mass (22,25,28).

Our findings provide a convincing explanation as to how the fat mass decreases in response to CNS GIP/GIPr deficiency and thereby protecting from HFD-induced obesity. Thus, the regulation of peripheral adipose tissue by CNS GIPr suggests a requirement of central GIPr for HFD-induced obesity prevention. Nevertheless, we cannot rule out the involvement of a modest reduction of lean mass and body length in hGIPr knockout mice, even though the effect was not significant. Supporting the involvement of GIPr in lean mass regulation, recently an increase in lean mass in transgenic mice overexpressing hGIPr has been reported (24). GIP also exerts an anabolic effect in bone as *Gipr*$^{-/-}$ mice exhibit reduced bone mass (29). This finding may explain the modest decrease in body length in our mouse model. It is interesting to note, that, GIP does not modulate bone resorption in human subjects (30). Over all our findings suggests that the CNS GIPr controls HFD-induced whole body fat mass reduction rather than lean mass.

It is well known that GIP contributes substantially to the insulin releasing actions of the entero-insular axis and represents the major physiological incretin compared with GLP-1 (31). It regulates insulin release by improving physiology of the β cells (30,32); hence GIP is considered a candidate for type II diabetes treatment (33,34). However, DIRKO mice results in a modest deterioration of glucose homeostasis (35,36) indicating a possible compensatory mechanisms during life-long deletion of GLP-1 and GIP receptors (31). In the current study, hGIPr knockout mice challenged with HFD exhibit enhanced insulin sensitivity, as shown by decreased fasting blood glucose levels and improved intraperitoneal glucose clearance and oral glucose tolerance. Consequently, glucose tolerance was accompanied by decreased fasting plasma insulin concentration and more response in an insulin tolerance test, as revealed by a significant reduction of glucose clearance upon exogenous insulin administration. Hence, the data demonstrate the decreased need of insulin possibly due to improved insulin sensitivity together with a reduced demand resulting from circulating glucose and lipids.

Consistent with our findings *Gipr*$^{-/-}$, *Lep*^{ob}*/Lep*^{ob} mice exhibit improved glucose homeostasis (22), moreover daily administration of the GIP antagonist (Pro3)-GIP to *ob/ob* mice markedly lowered levels of glucose and insulin in association with increased insulin sensitivity (19,31). In addition, DIRKO have been reported to be protected against HFD-induced insulin resistance as previously reported in the context of lower fasting glycaemia and insulinemea (28). *Gipr*$^{-/-}$ mice fed a regular diet exhibit a modest impairment of oral glucose tolerance (10). Here for the first time we showed a marked decrease in fasting blood glucose levels in a regular diet fed CNS-specific hGIPr knockout mice. These observations demonstrate that hGIPr can regulate insulin resistance independently of the effects of hGIPr on HFD-induced weight gain. Taken together our findings, clearly indicate that CNS-specific hGIPr knockout mice are protected against HFD-induced insulin resistance and improve fasting glucose levels in regular diet fed mice.

To investigate the CNS-GIP effect on adipokine secretion, we measured leptin and adiponectin levels. Interestingly, an increase in plasma leptin and a decrease in adiponectin level in HFD-fed hGIPr $^{p/p}$ control mice were found. Consistent with the decreased fat mass in a HFD-fed hGIPr knockout mice, the observed plasma leptin levels correlated with body fat mass (3,22), while the circulating levels of adiponectin

were inversely correlated with fat mass storage as demonstrated previously (4,37). Previous studies have reported that *Gipr*$^{-/-}$ mice show no difference in plasma adiponectin levels between regular diet and HFD-fed mice (25). In contrast, significantly increased mRNA expression and plasma levels of adiponectin in HFD-fed *Gipr*$^{-/-}$ mice compared with regular diet fed *Gipr*$^{-/-}$ mice have been shown (19). This finding is in line with our findings. Adiponectin has been considered to be a promising biomarker for indicating insulin sensitivity (4,37). A notable improvement of insulin sensitivity in HFD-fed hGIPr knockout mice could be partly explained by adiponectin levels but does not play a major role in this strain as the modest increase of adiponectin concentration was observed. However, this finding suggests inhibition of GIP signaling modulates adiponectin levels to enhance insulin sensitivity.

Consistent with *Gipr*$^{-/-}$ mice on HFD (22) and pharmacological inhibition of GIPr in *ob/ob* mice (24), endogenous GIP was increased in HFD-fed hGIPr$^{p/p}$ mice compared with hGIPr$^{d/d}$ mice. The elevation of GIP in hGIPr$^{p/p}$ mice fits with the elevation of GIP in *ob/ob* mice (31). Furthermore, fatty acids stimulate K-cell hyperplasia and GIP secretion as shown in *ob/ob* mice (31). Hence, the reduction of GIP in hGIPr$^{d/d}$ mice could be linked to the reduction of fatty acid circulation. Thus, decreased insulin level in hGIPr knockout mice are in line with decreased GIP circulation, as GIP is known to be the prominent insulin releasing factor other than GLP-1. Moreover, due to a potential compensatory mechanism an increase in circulating GLP-1 levels was observed in hGIPr knockout mice. However, the difference we observed might not be big enough to explain the overt phenotypic differences; therefore, we cannot consider GLP-1 as the major driving force for a notable improvement of insulin sensitivity in HFD-fed hGIPr knockout mice.

It is well known that consumption of a HFD results in an increased fat deposition in adipocytes as well as in liver and skeletal muscle in both humans and animals (19). This excessive fat deposition interferes with insulin action giving rise to increased insulin resistance (38-40). The absence of fat storage in hepatocytes and decreased adipocytes size (hyperplasia) in HFD fed hGIPr knockout mice may account for the observed improvements of insulin sensitivity, blood glucose, lipids and glucose tolerance in these transgenic animals. Hence, the genetic disruption of CNS-GIP action protected diet induced obesity, ameliorates diabetes and prevents hepatic steatosis, most likely through

the modulation of fat accumulation in adipocytes and liver, thereby leading to diminished insulin resistance.

To determine the effects of CNS-specific hGIPr deficiency on energy metabolism, we evaluated energy expenditure. Human GIPr knockout mice and $hGIPr^{P/P}$ mice fed a HFD showed no difference in RER, energy expenditure and water consumption. In contrast previous studies have shown increased energy expenditure in DIRKO mice (22,25,28), increased fat oxidation and energy expenditure in $Gipr^{-/-}$, and $Gipr^{-/-}$, Lep^{ob}/Lep^{ob} mice (22). The difference between these findings and our study might be due to the global and specific *Gipr* knockout effect. Interestingly, hGIPr knockout mice exhibited decreased physical activity during light phase whereas activity was significantly increased during the dark phase compared with the control mice. Supporting this, $Gipr^{-/-}$ and DIRKO mice showed higher locomotor activity (18,28). The maintenance of physical activity during the light and dark phase in hGIPr knockout mice, in part, contributes to the protection of weight gain when fed a HFD.

Surprisingly, cumulative absolute food intake in hGIPr knockout mice significantly lower compared with $hGIPr^{P/P}$ mice fed a HFD. In the current study, we report for the first time decreased food intake in hGIPr knockout mice. In contrast, previous studies have reported (22,25) no significant difference in food intake between WT and $Gipr^{-/-}$ mice. However, consistent with our findings (41) decreased food intake in ovariectomized (OVX $Gipr^{-/-}$) mice has been shown, suggesting the influence of GIP on the estrogen signaling pathway to regulate food intake. The effect of CNS-hGIPr on energy intake indicates the major determinant of central GIP signaling to regulate obesity and metabolic disorders, suggesting that the CNS is the main site accounting for HFD-induced obesity resistance in global GIPr knockout mice. The results showed an independent effect of central and peripheral GIP action on the regulation of energy homeostasis, most importantly the opposite effect of GIP and GLP-1 on food intake.

The hypothalamus is the major brain center that regulates food intake and body weight. Although the importance of GIP action in the CNS is not well understood, both GIP and the GIPr are expressed in the hypothalamus (21). Several neuropeptides such as NPY, AgRP, CART, POMC and α-melanocyte-stimulating hormone have been shown to control energy homeostasis by modulating energy intake or energy expenditure (22).

Thus, we investigated the neuropeptide hormone expression in a HFD fed hGIPr$^{d/d}$ and hGIPr$^{P/P}$ mice. Hypothalamic POMC, CART and BDNF mRNA expression were highly up-regulated in hGIPr$^{d/d}$ compared with hGIPr$^{P/P}$ mice whereas, NPY, AgRP, PMCH, MCR-3 and MCR-4 expression showed no significant difference between the two strains. The induced POMC and BDNF expression in hGIPr knockout mice might explain the difference in food intake between hGIPr$^{d/d}$ and hGIPr$^{P/P}$ mice groups. BDNF is a neurotrophin that plays a fundamental role in development and plasticity of the central nervous system. In addition, BDNF is currently recognized as a major factor in the regulation of food intake (42). Low levels of circulating BDNF have been found in individuals with obesity and T2D (43,44). Moreover, BDNF infusions in rats have been shown to decrease food intake and body weight gain (45). POMC neurons also inhibit food intake and body weight through melanocortin receptors (46). Therefore, GIP/GIPr signals via POMC and BDNF, which are the crucial neuropeptides hormones to regulate food intake and maintenance energy homeostasis.

The brain through IGF-1/insulin axis plays a major role in the regulation of energy homeostasis and development. IGF-1 and growth hormone (GH) interact with insulin to modulate carbohydrate metabolism (47). Interestingly, blocking the effect of GH in the presence of low serum IGF-1 concentrations enhances insulin sensitivity (47) consistent with the low expression and low levels of plasma IGF-1 in hGIPr knockout mice. This finding indicated that the presence of low concentration of IGF-1 results in a major improvement in insulin sensitivity, suggesting CNS-GIP/GIPr signaling is a major determinant of insulin action in hGIPr deficient animals. Interestingly, previous studies have reported that low IGF-1 levels in mouse correlate with longevity (48). Therefore, this finding draws attention to understand the molecular mechanism regulating GIP/IGF-1 signaling to control mice development and metabolic status.

IGF-1 is produced by the liver in response to GH secreted from the pituitary gland, hence measuring the concentration levels of GH is very important to partially understand the levels of IGF-1 secretion in hGIPr knockout mice and to determine whether GIP signaling affects the pituitary axis to control mouse development and metabolic status via IGF-1.

In conclusion, CNS-specific hGIPr deletion in mice protected from HFD-induced obesity, insulin resistance and liver steatosis by increasing physical activity and satiety then decreasing body fat mass storage and preventing lipid accumulation in hepatocytes. Notably, CNS-hGIPr deficient mice exhibited improved insulin sensitivity, up-regulation of BDNF, adiponectin and GLP-1 secretion and down regulation of IGF-1 and insulin release. Furthermore, these mice exhibited improved glucose tolerance and were protected from the development of T2D and metabolic disorders. In this respect, central GIPr inhibition may provide another pharmacological function to regulate excessive adipose accumulation by decreasing energy intake.

3.6. References

1. Ouchi, N., Parker, J. L., Lugus, J. J., and Walsh, K. (2011) *Nature reviews. Immunology* **11**, 85-97
2. MacDougald, O. A., and Burant, C. F. (2007) *Cell Metab* **6**, 159-161
3. MacDougald, O. A., and Burant, C. F. (2007) *Cell Metab* **6**, 159-161
4. Goossens, G. H. (2008) *Physiol Behav* **94**, 206-218
5. Challa, T. D., Beaton, N., Arnold, M., Rudofsky, G., Langhans, W., and Wolfrum, C. (2012) *J Biol Chem* **287**, 6421-6430
6. Hajer, G. R., van Haeften, T. W., and Visseren, F. L. (2008) *Eur Heart J* **29**, 2959-2971
7. Yabe, D., and Seino, Y. (2011) *Progress in biophysics and molecular biology* **107**, 248-256
8. Creutzfeldt, W. (1979) *Diabetologia* **16**, 75-85
9. Creutzfeldt, W. (2005) *Regul Pept* **128**, 87-91
10. Miyawaki, K., Yamada, Y., Yano, H., Niwa, H., Ban, N., Ihara, Y., Kubota, A., Fujimoto, S., Kajikawa, M., Kuroe, A., Tsuda, K., Hashimoto, H., Yamashita, T., Jomori, T., Tashiro, F., Miyazaki, J., and Seino, Y. (1999) *Proc Natl Acad Sci U S A* **96**, 14843-14847
11. Brown, J. C., Pederson, R. A., Jorpes, E., and Mutt, V. (1969) *Canadian journal of physiology and pharmacology* **47**, 113-114
12. Dupre, J., Ross, S. A., Watson, D., and Brown, J. C. (1973) *J Clin Endocrinol Metab* **37**, 826-828
13. Brown, J. C., Dryburgh, J. R., Frost, J. L., Otte, S. C., and Pederson, R. A. (1978) *Adv Exp Med Biol* **106**, 169-171
14. Usellini, L., Capella, C., Solcia, E., Buchan, A. M., and Brown, J. C. (1984) *Histochemistry* **80**, 85-89
15. Schieldrop, P. J., Gelling, R. W., Elliot, R., Hewitt, J., Kieffer, T. J., McIntosh, C. H., and Pederson, R. A. (1996) *Biochim Biophys Acta* **1308**, 111-113
16. Volz, A., Goke, R., Lankat-Buttgereit, B., Fehmann, H. C., Bode, H. P., and Goke, B. (1995) *FEBS Lett* **373**, 23-29
17. Harada, N., Yamada, Y., Tsukiyama, K., Yamada, C., Nakamura, Y., Mukai, E., Hamasaki, A., Liu, X., Toyoda, K., Seino, Y., and Inagaki, N. (2008) *Am J Physiol Endocrinol Metab* **294**, E61-68
18. Faivre, E., Gault, V. A., Thorens, B., and Holscher, C. (2011) *J Neurophysiol* **105**, 1574-1580
19. McClean, P. L., Irwin, N., Cassidy, R. S., Holst, J. J., Gault, V. A., and Flatt, P. R. (2007) *American journal of physiology. Endocrinology and metabolism* **293**, E1746-1755
20. Nyberg, J., Jacobsson, C., Anderson, M. F., and Eriksson, P. S. (2007) *J Neurosci Res* **85**, 2099-2119
21. Nyberg, J., Anderson, M. F., Meister, B., Alborn, A. M., Strom, A. K., Brederlau, A., Illerskog, A. C., Nilsson, O., Kieffer, T. J., Hietala, M. A., Ricksten, A., and Eriksson, P. S. (2005) *J Neurosci* **25**, 1816-1825
22. Miyawaki, K., Yamada, Y., Ban, N., Ihara, Y., Tsukiyama, K., Zhou, H., Fujimoto, S., Oku, A., Tsuda, K., Toyokuni, S., Hiai, H., Mizunoya, W., Fushiki, T., Holst, J. J., Makino, M., Tashita, A., Kobara, Y., Tsubamoto, Y., Jinnouchi, T., Jomori, T., and Seino, Y. (2002) *Nat Med* **8**, 738-742

23. Lenard, N. R., and Berthoud, H. R. (2008) *Obesity (Silver Spring)* **16 Suppl 3**, S11-22
24. Ugleholdt, R., Pedersen, J., Bassi, M. R., Fuchtbauer, E. M., Jorgensen, S. M., Kissow, H. L., Nytofte, N., Poulsen, S. S., Rosenkilde, M. M., Seino, Y., Thams, P., Holst, P. J., and Holst, J. J. (2011) *J Biol Chem* **286**, 44632-44645
25. Hansotia, T., Maida, A., Flock, G., Yamada, Y., Tsukiyama, K., Seino, Y., and Drucker, D. J. (2007) *The Journal of clinical investigation* **117**, 143-152
26. Fulurija, A., Lutz, T. A., Sladko, K., Osto, M., Wielinga, P. Y., Bachmann, M. F., and Saudan, P. (2008) *PLoS One* **3**, e3163
27. Naitoh, R., Miyawaki, K., Harada, N., Mizunoya, W., Toyoda, K., Fushiki, T., Yamada, Y., Seino, Y., and Inagaki, N. (2008) *Biochemical and biophysical research communications* **376**, 21-25
28. Ayala, J. E., Bracy, D. P., Hansotia, T., Flock, G., Seino, Y., Wasserman, D. H., and Drucker, D. J. (2008) *Diabetes* **57**, 288-297
29. Xie, D., Cheng, H., Hamrick, M., Zhong, Q., Ding, K. H., Correa, D., Williams, S., Mulloy, A., Bollag, W., Bollag, R. J., Runner, R. R., McPherson, J. C., Insogna, K., and Isales, C. M. (2005) *Bone* **37**, 759-769
30. Drucker, D. J. (2006) *Cell metabolism* **3**, 153-165
31. Gault, V. A., Irwin, N., Green, B. D., McCluskey, J. T., Greer, B., Bailey, C. J., Harriott, P., O'Harte F, P., and Flatt, P. R. (2005) *Diabetes* **54**, 2436-2446
32. Baggio, L. L., and Drucker, D. J. (2007) *Gastroenterology* **132**, 2131-2157
33. Green, B. D., Gault, V. A., O'Harte F, P., and Flatt, P. R. (2004) *Current pharmaceutical design* **10**, 3651-3662
34. Irwin, N., McClean, P. L., Cassidy, R. S., O'Harte F, P., Green, B. D., Gault, V. A., Harriott, P., and Flatt, P. R. (2007) *Diabetes/metabolism research and reviews* **23**, 572-579
35. Hansotia, T., Baggio, L. L., Delmeire, D., Hinke, S. A., Yamada, Y., Tsukiyama, K., Seino, Y., Holst, J. J., Schuit, F., and Drucker, D. J. (2004) *Diabetes* **53**, 1326-1335
36. Preitner, F., Ibberson, M., Franklin, I., Binnert, C., Pende, M., Gjinovci, A., Hansotia, T., Drucker, D. J., Wollheim, C., Burcelin, R., and Thorens, B. (2004) *The Journal of clinical investigation* **113**, 635-645
37. Karastergiou, K., and Mohamed-Ali, V. (2010) *Mol Cell Endocrinol* **318**, 69-78
38. Goodpaster, B. H., He, J., Watkins, S., and Kelley, D. E. (2001) *The Journal of clinical endocrinology and metabolism* **86**, 5755-5761
39. Ryysy, L., Hakkinen, A. M., Goto, T., Vehkavaara, S., Westerbacka, J., Halavaara, J., and Yki-Jarvinen, H. (2000) *Diabetes* **49**, 749-758
40. Shulman, G. I. (2000) *The Journal of clinical investigation* **106**, 171-176
41. Isken, F., Pfeiffer, A. F., Nogueiras, R., Osterhoff, M. A., Ristow, M., Thorens, B., Tschop, M. H., and Weickert, M. O. (2008) *American journal of physiology. Endocrinology and metabolism* **295**, E350-355
42. Rosas-Vargas, H., Martinez-Ezquerro, J. D., and Bienvenu, T. (2011) *Archives of medical research* **42**, 482-494
43. Krabbe, K. S., Nielsen, A. R., Krogh-Madsen, R., Plomgaard, P., Rasmussen, P., Erikstrup, C., Fischer, C. P., Lindegaard, B., Petersen, A. M., Taudorf, S., Secher, N. H., Pilegaard, H., Bruunsgaard, H., and Pedersen, B. K. (2007) *Diabetologia* **50**, 431-438
44. Lommatzsch, M., Zingler, D., Schuhbaeck, K., Schloetcke, K., Zingler, C., Schuff-Werner, P., and Virchow, J. C. (2005) *Neurobiology of aging* **26**, 115-123

45. Pelleymounter, M. A., Cullen, M. J., and Wellman, C. L. (1995) *Experimental neurology* **131**, 229-238
46. Mineur, Y. S., Abizaid, A., Rao, Y., Salas, R., DiLeone, R. J., Gundisch, D., Diano, S., De Biasi, M., Horvath, T. L., Gao, X. B., and Picciotto, M. R. (2011) *Science* **332**, 1330-1332
47. Clemmons, D. R. (2004) *The Journal of clinical investigation* **113**, 25-27
48. Henis-Korenblit, S., Zhang, P., Hansen, M., McCormick, M., Lee, S. J., Cary, M., and Kenyon, C. (2010) *Proceedings of the National Academy of Sciences of the United States of America* **107**, 9730-9735

Chapter 4

4. The regulation of adipogenesis through novel adipokines secreted by adipocytes and adipose tissue explants

Tenagne Delessa Challa[1], Leon Gabriel Straub[1] and Christian Wolfrum[1]

[1]Swiss Federal Institute of Technology, ETH Zürich, Institute of Food Nutrition and Health, Schorenstrasse 16, 8603 Schwerzenbach, Switzerland

4.1. Abstract

Adipose tissue plays a key role in the regulation of whole body energy metabolism by secreting adipokines. The differential secretion of adipokines and divergent metabolic effects of adipose depot on adipocyte development is however still not fully understood. We have developed a co-culture method of pre-adipocytes with primary subcutaneous adipocyte or subcutaneous adipose tissue explants (SA, SE, respectively), visceral adipocyte or visceral adipose tissue explants (VA, VE, respectively). SA, SE, VA or VE were cultured on the co-culture insert membrane integrated with fractionation of the secretions by FPLC. A proteomic approach was used to identify differentially secreted adipokines by SA *vs* SE, VA *vs* VE that regulate adipogenesis. SA, SE, VA or VE inhibited pre-adipocyte differentiation in co-culture. Adipocytes or adipose tissue explants secretion were also able to decrease adipocyte formation. However, these effects were abolished upon heat inactivation or by charcoal treatment. In contrast to global effects, fractions of SA, SE, VA or VE secretions showed both induction and inhibition of pre-adipocyte differentiation.

Based on the different fraction effect on adipogenesis, we identified Slc27a1, Vim, Cp and Ecm1 proteins to be secreted by SA, SE, VA or VE, which subsequently induced pre-adipocyte differentiation. Among other identified proteins Got2, Cpq, Il1rl1, SPARC, Ces1d, Fbln2, Lgals3bp and Tf which decreased adipogenesis up on their knockdown. These 12 differentially secreted proteins were expressed in 3T3-L1 cells in addition to, subcutaneous and visceral adipose tissue. Moreover, we validated the effects of Vim and Il1rl1 among other selected candidates on adipocyte formation. Vim recombinant protein induced 3T3-L1 pre-adipocyte differentiation while, IL-33, an Il1rl1 ligand, dramatically decreased adipocyte formation. In addition to the secreted proteins with known effects on adipocytes formation we identified 4 novel secreted molecules (i.e. Got2, Cpq, Il1rl1 and Ces1d) that have not been previously shown to be secreted, expressed nor regulate the process of adipogenesis. These novel adipokines which are differentially secreted by adipose depots may broadly affect adipose and non-adipose metabolic organ function, thereby regulating systemic metabolism. To understand the molecular mechanism underlying the roles of these novel adipokines in adipocytes development additional *in vitro* and *in vivo* studies will be necessary.

4.2. Introduction

Obesity, defined as an excessive accumulation of white adipose tissue, is the core component of the metabolic syndrome and strongly associated with the development of insulin resistance and type II diabetes mellitus (T2D) (1-4). Over the past several years, our understanding of adipose tissue has dramatically changed from an inert energy storage organ to an active multifunctional endocrine tissue (5-9). Thus, adipose tissue serves as a key organ for the regulation of whole body energy metabolism by secreting adipokines (3,10). Some of these secreted adipokines include tumor necrosis factor α, (TNF-α), interleukin-6 (IL-6), adipsin, adiponectin, renin, leptin and resistin (7-9,11,12). Adipokines secreted by adipocytes or adipose tissue are involved in the regulation of food intake, glucose and lipid metabolism (13,14) through endocrine action. They are also capable of acting locally (autocrine and/or paracrine) for the regulation of adipocyte development in addition to having a role in the recruitment of inflammatory cells (6,12).

Development of adipose tissue is through cellular hypertrophy (increase in cell size) and hyperplasia (increase in cell number) (8,15,16). Hypertrophy, an excess lipid accumulation in the existing adipocytes, is strongly associated with the development of insulin resistance, T2D and cardiovascular disease (CVD) and leads to an enhanced secretion of pro-inflammatory adipokines from adipose tissue (15,17). In contrast, hyperplasia is the recruitment of new smaller adipocytes from precursor cells. This process involves the proliferation and differentiation of pre-adipocytes (8,16,18) and is associated with more insulin sensitivity (19) and increased secretion of anti-inflammatory adipokines (17). Adipose tissue development involves complex interactions between endocrine, paracrine, and autocrine systems (20). Moreover, adipocytes express adipokine receptors, which modulate adipogenesis directly by autocrine and/or paracrine mechanisms (15).

Well-studied adipokines that influence adipocyte growth through both central and peripheral mechanisms include leptin, adiponectin, TNFα, IL-6, visfatin, and resistin (8,9,15,20). Therefore, adipokines may contribute to the development of metabolic disorders, partly by inhibiting adipogenesis and causing adipocytes hypertrophy (15). Different studies show the alteration of adipokine profile in obese subjects due to increased pro-inflammatory adipokine secretion, which subsequently promotes insulin resistance, whereas adiponectin and other anti-inflammatory adipokine secretion are

reduced (17). Consequently, dysregulation of the production of adipokines contributes to the development of obesity and obesity related disease 'metabolic syndrome' (21).

Interestingly, different adipose depots have distinct patterns of adipokine secretion. Subcutaneous adipose tissue (SAT) secretes higher amounts of metabolically beneficial adipokines including, leptin and adiponectin, whereas pro-inflammatory adipokines secretion such as RBP4, TNF-α, MCP-1, IL-8, and IL-6 are increased in visceral adipose tissue (VAT) (4,22). In addition, different adipose depots also have different adipogenic capacity. For example, pre-adipocytes from SAT have a higher capacity of adipocyte formation compared with those from visceral depots (23). Together, these observations show that subcutaneous and visceral depot differ in their intrinsic characteristics, including levels of adipokine secretion profiles, insulin sensitivity, lipolysis rate and capacity of adipogenesis (22,23). This differential secretion of adipokines and the divergent metabolic effects may be due to the intrinsic, cell-autonomous/cells resident differences between VAT and SAT that contributes to the differing metabolic consequences of fat depot. Therefore, the identification and quantitative comparison of novel adipokine secretion from subcutaneous adipocytes, visceral adipocytes, SAT and VAT, will be of importance to delineate this process. Furthermore, it will be important to define the role of differentially secreted adipokines in adipocyte development to identify novel molecular targets for therapeutic approaches to treat the epidemic of obesity and type II diabetes.

Multiple studies in recent years have used primary mature adipocytes isolated from SAT and VAT, since the well-established 3T3-L1 cell-line is unable to provide depot specificity, as reported previously (4). However, primary adipocytes also have their limitations, since the cross-talk between these cells and other non-adipose cells within adipose tissue is lost (4). One possibility is the use of SAT and VAT explants, but using whole adipose tissue explants also has inherent problems due to less uniform sample preparation and the reduction of the quality of secretome sample. This will affect the relevance of the identified proteins source (secreted, serum, or intracellular) because of contaminant proteins (4,21). Moreover, the duration of the culturing of mature primary adipocytes and adipose tissue explants influences the level of secreted proteins (21).

4.3. Experimental procedures

Materials

Recombinant human vimentin and mouse IL-33 were obtained from R&D Systems (England). Dexamethasone (Dexa), 3-isobutyl-1-methylxanthine (IBMX), insulin and formaldehyde were obtained from Sigma-Aldrich. Dulbecco's modified Eagle's medium (DMEM), heat inactivated fetal bovine serum (FBS), penicillin streptomycin, trypsin-EDTA solution, Bodipy493/503, Hoechst, Syto60, TRIzol reagent and fast SYBR Green master mix were purchased from Invitrogen Life Science (Basel, Switzerland).

Animals

All animal studies were approved by the Canton of Zurich Veterinary Office. C57BL/6 male mice (10-16 weeks old) were obtained from Charles River and housed in a pathogen-free animal facility on a (reversed) 12 h dark/light cycle.

Adipose tissue explants culturing

Paired VAT (epididymal) and SAT (inguinal) depots were obtained from 12-weeks old C57BL/6J mice. For each experiment, 8-12 mice were used as tissue donors. The adipose tissue explant culturing protocls were developed and optimized from Alvarez-Llamas., et al. (21). After the animals were sacrificed the fat depot was dissected and adipose tissue was finely minced into smaller pieces. The minced tissues were washed thoroughly with 100 ml of PBS over a 40 µm filter blue mesh. The tissue was gently shaken for a short period and washed on the 40 µm mesh with 200 ml of warm PBS then centrifuged for 1 min at 1000 rpm to remove erythrocytes and debris. After that 1 g of the tissues were cultured in serum-free media at 37 °C and 5% CO_2 and washed every 2 h for 8 h followed by one time washing after 24 h culture. Thereafter tissue was cultured on co-cultured insert membrane (Fig.1).

Stromal vascular fraction (SVF) and adipocyte isolation and culture

SVF isolation was performed as described previously (24,25). Brifely, 8 to 12 weeks old male C57BL/6J mice were sacrificed and dissected, fat tissues were obtained from SAT

and VAT depots. Fat tissue were immediately minced and incubated with collagenase type II buffer (1mg/ml) for 45 min at 37°C with gentle shaking. Floating adipocytes and free oil were separated from SVF by centrifugation at 1000 rpm for 5 min. Adipocytes were gently transferred to 50 ml falcon tubes and intensively washed with PBS and centrifuged for 1 min at 1000 rpm. Approximately 200 µl adipocytes were cultured on co-cultured insert membrane in serum-free media at 37 °C and 5% CO_2 overnight (Fig.1). After 24 h incubation adipocytes were washed once and subsequently cultured for 120 h. SVF pellet were filtered with 40 µm net and erythrocytes were lysed. The pellet was resuspended in media containing 1% Pen Strep and 10% FBS and cultured at equal density at 37 °C and 5% CO_2 and induced to differentiation as described in section below.

Co-culture experiments

To avoid the leakage of dead cell and other contaminant to the secretome sample, we established a co-culture system by using cell culture insert (BD Falcon). The inserted membrane has a pore size of 3.0 µm and permits free exchange of media between insert and the well (Fig.1). SE, VE, SA or VA were cultured on the insert membrane sieve and the secretome sample were harvested every 24 h for 120 h. The secreted sample was collected and centrifuged at 1000 rpm for 5 min and stored in -80°C. At the end of the exeperiment the adipose tissue explants or adipocytes were lysed with lysis buffer and harvested to analyse LDH leakage.

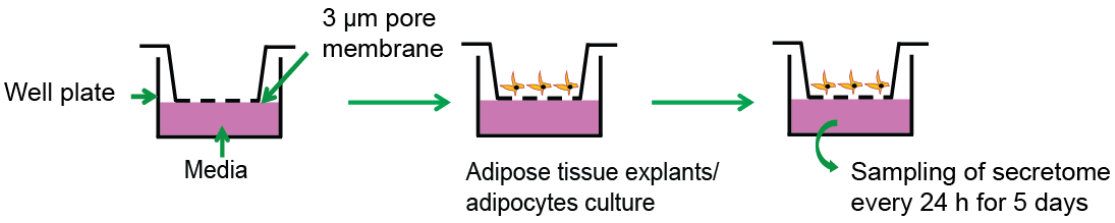

Figure 1**. Schematic representation of culturing cell/tissue on the inseret membrane co-cultutre.**

To assess whether adipocytes or adipose tissue explants can affect pre-adipocyte differentiation, 3T3-L1 cells or primary pre-adipocytes isolated from SAT or VAT were cultured on the bottom chambers of 6 well-plates at the density of 4.66×10^5 and 8.7×10^6 cells/well, respectively. SA, SE, VA or VE were cultured separately on the insert

membrane sieves for 48 h. The pre-adipocytes were cultured for 3 days and on the third day, SA, SE, VA or VE cultured on the membrane inserts for 48 h were transferred to the culture plates and co-cultured together (Fig 2). The pre-adipocytes were induced for differentiation as described below. The co-culture was conducted for 3 days, then the adipocytes or adipose tissue explants in the insert were discarded.

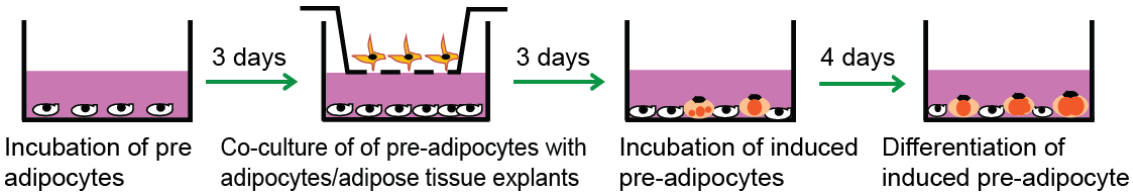

Figure 2. **Schematic representation of co-culture experiment.** Differentiation of adipocytes was evaluated on day 8 by using a light microscope.

Measurement of cell cytotoxicity

Cytotoxicity Detection Kit, lactate dehydrogenase (LDH) (Roche, Germany) were used to evaluate cell vaibilty by measuring LDH enzyme activity in the secretome sample and lysed cells according to the manufacturer's instructions. This test is a colorimetric assay used for the quantification of cell death and cell lysis based on LDH release from the cytosol of dead cells or cells with damaged plasma membranes into the media. The assay was peformed in 96-well plates and enzyme activity was measured at 490 nm using an ELISA plate reader.

Sample pre-treatement

The secretome sample was concentrated by 15 to 20-fold by ultrafiltration (Amicon, 3-kDa cutoff, Millipore) at 4^{o}C. The concentrated sample was used for total protein concentration measurement by BCA protein assay kit, (Thermo Fisher Scientific, Switzerland). Equal amounts of concentrated total proteins (20 µg to 1 ng) were used for pre-adipocyte treatment during differentiation. The concentrated total proteins were also used for fractionation.

Silver staining

To determine the protein composition of the sample, equal amounts of concentrated total proteins were resolved on 12% SDS-PAGE gel and silver-stained with SilverQues Silver Staining Kit (Invitrogen Life Science, Switzerland) according to the manufacturer's protocols. Briefly, the gels were fixed with 40% ethanol and 10% acetic acid for 20 min. After several washes with 30% ethanol and water, the gels were sensitized, stained and developed for visualization of the band and then scanned.

Fast protein liquid chromatography (FPLC)

FPLC was used for total proteins mixture separation by rapid fractionation. The concentrated sample was adjusted to the composition of the start buffer (20 mM Tris-HCl**,** pH 8.0) by diluting with the buffer then filtered with a 0.22 μm filter and centrifuged immediately before it was applied to the column. The samples were applied to the HiTrap Q HP, 1 ml an anion exchange column connected to FPLC (ÄKTA, GE Healthcare, Sweden) by using super loop with a flow rate of 1 ml/min. Before injecting the sample solution, the column was equilibrated with 5 column volumes of start buffer. A total of 1 mg concentrated protein solution was injected. The samples were eluted with 5 to 10 column volumes of elution buffer. An elution buffer was applied based on gradient elution, with highest gradient of elution buffer containing up to 1M NaCl **(**20mM Tris-HCl**,** 1M NaCl, pH 8.0).

The fractionation was carried out at 4^{o}C. Each sample (SA, SE, VA or VE) was fractionated into three fractions (F1, F2 and F3) and 5 ml were collected for each. In short, SA fractionated into SA1, SA2 or SA3, SE fractionated into SE1, SE2 or SE3, VA fractionated into VA1, VA2 or VA3, VE fractionated into VE1, VE2 or VE3. The fractions were desalted and concentrated by ultrafiltration at 4^{o}C and filtered with a 0.22 μm filter. Equal amount of fraction protein were resolved by SDS-PAGE gel and stained with silver to determine protein composition. The effects of the fractions were evaluated on adipogenesis.

Protein identification by LC/ESI/MS/MS

Protein identification and characterization was carried out at Zurich Functional Genomics Center. In brief, 60 µg of (SA1, SA2, SA3, SE1, SE2, SE3, VA1, VA2, VA3, VE1, VE2 or VE3) were precipitated with 16.6 µl 100% TCA and washed twice with cold acetone. The samples were dried and dissolved in 40 µl buffer (10 mM Tris/2 mM CaCl2, pH 8.2) + 5 µl trypsin (100 ng/ µl in 10 mM HCl) + 5 µl Rapi Gest (1% in water). The samples were incubated overnight at 37°C then incubated for 30 min with 3 µl of 1 M HCl at 37°C. After centrifugation the samples were desalted on ZipTip C18 and were dried. When a white precipitate (salt) was observed the desalting step was repeated and samples were dried, dissolved in 15 µl 0.1% formic acid/3% acetonitrile and transferred to auto-sampler vials for LC/MS/MS analysis. For protein identification 5 µl was injected into LC/MS/MS. Database searches were performed by using the Mascot (SwissProt restricted to *Mus musculus*). Mass spectrometry tolerance was set at 0.5 Da, and MS/MS was set at 0.05 Da and quantitative normalized total spectral count (QNTSC) was used for protein identification and relative quantifications. Protein identifications were accepted at Protein threshold ≥ 99% probability confidence and if they contained at least 5 or more identified peptides. Spectral counts were calculated by Scaffold. To classify secreted and non-secreted identified proteins, SecretomeP 2.0 Server (26) and SignalP 3.0 (4) were used. Signal peptides were determined by using SignalP 3.0 (4). Protein with a signal peptide was considered as secreted proteins via the classical pathway (endoplasmic reticulum/Golgi dependent pathway) (21). If no signal peptide was predicted but the Neural Network (NN) score value was ≥ 0.5, proteins were classified as secreted via the non-classical pathway.

Differentiation of pre-adipocytes

Subcutanous (Sub) and visceral (Vis) primary pre-adipocytes and 3T3-L1 fibroblasts were grown and induced to differentiate with induction medium containing 10 mg/ml insulin, 10 mM Dexa, 11.5 µg/ml IBMX, 10% FBS and 1% penicillin streptomycin as described previously (24,25). High throughput image analysis to calculate adipogenesis was performed as described before (24,25). Briefly, Sub, Vis and 3T3-L1 pre-adipocytes were cultured on collagen coated black 96-well plates with clear bottoms.

Fluorescent image pictures were taken with high throughput imaging system Operetta (Perkin Elmer). Images were analyzed using Harmony software (Perkin Elmer) (24).

Reverse transfection of pre-adipocytes

For the RNA interference assay, 25 µl of Optimem media and 100 nM of small interfering RNA (siRNA) were mixed in collagen coated 96 well plates. Transfection reagent, Lipofectamine RNAiMax (Invitrogen Life Science, Switzerland) was used and pre-adipocyte was cultured for 24 h. After 24 h of incubation the medium was changed to complete medium. Following the differentiation procedure automated differentiation quantifications were performed as described above (24,25). Both custom library siRNA targeting and non-targeting siRNA control were purchased from Dharmacon (USA). Custom SMARTpool siRNA library sequences are (Table 4, Appendix 3).

RNA isolation and quantitative real-time RT-PCR

Total RNA was extracted using TRIzol reagent according to the manufacturer's protocol. One µg of total RNA was converted into first-strand cDNA using high capacity cDNA reverse transcription kit (Invitrogen). Real-time PCR quantification was performed using a fast SYBR Green master mix and gene specific primer sets (Table 1, Appendix 4).

Charcoal depletion

To strip free hormones from the secretome and fractionated sample, dextran-coated charcoal (Sigma) was used according to the manufacturer's instructions. In short, 20 mg of dextran-coated charcoal was added to 1 ml of sample and mixed overnight with an overhead mixer at 4°C. Charcoal was removed from the suspension by centrifugation at 2000 x *g* for 15 minutes at 4 °C. The supernatant was taken for protein measurement and differentiation.

Statistical analysis

All data are expressed as mean ± SEM. The significance of differences between groups was determined using a two tailed Student’s t test.

4.4. Results

Analysis of mature adipocytes and adipose tissue explants secretion quality

Different adipose depots have distinct patterns of adipokine secretion; therefore, we used primary subcutaneous adipose tissue explants (SE) and visceral adipose tissue explants (VE). However, adipose tissue explants represent a big challenge regarding the quality of secretome sample due to the presence of SVF. Notably, the release of damaged cell content because of the effects associated with cutting the tissue to smaller pieces and leakage of serum proteins present in the tissue pieces. Hence, we used primary adipocytes isolated from subcutaneous (SA) and visceral (VA) adipose tissue, to examine if the depot-specific difference in adipokine secretion could persist in adipocytes, and could influence pre-adipocyte differentiation. On the other hand culturing of mature primary adipocytes *in vitro* is also very challenging since mature adipocytes have large lipid droplets and they float on the top of the media. Additionally, they clump together and as such, access to sufficient media may be unequal.

To solve these problems and obtain serum and intracellular protein free secretome sample from mature adipocytes and adipose tissue explants, we performed several washing steps before starting culturing and applied different culturing time points as described in the experimental procedure. After several washing steps, we used a co-culture system and adipocytes or adipose tissue explants were cultured on the insert membrane sieve of co-culture well with serum-free media (Fig.1). The adipocytes were cultured on the sieve without media, but they had contact with media through the pores of the insert membrane. Therefore, they were attached to the sieve and were not floating (Fig.1). In addition, adipocytes were cultured at very low density (thin layer) to increase the surface area or to spread the cells all over the sieve; therefore, they can equally access the media without floating (Fig.1). Beside these points, the insert membranes have additional advantages as they obviate dead cell leakage or any other contaminants to the media. Hence, this method is very useful to maintain viable mature adipocytes and adipose tissue explants in culture for more than 120 h. Furthermore, it is very helpful to harvest samples mainly consisting of adipocytes and adipose tissue-derived secreted proteins as a subsequent means to investigate their possible potential role on adipogenesis and to use for secretome analyses.

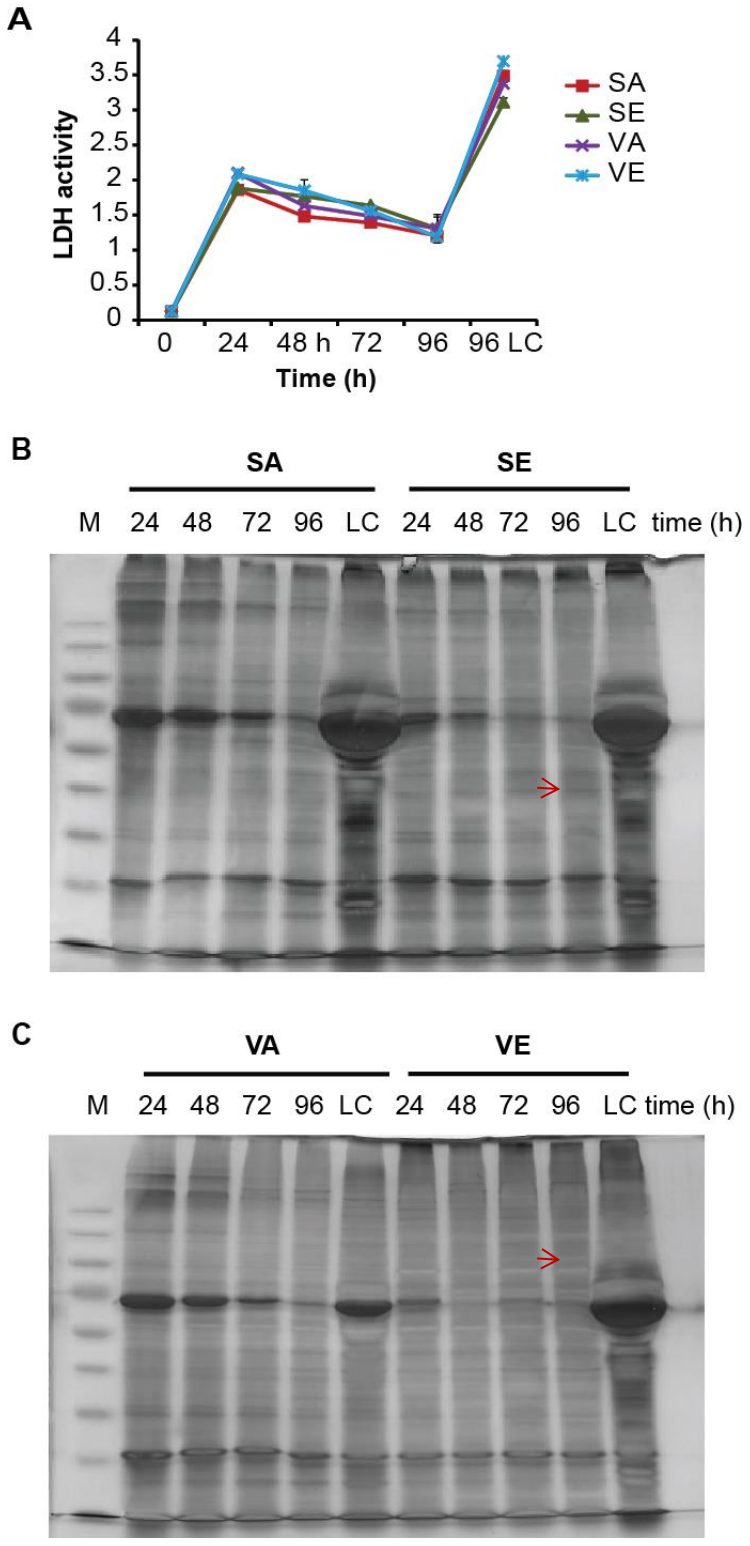

Figure 3. **Cell viability and protein composition of secretome sample.** Subcutaneous adipocytes (SA), subcutaneous adipose tissue explants (SE), visceral adipocytes (VA) and visceral adipose tissue explants (VE) were cultured on the insert membrane sieve for the indicated time points and the secreted samples were harvested. A) Cell viability was determined by release of lactate dehydrogenase (LDH) into the media. B and C) Protein composition of SA, SE, VA and VE secretome sample were resolved on SDS-PAGE gel and detected with silver-staining. Lysed cells (LC).

Based on these findings, we further analyzed the leakage of these abundant proteins and cell viability of adipocytes and adipose tissue explants cultured on the insert membrane up to 96 h by using LDH enzyme activity as shown in figure 3A. The release of LDH to the media was detected after 24 h incubation of SA, SE, VA and VE, indicating more cell damage during isolation and culturing at 24 h; afterwards LDH release was reduced from 48 h up to 96 h (Fig. 3A).When SA, SE, VA and VE were lysed (lysed cells = LC) at 96 h the LDH activity was dramatically increased (Fig. 3A) demonstrating that more than 85 % of the cells were alive at the end of the experiment.

The protein composition of SA, SE, VA and VE obtained during culturing time points and lysed cells at the end of the experiments was investigated by SDS-PAGE (Fig. 3, B and C). When secreted samples were harvested at 24 h and compared with 48, 72 and 96 h, protein staining showed less uniformity in intensity of bands than 48, 72 and 96 h, due to high abundance of contaminating proteins (Fig. 3, B and C). However, with intensive washing and culturing on the insert membrane sieve the high abundance contaminant proteins leakage decreased in all secreted samples as clearly shown in lanes 48, 72 and 96 h. This data demonstrates the increased leakage of serum and intracellular proteins even after intensive washing at 24 h, but a decreased leakage after 72 and 96 h. In addition, the bands observed have the same intensity, indicating that they may represent constitutively secreted proteins.

To further confirm the viability of these cells and adipose tissues explants, the cells were lysed by sonication and the proteins were resolved on the gel as shown in the lanes bands under lysed cell. Confirming the LDH data the adipocytes or adipose tissue explants were viable as shown by its high protein content after silver staining comparing LC to 24, 48, 72 and 96 h culturing time points (Fig. 3, B and C). The bands at 24 h and LC were expressed highly by all samples: SA, SE, VA, and VE compared to 72 and 96 h. Interestingly, some of these bands completely disappeared at 72 and 96 h; furthermore some bands expressed in SE were not detected in SA. Similar results were observed for VA and VE (see red arrow in the figures (Fig. 3, B and C)). These findings suggested that SA and VA as well as VA and VE show different protein secretion. Taken together this data demonstrated that high serum and intercellular contaminant proteins in adipocytes and adipose tissue explants are present at 24 h, but their secretion was decreased or was no longer detectable with our culturing setup time points at 48, 72 and 96. Based on the observed protein concentration, LDH leakage and protein composition; 48, 72 and 96 h culturing time points were selected to harvest secretome samples for further investigation.

These data taken together indicate that our culturing system is very helpful to maintain viable adipocyte and adipose tissue explant in the culture and decrease the leakage of contaminant proteins, to study the role of SA, SE, VA and VE secretion on adipocyte development and to identify novel adipokine secretion.

Adipocytes or adipose tissue explants co-culture regulates adipogenesis

After we established the optimal culture setup for mature adipocytes or adipose tissue explants, we studied the effect of their secretion on adipogenic differentiation via cross-talk between mature adipocytes, adipose tissue and pre-adipocytes. As different adipose depots have different adipogenic capacity, isolated primary pre-adipocytes from subcutaneous (Sub) and visceral (Vis) adipose tissue and 3T3-L1 cells were used. Sub and Vis primary pre-adipocytes as well as 3T3-L1 cells were co-cultured with or without SA, SE, VA or VE for 3 days during induction of differentiation (Fig. 4, A-C). Co-culture of mature adipocytes (SA, VA) or adipose tissue explants (SE, VE) inhibited differentiation of Sub, Vis or 3T3-L1 pre-adipocytes compared to control cells, as evidenced by marked reduction of lipid droplet accumulation (Fig. 4, A-C). These data demonstrated that co-culture of mature adipocytes or adipose tissue explants suppresses adipogenesis via secretion of active biological molecules.

Adipocytes or adipose tissue explants secretion suppresses adipocyte formation

To verify the co-culture effects of adipocytes or adipose tissue explants on adipocyte differentiation: SA, SE, VA or VE were cultured on the insert membrane in serum-free media and secretome samples were harvested at 72 and 96 h. Cultured Sub, Vis or 3T3-L1 cells were treated with or without the secreted samples for 3 days during induction of differentiation and lipid droplet formation was quantified (Fig. 5). The observed data showed a reduction of Sub, Vis or 3T3-L1 pre-adipocyte differentiation into adipocytes as shown in Figure 5, A-C. In agreement with the co-culture data, mature adipocytes or adipose tissue explants secretion significantly decreased adipocyte formations in Sub, Vis and 3T3-L1 cells.

These data together indicate that both co-culture of primary adipocyte or adipose tissue explants and their secretions halted adipogenic differentiation of pre-adipocyte, suggesting that there are inhibitory factors secreted by primary adipocytes or adipose tissue explants, which affect adipogenesis via cross-talk between adipose tissue cells and their precursors.

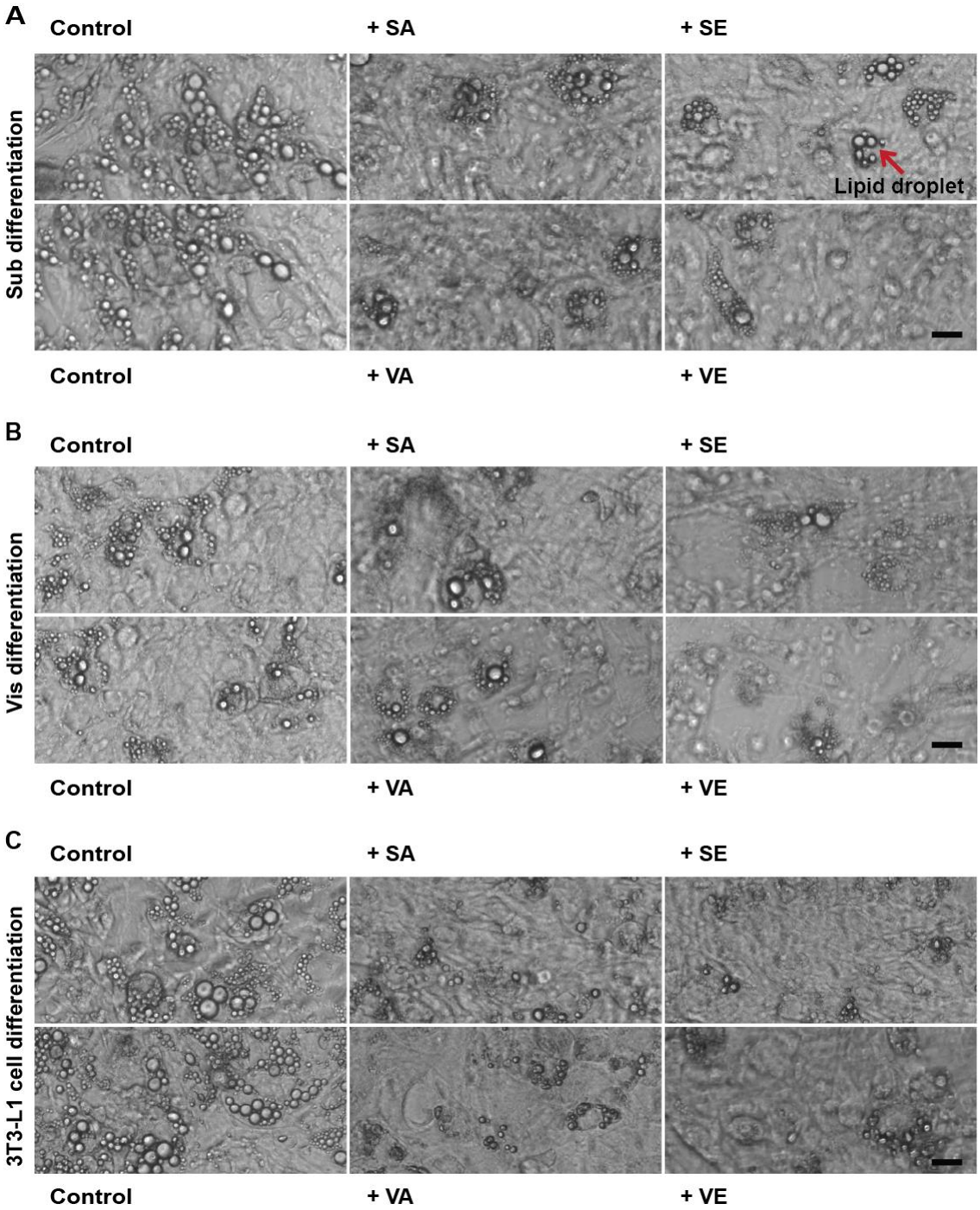

Figure 4. **Co-culture of adipocytes or adipose tissue explants regulates adipogenesis.** Subcutaneous (Sub), visceral (Vis) or 3T3-L1 pre-adipocytes were cultured on the bottom of well for 72 h (A-C). SA, SE, VA or VE were cultured separately on the insert membrane for 48 h as shown above. SA, SE, VA or VE were transferred to confluent pre-adipocytes and co-cultured together for 3 days during induction of differentiation. SA, SE, VA or VE were separated after 3 days. Lipid droplet formation was assessed by light microscope on day 8 (n = 12) at 10 x magnification. Co-culture of pre-adipocytes with: + SA = subcutaneous adipocytes, + SE = subcutaneous adipose tissue explants, + VA = visceral adipocytes, + VE = visceral adipose tissue explants.

Inhibition of adipogenesis by adipocytes or adipose tissue explants secretome reversed by heat inactivation or charcoal suspension

We tested whether adipose tissue explants or adipocyte secretions - inhibited adipocyte differentiation is heat sensitive or depleted by dextran-coated charcoal stripping. Similar to the above mentioned data; SA, SE, VA or VE secretion significantly inhibited adipogenic differentiation of Sub, Vis and 3T3-L1 pre-adipocytes compared to control cells (Fig. 6, A-C). However, this effect was completely reversed by heat inactivation of SA, SE, VA or VE secretion and resulted in significant increase in the number of differentiated Sub, Vis and 3T3-L1 adipocytes compared to control cells (Fig. 6, A-C). As shown in the figures charcoal stripped VA and VE secretion showed just a trend toward increased sub pre-adipocyte differentiation, while SA and SE Charcoal stripped secretion significantly increased sub adipogenesis compared to control cells (Fig. 6A). Charcoal stripped secretion of SA, SE, VA or VE significantly abolished Vis adipocyte differentiation compared to control cells (Fig. 6B), but showed a trend toward induced adipocyte formation in 3T3-L1 cells compared to the control cells (Fig. 6C).

Taken together these results indicate that secretion from mature adipocytes or adipose tissue explants which inhibited adipogenesis is heat sensitive and can be partially depleted by charcoal suspension, suggesting the presence of active protein factors in the secretome sample.

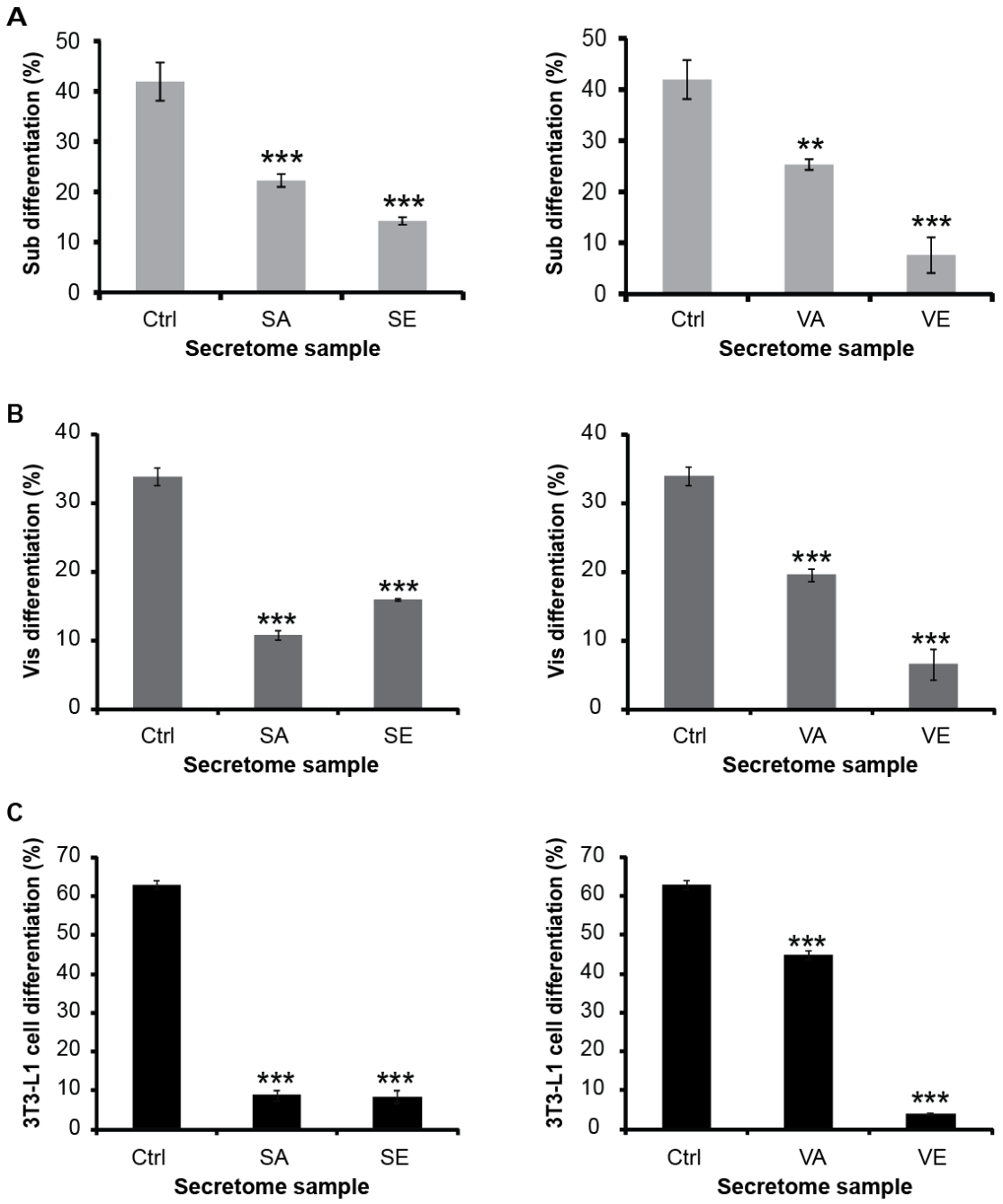

Figure 5. **Secretion of mature adipocytes or adipose tissue explants suppresses pre-adipocyte differentiation.** A) Subcutaneous (Sub) primary pre-adipocytes were treated without or with 10 µg/ml of SA, SE, VA, or VE secretion during induction of adipogenesis. Differentiation was quantified using automated image based analysis (n = 6). B) Visceral (Vis) primary pre-adipocytes were treated with or without 10 µg/ml of SA, SE, VA, or VE secretion during induction of adipogenesis. Differentiation was quantified as described above (n = 6). C) 3T3-L1 pre-adipocytes were treated with 10 µg/ml of SA, SE, VA, or VE secretion during induction of adipogenesis. Differentiation was quantified as described above (n = 12). SA = subcutaneous adipocytes, SE = subcutaneous adipose tissue explants, VA = visceral adipocytes, VE = visceral adipose tissue explants. All values are shown as mean ± SEM (**p<0.01, ***p<0.001).

Fractionation of adipocytes or adipose tissue explants secretion regulates adipocyte differentiation

To screen the factors present in SA, SE, VA and VE secretion which influence adipogenic differentiation, the secretions were fractionated by using FPLC. To separate the complexity of the secreted factors we used an anion exchange column for fractionation. Cultured 3T3-L1 pre-adipocytes were treated with different fractions as shown in Fig. 7A. The observed data showed the inhibitory effects of SA secretions on adipogenesis was changed after the secretion was fractionated. Fractions (F1 and F3) obtained from SA fractionation resulted in significantly increased adipocytes formation while SA fraction 2 (F2) decreased differentiation compared to control cells. The inhibitory effects of SE secretion remained the same. Fractions (F1, F2 or F3) of SE reduced lipid droplet formation compared to control cells (Fig. 7A). Similar to SA fractions, F1 and F3 of VA led to significant induction of adipocyte differentiation whereas VA F2 reduced compared to the control cells. On the other hand, VE F3 showed a trend toward increased adipocytes formation whereas VE F1 or F2 resulted in reduced differentiation (Fig. 7A). When we compared SA F1 and F3 with SE F1 and F3 the opposite effect was observed, except SA F2 and SE F2 both led to significant reduction of adipocyte formation. VA F1 *vs* VE F1 also showed the opposite effect, while VA F2 or VE F2 significantly inhibited adipocytes formation. In contrast, VA F3 or VE F3 promoted adipocyte differentiation (Fig. 7A).

Furthermore, the fractionated samples were heat inactivated or charcoal stripped, to investigate if the fractionated samples which inhibited or promoted adipogenesis are heat sensitive or can be affected by charcoal. Interestingly, heat inactivation or charcoal suspension completely reversed the stimulatory or inhibitory effects of SA fractions (F1, F2 and F3; Fig.7B). Similarly, the inhibitory effect of SE fractions (F1, F2 and F3) was abolished by heat inactivation or charcoal depletion (Fig.7B). Heat inactivation or charcoal depletion also overcomes the stimulatory or inhibitory effects of VA (F1, F2 or F3) and VE (F1, F2 or F3) fractions as shown in figure 7 C and D.

Taken together these data demonstrated that fractionation of SA, SE, VA or VE secretion regulates adipogenesis, the effect of these fractions can be reversed by heat

inactivation or charcoal depletion, indicating there are biologically active factors present in these fractions.

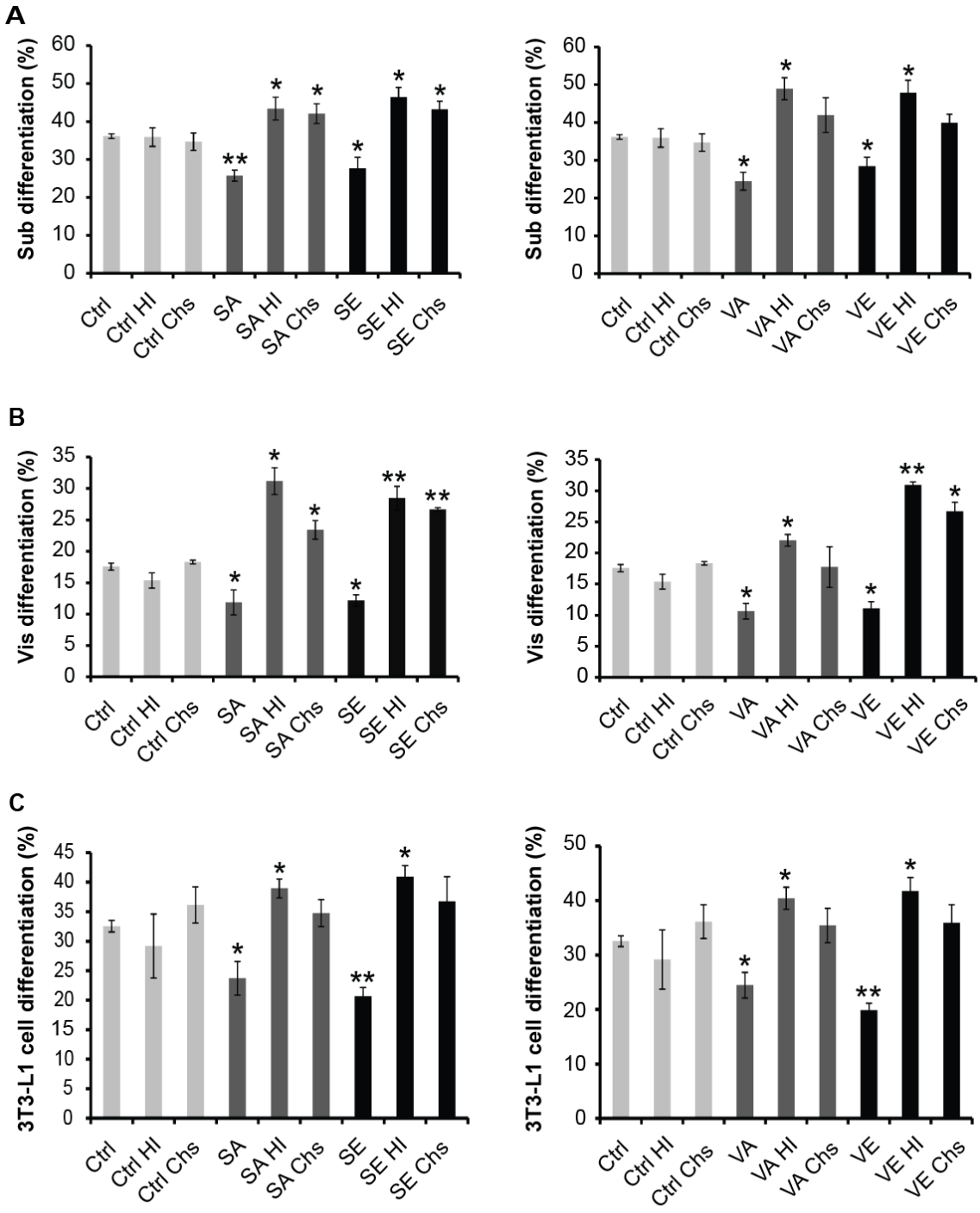

Figure 6. **Heat inactivation or charcoal suspension of adipocytes or adipose tissue secretome induced adipogenesis.** A-C) Sub, Vis or 3T3-L1 cells were treated in the presence or absence of either 10 µg/ml secretions of SA, SE, VA or VE, heat inactivated for 20 min at 95 ^{o}C or dextran-coated charcoal stripped, during induction of differentiation. Control cells were treated with normal media or media heat inactivated

or charcoal stripped. Quantitative analysis of adipocyte differentiation was preformed, using high-throughput image analysis (n = 4). Sub = subcutaneous, Vis = visceral. Ctrl = Control, Ctrl HI = Control heat inactivated, Ctrl Chs = Control charcoal stripped, SA = subcutaneous adipocytes secretion, SA HI = subcutaneous adipocytes secretion heat inactivated, SA Chs = subcutaneous adipocytes secretion charcoal stripped, SE = subcutaneous adipose tissue explants secretion, SE HI = subcutaneous adipose tissue explants secretion heat inactivated, SE Chs = subcutaneous adipose tissue explants secretion charcoal stripped. VA = visceral adipocytes secretion, VA HI = visceral adipocytes secretion heat inactivated, VA Chs = visceral adipocytes secretion charcoal stripped, VE = visceral adipose tissue explants secretion, VE HI = visceral adipose tissue explants secretion heat inactivated, VE Chs = visceral adipose tissue explants secretion charcoal stripped. All values are shown as mean ± SEM (*<0.05, **p<0.01, ***p<0.001).

Identification of secreted factors by adipocyte and adipose tissue explants which regulates adipogenesis

Before analyzing the fractions by MS, we established the optimal culture setup to diminish the contaminant protein leakage to the secretome samples as described above. After insolution digestion SA, SE, VA or VE fractions were subjected to MS analysis (Fig. 8, A-C; supplemental Table, S1-3, Appendix 4) and protein threshold ≥ 99% confidence were analyzed for the presence of signal peptides to identify secreted proteins by using SecretomeP 2.0 and SignalP 3.0. To further confirm whether the identified proteins were secreted by adipocytes and adipose tissue explants a series of published literature was used.

Based on this analysis a total of 49 secreted proteins were identified from subcutaneous adipocyte fraction 1 (SA1), subcutaneous adipose tissue explant fraction 1 (SE1), visceral adipocyte fraction 1 (VA1) and visceral adipose tissue explant fraction 1 (VE1) (Fig. 8A). Out of these 3 proteins were present in SA1, 1 protein in VA1 and 3 proteins present in VE1. When the secretomes of SA1, SE1, VA1 and VE1 were compared, 28 common secreted proteins were identified. Five secreted proteins were shared between SA1 and VA1. A total of 35 secreted proteins were identified from fraction 2 (SA2, SE2, VA2 and VE2), of these 26 were secreted common proteins (Fig. 8B). Only 14 secreted proteins were identified from fraction 3 (SA3, SE3, VA3 and VE3), of which 3 proteins were present in SE3 and 3 proteins in VE3 (Fig. 8C). Common secreted proteins from SA3, SE3, VA3 and VE3 were six (Fig. 8C).

Taken together the data demonstrated that, our culturing set up with several washing steps and culturing adipocytes and adipose tissue explants in serum free media on the insert membrane dramatically decreased serum and intracellular abundant protein leakage. It enhances the identification of secreted protein by MS.

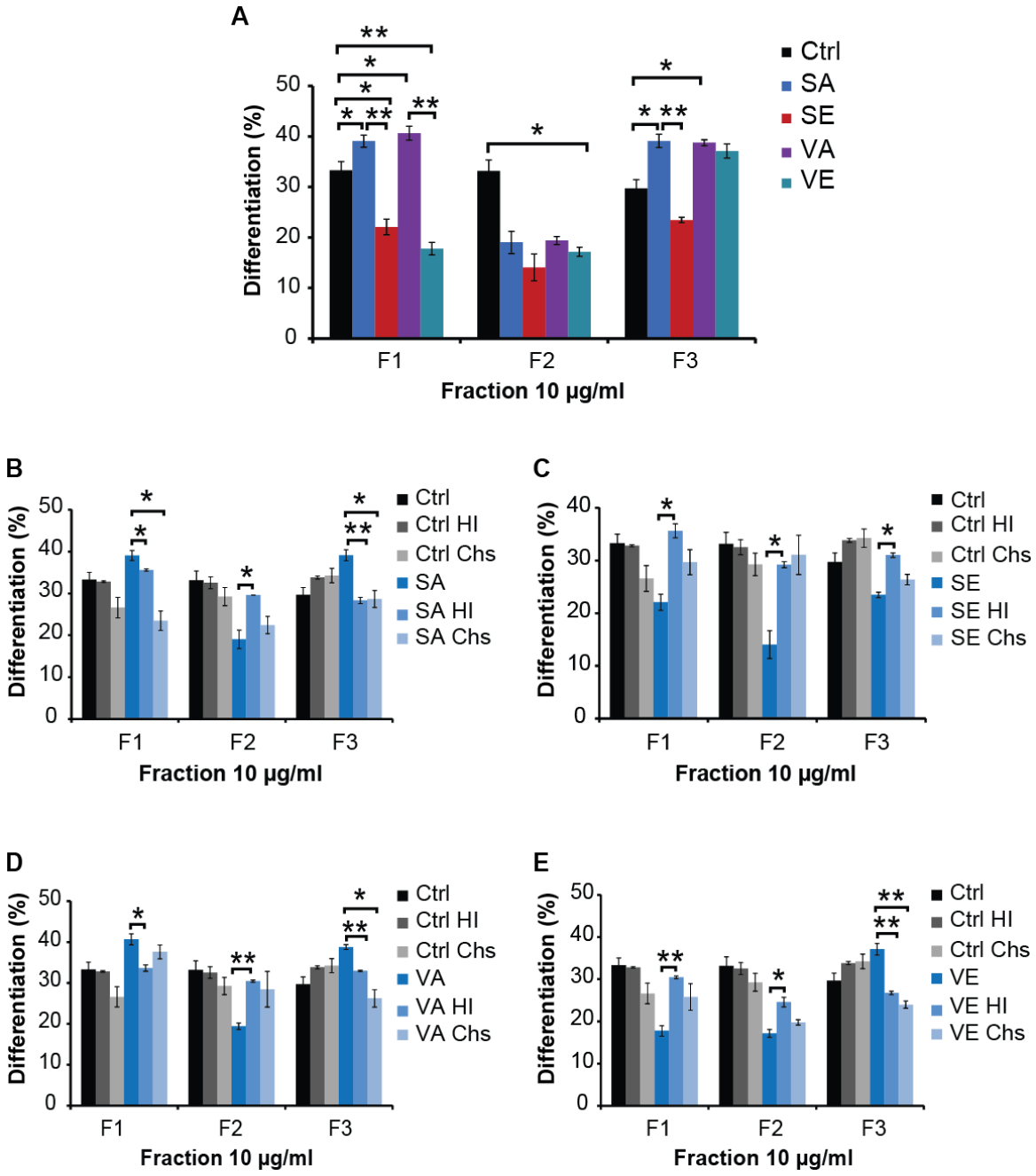

Figure 7. **Effects of SA, SE, VA or VE secretion fractionation on adipogenesis.** Secretion of SA, SE, VA or VE was fractionated into F1, F2 and F3 with anion exchange by using fast protein liquid chromatography (FPLC). A) Cultured 3T3-L1 pre-adipocytes were treated with or without 10 µg/ml fractions during induction of differentiation. Differentiation was quantified using automated image based analysis (n

= 12). B-E) Cultured 3T3-L1 pre-adipocytes were treated in the presence or absence of either 10 µg/ml of SA, SE, VA or VE fractions, heat inactivated or dextran-coated charcoal stripped fractions during induction of differentiation. Control cells were treated with fractionated media or fraction heat inactivated or charcoal stripped. Differentiation was quantified as described above (n = 6). Ctrl = Control, Ctrl HI = Control heat inactivated, Ctrl Chs = Control charcoal stripped, SA = subcutaneous adipocytes fraction, SA HI = subcutaneous adipocytes fraction heat inactivated, SA Chs = subcutaneous adipocytes fraction charcoal stripped, SE = subcutaneous adipose tissue explants fraction, SE HI = subcutaneous adipose tissue explants fraction heat inactivated, SE Chs = subcutaneous adipose tissue explants fraction charcoal stripped. VA = visceral adipocytes secretion, VA HI = visceral adipocytes secretion heat inactivated, VA Chs = visceral adipocytes secretion charcoal stripped, VE = visceral adipose tissue explants secretion, VE HI = visceral adipose tissue explants secretion heat inactivated, VE Chs = visceral adipose tissue explants secretion charcoal stripped. F1=fraction 1, F2= fraction 2, F3= fraction 3. All values are shown as mean ± SEM (*<0.05, **p<0.01, ***p<0.001).

Effects of secreted proteins by adipocytes and adipose tissue explants on adipogenesis

To screen the possible potential candidates among the identified secreted proteins, which influence adipogenesis when the cells were treated with FPLC fractions, we used a short interference (siRNA) custom library. 3T3-L1 pre-adipocytes were reverse transfected with siRNA targeting or non-targeting siRNA control and differentiation was quantified. Among all the identified secreted proteins from SA, SE, VA and VE fraction 1, knockdown of long-chain fatty acid transport protein 1 (Slc27a1) or vimentin (Vim) decreased differentiation whereas aspartate aminotransferase, mitochondrial (Got2), Carboxypeptidase Q (Cpq) or interleukin-1 receptor-like 1 (Il1rl1) promoted differentiation compared to the siRNA control (Fig. 9A). The top secreted protein candidates were chosen from spectral count ≥ 2-fold change plotted against differentiation ≥ 1.3-fold (ratio of adipocyte differentiation with siRNA / siRNA control). We used this cut off to identify factors present in FPLC fractions of SA1 *vs* SE1 and VA1 *vs* VE1 that significantly regulated differentiation. Hence, these selected secreted candidate proteins represent factors present in SA, SE, VA and VE fraction 1 which influence adipogenesis.

Reduction of SPARC, carboxylesterase 1D (Ces1d), fibulin-2 (Fbln2) or Cpq expressions decreased adipocyte differentiation, among other secreted proteins by SA2, SE2, VA2 and VE2 (fraction 2) compared to the siRNA control (Fig. 9B). When the

secreted proteins by SA3 and SE3 were reduced by siRNA mediated knock down, ceruloplasmin (Cp) reduced adipocytes differentiation, while Galectin-3-binding protein (Lgals3bp) or Serotransferrin (Tf) induced differentiation (Fig. 9C). These differentially secreted candidate proteins by SA3/SE3 represent factors which regulate adipocytes formations when the cells were treated with SA or SE fractions 3. Among secreted proteins by VA3 and VE3, knockdown of Cp or Extracellular matrix protein 1 (Ecm1) were found to reduce adipocyte differentiation (Fig. 9D). On the other hand both VA3 and VE3 FPLC fractions were induced differentiation as shown above.

Taken together these results indicate that adipocytes or adipose tissue fractions regulate adipogenesis via differentially secreted factors present in fraction 1; Slc27a1, Vim, Got2, Cpq or Il1rl1, fraction 2: SPARC, Ces1d, Fbln2 or Cpq and fraction 3: Cp, Lgals3bp, Tf or Ecm1.

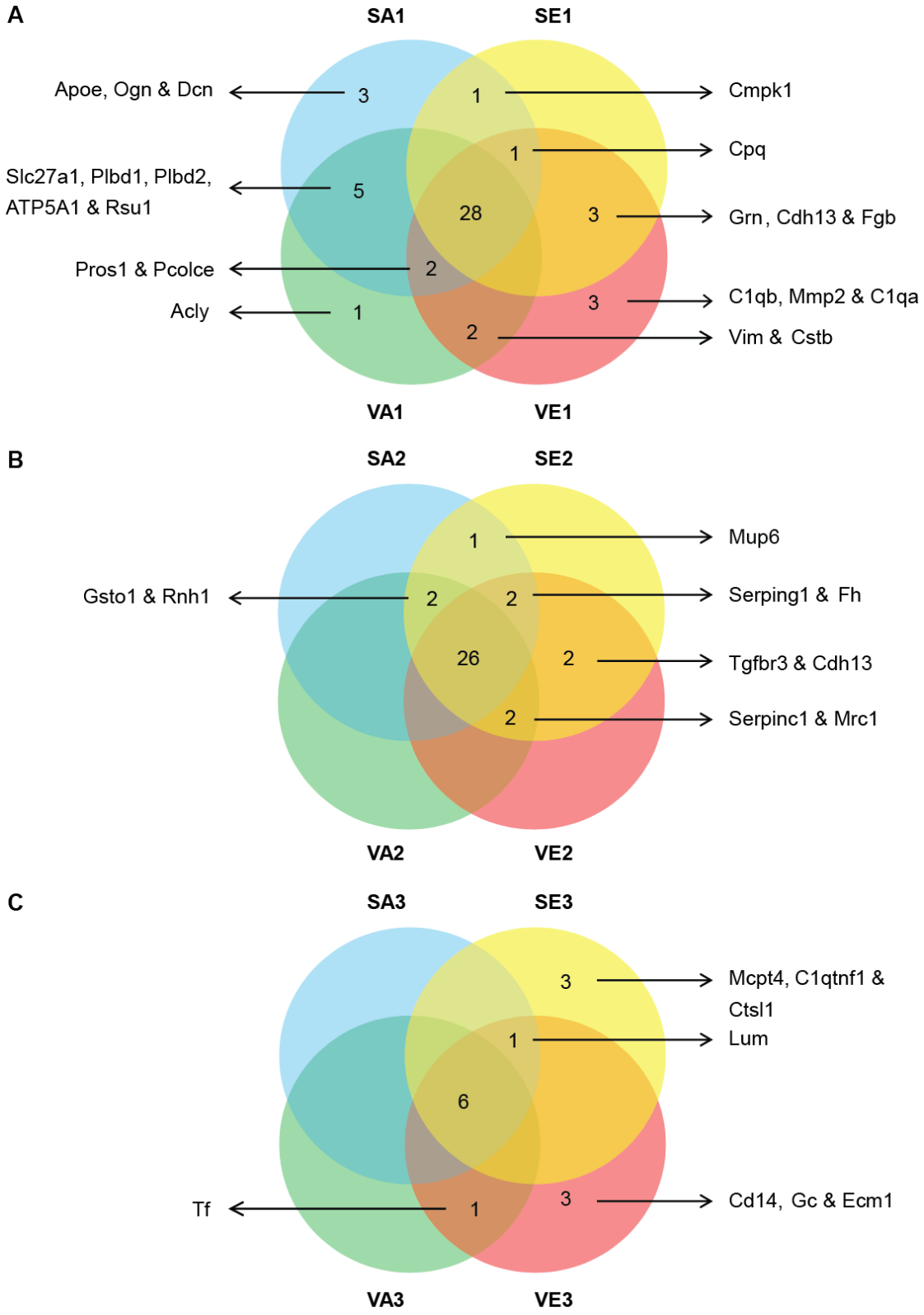

Figure 8. **Identified proteins secreted by adipocyte and adipose tissue explants.** **A**dipocytes or adipose tissue secretion fractions were analyzed by mass spectrometry (MS). A) Venn diagram showing the overlap of secreted protein from SA1, SE1, VA1 and VE1. B) Venn diagram showing the overlap of secreted protein from SA2, SE2, VA2 and VE2. C) Venn diagram showing the overlap of secreted protein from SA3,

SE3, VA3 and VE3. SA1 = subcutaneous adipocytes fraction 1, SE1 = subcutaneous adipose tissue explants fraction 1, VA1 = visceral adipocytes fraction 1, VE1 = visceral adipose tissue explants fraction 1. SA2 = subcutaneous adipocytes fraction 2, SE2 = subcutaneous adipose tissue explants fraction 2, VA2= visceral adipocytes fraction 2, VE2 = visceral adipose tissue explants fraction 2. SA3 = subcutaneous adipocytes fraction 3, SE3 = subcutaneous adipose tissue explants fraction 3, VA3 = visceral adipocytes fraction 3, VE3 = visceral adipose tissue explants fraction 3.

Selected candidate proteins and their effect on differentiation

We identified Slc27a1 in SA1 and VA1. This protein was not detected in SE1 and VE1. Knockdown of Slc27a1 significantly decreased differentiation (Table1). In contrast, Got2 and Cpq secretion increased in VE fraction 1 and their knockdown significantly increased adipocyte formation. Vim secretion was detected only in VA and VE fraction 1 and its secretion increased in VA1, and knockdown of Vim led to significant reduction of lipid droplet formation (Table1). On the other hand, Il1rl1 was highly secreted in SE and VE fraction 1, whereas its knockdown significantly suppressed differentiation.

The secretion of SPARC, Ces1d, Fbln2 and Cpq was detected in all fractions 2 of SA, SE, VA and VE and reduction of their expression significantly induced adipocyte formation (Table1). Secretion of Cp was high in SA3, reduction of Cp expression significantly reduced differentiation, whereas secretion of Lgals3bp and Tf increased in SE3, and their expression reduction significantly induced differentiation (Table1). Ecm1 was only detected in VE3. Its knockdown resulted in reduction of differentiation.

Taken together the data indicate that these differentially secreted identified proteins are biologically active factors present in adipocytes or adipose tissue explants fractions which up regulated or down-regulated adipogenesis.

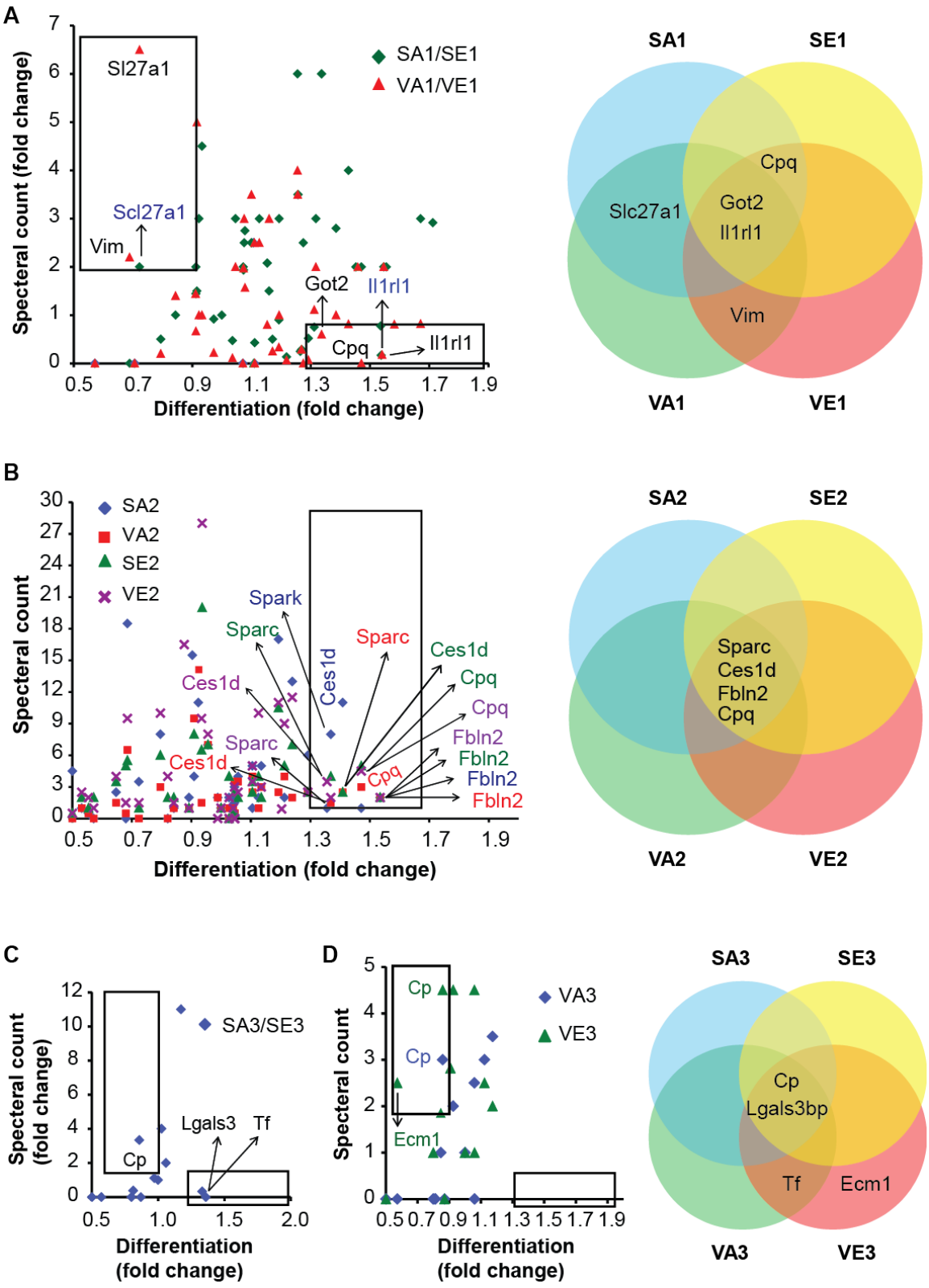

Figure 9. **Regulation of adipocytes formations via identified secreted proteins by adipocyte and adipose tissue explants.** 3T3-L1 pre-adipocytes were reverse transfected with 100 nM of siRNA targeting or non-targeting siRNA control. A-D) Quantitative adipocyte differentiation was analyzed with high-throughput image analysis in cells

transfected with siRNA or siRNA control. Differentiation fold change was obtained by ration of adipocyte formation in cells transfected with siRNA targeting genes and cells transfected with non-targeting siRNA control. A) Differentiation fold changes were plotted against protein spectral count fold change. A) Venn diagram selected candidates of secreted proteins, which regulates adipogenesis based on spectral count ≥ 2-fold change and differentiation ≥ 1.3-fold cut off. B) Differentiation fold changes were plotted against protein spectral count. B) Venn diagram selected candidates of secreted proteins, which regulate adipogenesis based on ≥ 2 spectral count and differentiation ≥ 1.3-fold. C) Differentiation fold changes were plotted against protein spectral count fold change. C) Venn diagram selected candidates of secreted proteins, which regulate adipogenesis ≥ 2-fold spectral count and differentiation ≥ 1.3-fold. D) Differentiation fold change plotted against protein spectral count. D) Venn diagram selected candidates of secreted protein, which regulates adipogenesis ≥ 2 spectral count and differentiation ≥ 1.3-fold.

Expressions of candidate proteins and their feedback loop effect on the regulation of adipogenesis

To validate the secretion of candidate proteins, their expression was evaluated. In agreement with our proteomic data, we found Slc27a1, Cpq, Got2, Vim and Il1rl1 to be expressed both in undifferentiated and differentiated 3T3-L1 cells (Fig. 10A). However, the expression of Cpq, Got2 and Vim mRNA was up regulated during late phase adipocyte differentiation. The expression of Il1rl1 increased in pre-adipocytes then decreased after induction of differentiation from 24 h and onwards. Slc27a1 expression was very low both in pre-adipocytes and adipocytes cells.

The selected candidates from fraction 2; Sparc, Ces1d, Fbln2 and Cpq were expressed during the process of adipocyte differentiation (Fig. 10B), supporting our protein secretion results. The expression of Sparc mRNA was markedly increased during the adipogenic differentiation, whereas Cpq expression up-regulated at 72 h post induction of differentiation. However, Ces1d and Fbln2 expression was found to be very low during adipogenic differentiation of 3T3-L1 cells. The selected candidates from fraction 3 were also expressed in 3T3-L1 cells during adipogenic events (Fig. 10C), confirming the secreted proteins. The expression of Lgals3bp and Cp was low in pre-adipocytes and adipocytes, while Tf expression was highly up regulated only in pre-adipocytes. Ecm1 expression was increased from 6 h up to 48 h during adipocyte differentiation.

Table 1. Candidate proteins secreted by adipocytes and adipose tissue explants, and their effect on adipogenesis. Protein secretion up-regulated, decreased, present or absent in SA, SE, VA and VE fraction 1, 2 and 3.

Accession	Gene name	Description	Spectral count (QNTSC)				Signal peptide NN score	P value	Adipogenesis
			SA	SE	VA	VE			
		Fraction 1							
Q60714	Slc27a1	Long-chain fatty acid transport protein 1	2.0	0.0	6.5	0.0	0.846	0.05	↓
Q9WVJ3	Cpq	Carboxypeptidase Q	2.0	0.5	0.0	1.5	0.599	0.01	↑
P05202	Got2	Aspartate aminotransferase, mitochondrial	6.0	0.2	0.6	1.7	0.51	0.01	↑
P20152	Vim	Vimentin	0.0	0.0	2.2	0.5	0.728	0.03	↓
P14719	Il1rl1	Interleukin-1 receptor-like 1	0.2	6.0	0.2	5.0	0.592	0.02	↑
		Fraction 2							
P07214	Sparc	SPARC	2.0	0.8	0.5	1.3	0.921	0.04	↑
Q8VCT4	Ces1d	Carboxylesterase 1D	4.4	0.8	0.2	1.2	0.757	0.04	↑
P37889	Fbln2	Fibulin-2	2.0	1.0	2.0	2.0	0.58	0.04	↑
Q9WVJ3	Cpq	Carboxypeptidase Q	0.2	0.7	5.0	1.5	0.599	0.01	↑
		Fraction 3							
Q61147	Cp	Ceruloplasmin	3.3	0.3	0.7	1.5	0.632	0.05	↓
Q07797	Lgals 3bp	Galectin-3-binding protein	0.3	3.0	1.2	0.8	0.81	0.05	↑
Q921I1	Tf	Serotransferrin	0.0	3.5	0.0	1.0	0.609	0.04	↑
Q61508	Ecm1	Extracellular matrix protein 1	0.0	0.0	0.0	2.5	0.587	0.05	↓

Identified proteins by mass spectrometry (MS). 3T3-L1 pre-adipocytes were reverse transfected with 100 nM of siRNA targeting or non-targeting siRNA control. Quantitative adipocyte differentiation was analyzed with high-throughput image analysis in cells transfected with siRNA or siRNA control. P value shows effects of selected candidates on differentiation up on knockdown with siRNA. ↑ shows induced adipogenesis, ↓ indicates decreased adipogenesis up on siRNA knockdown. QNTSC = Quantitative normalized total spectral count. SA = subcutaneous adipocytes, SE = subcutaneous adipose tissue explants, VA = visceral adipocytes, VE = visceral adipose tissue explants.

In addition to 3T3-L1 cells, Cpq, Slc27a1, Got2, Vim, Il1rl1, SPARC, Ces1d and Tf were also expressed in white and brown adipose tissue of mice (Supplemental Fig. 1, A-H; Appendix 4). In line with protein secretion, expression of Cpq and Got2 increased in VAT. Expression of Il1rl1 up-regulated both in SAT and VAT while Ces1d increased in

SAT and BAT and Vim was highly up-regulated in BAT (Supplemental Fig. 1, A-H, Appendix 4).

Functional studies revealed the role of candidate proteins in regulating adipogenesis as shown above. To further confirm these effects, cultured 3T3-L1 pre-adipocytes were treated with or without Vim or IL-33 recombinant proteins at the indicated concentrations (Fig. 10, D and E). Recombinant Vim showed a trend toward induced adipocytes differentiation and rescued the suppression effects of Vim on adipogenesis upon its knock down (Fig. 10D). Interestingly, cells treated with IL-33, a specific ligand of Il1rl1 (a secreted soluble ST2 (sST2)), dramatically suppressed differentiation (Fig. 10E). Moreover, treatment of 3T3-L1 with IL-33 during adipocyte differentiation showed a dose-dependent inhibition of adipogenic differentiation as clearly shown in the figures and pictures (Fig. 10E). Confirming the inhibitory effects of Il1rl1 on the number of adipocytes formation, as observed above knocked down of Il1rl1 by siRNA, showed stimulatory effects.

Taken together these results indicate that the secreted candidate proteins were present in pre-adipocytes and adipocytes and regulate adipogenesis via negative or positive feedback loop mechanisms.

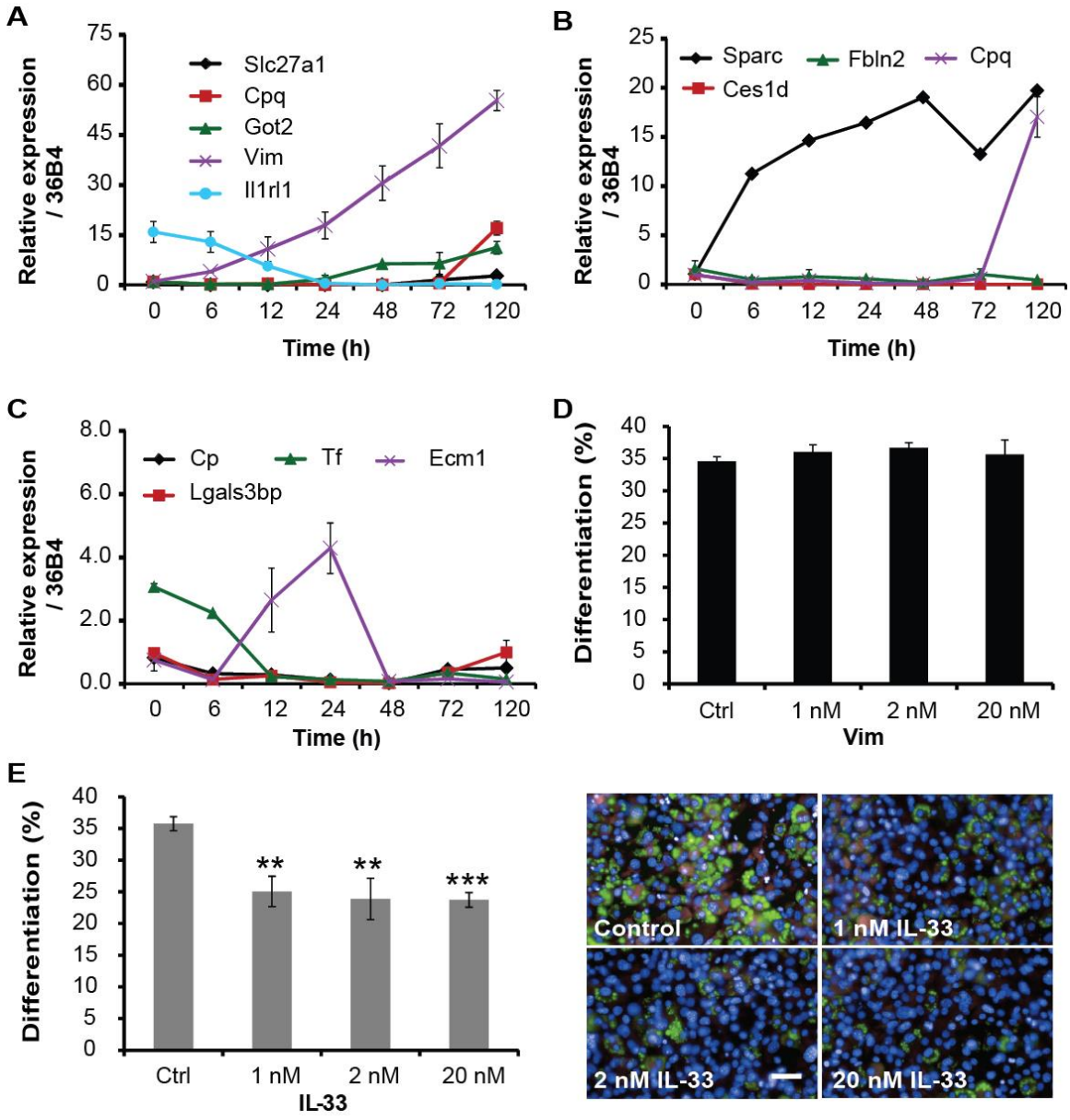

Figure 10. **Candidate proteins expressions and their effect on adipogenesis via feedback loop mechanisms.** A-C) Analysis of Slc27a1, Cpq, Got2, Vim, Il1rl1, SPARC, Ces1d, Fbln2, Lgals3bp, Cp, Tf and Ecm1 mRNA expression at different time points during 3T3-L1 adipocyte differentiation (n = 4). D, E) 3T3-L1 pre-adipocyte was treated with the indicated concentrations of Vim or IL-33 during induction of adipogenesis. Differentiation was quantified as described above (n = 8). All values are shown as mean ± SEM (**p<0.01, ***p<0.001).

4.5. Discussion

Adipose tissue is a crucial organ for the regulation of the whole-body energy metabolism by secreting adipokines that regulate energy intake and expenditure (3,10). Studies have been reported that obesity and its associated metabolic disorders, insulin resistance, diabetes and cardiovascular disease are influenced by actions of impaired secretion of adipokines (27). Interestingly different adipose depots have distinct patterns of adipokine secretion and adipogenic capacity (22); however the differential secretion of adipokines and divergent metabolic effects of adipose depots, especially on adipocytes development has still not been fully elucidated.

In the present study, we hypothesized that there are novel molecules differentially secreted from subcutaneous adipocytes or subcutaneous adipose tissue explants and visceral adipocytes or visceral adipose tissue explants which regulate adipogenesis. In the current study we optimized and established the best *in vitro* culture system for mature primary adipocytes and adipose tissue explant in order to minimize the leakage of serum and intracellular contaminant proteins to secretome sample. By intensive washing and culturing of adipocytes or adipose tissue explants on the insert membrane sieve of a co-culture well, a high quality sample was obtained. These result agreed with the previous findings (21) and confirmed by low protein concentration, protein composition and high cell viability.

Co-culturing of primary adipocytes (SA, VA) or adipose tissue explants (SE, VE) was found to inhibit adipogenic differentiation of primary (Sub, Vis) or 3T3-L1 pre-adipocytes. Consistent with our result, co-culture of primary mature human adipocytes have been reported to inhibit differentiation of pre-adipocytes (28). However, our data are inconsistent with previous findings showing that co-culture of rat mature primary adipocytes or adipose tissue induced pre-adipocyte differentiation (29). This discrepancy might be due to the difference in co-culturing technique used, duration of pre-adipocyte co-cultured with mature fat or fat cell and the difference in pore size of insert membrane, as they have previously used 0.4 µm, which in our system showed no exchange of media between the two co-culture compartments. It has been shown that impaired adipogenesis due to decreased formation of new smaller adipocytes in number and increased adipocytes size causes WAT dysfunction and plays a major role in the

development of obesity, insulin resistance and T2D which as a result lead to the development of metabolic disorders (20).

Treatment of Sub, Vis or 3T3-L1 pre-adipocytes with SA, SE, VA or VE secretion markedly decreased differentiation and confirming the inhibitory effects of these secretions. Similarly, the dysfunction of adipose tissue has been observed in obesity as characterized by decreased adipocyte formation and increased secretion of pro-inflammatory adipokines (30). In addition, our data suggest that there are inhibitory factors secreted from mature primary adipocytes or adipose tissue explants, which halted adipogenesis via cross-talk between mature adipocytes, adipose tissue and pre-adipocytes. In contrast, a conditioned medium collected from differentiating human adipose-derived stem cells (ASCs) showed a positive effect on adipogenic differentiation of human ASCs (31). This inconsistency may be due to the mixture of cells at different differentiation stages in human ASCs, which makes the source of the secreted factors, which induced differentiation unclear.

Interestingly, the inhibitory effects of SA, SE, VA or VE secretion were found to be completely reversed by heat inactivation or charcoal suspension and resulted in significant induction of pre-adipocyte differentiation. These data indicate the presence of protein and free hormones. A previous study has shown that a failure of the recruitment of new adipocytes due to impaired differentiation, decreased lipid storage in adipocytes especially in the postprandial state (20). Consequently, non-adipose tissues are highly exposed to ectopic fat deposition and insulin resistance may develop (9).

Our data demonstrated that the secretion of adipocytes or adipose tissue explants is heat sensitive and could be depleted by charcoal suspension, suggesting degradation or inactivation of the active components and indicating the involvement of a protein. The secretion of adipocytes and adipose tissue was also shown to affect the function of many other metabolic organs and tissues including; muscle, liver, vasculature, and brain (32). Impairment of insulin signaling and glucose uptake in skeletal muscle cells treated with conditioned medium of adipocytes and adipose tissue (32), and the occurrence of hepatotoxicity and insulin-resistance in primary rat hepatocytes co-cultured with adipose tissue explant (33) have been reported. Cumulative studies have also shown the inflammatory proteins secreted from adipocytes and adipose tissue derived macrophages

dramatically increase the risk of cardiovascular disease (34). These data together with our findings elucidate the hallmark of adipose tissue secretion involvement in the regulation of whole body energy metabolism via endocrine, paracrine and/or autocrine mechanisms.

To screen and further confirm the adipogenic differentiation inhibitory factors present in SA, SE, VA or VE secretion, the samples were fractionated by anion exchange column FPLC. So far, fractionation of adipocyte or adipose tissue explant secretions by FPLC is not widely used to investigate the secretome effect on adipogenesis. Surprisingly here, secretions fractionated by FPLC showed both inhibition and activation of adipocyte differentiation, and partly explains the inhibitory effects of SA, SE, VA or VE secretion on differentiation. SE fractions (F1, F2 or F3) or fraction 2 (SA, VA or VE) decreased adipocyte differentiation while SA fractions (F1 or F3), VA (F1 or F3) and VE fraction 3 induced adipocyte formation.

Interestingly, the inhibitory effects of SE secretion were persistent as we still observed the negative effect of SE F1, F2 or F3 on adipocyte formation, suggesting that SE secretes negative adipogenic differentiation factors contrary to VE, indicating the adipose intrinsic depot difference. In the same notion with our findings Du et al. (33) have also shown the up-regulation of inflammation factors secreted from subcutaneous but not from visceral adipose tissue explants in co-culture of adipose tissue explant with hepatocytes, suggesting that the differences were due to the cells in the SVF which secretes negative adipogenic differentiation factors. To our knowledge, this study for the first time showed the positive and negative effects of SA, SE, VA or VE secretion fractionated by FPLC on adipogenesis.

Adipose tissue directly contributes to the pathogenesis of obesity and obesity-related disorders via unbalanced adipokine secretion as mentioned above (27). For instance large adipocytes due to decreased new adipocytes formation secrete pro-inflammatory adipokines, compared to smaller adipocytes which secrete anti-inflammatory adipokines (30). Our data points out, the inhibitory factors of the whole secretion of adipocytes or adipose tissue explant were likely to suppress factors, which induced adipogenesis, and FPLC fractionation reveals the presence of positive factors in the secretion as well.

These findings suggest that, the inhibitory factors might be in high abundance and overshadow the low abundance activation factors present in the whole secretions.

To identify the negative and positive factors present in primary mature adipocytes or adipose tissue explant secretion fractionations, which regulate adipogenic differentiation, proteomic strategies were used. The optimal culture setup (21) followed by FPLC fractionation were integrated for the secretome identification. Based on databases and published literature proteins were identified and the presence of a signal peptide was investigated to distinguish those that are actively secreted by SA, SE, VA or VE from serum and intracellular proteins. With this technique we identified 49 proteins secreted by SA, SE, VA and VE fraction 1 including adiponectin, cystatin-C, resistin and retinol-binding protein 4: the classical proteins (4,21,35-38). Chemerin (3,10) and vimentin (vim) (38): novel adipokine were also among others identified proteins. Long-chain fatty acid transport protein 1 (Slc27a1) secretion by SA and VA fraction 1 was also detected and agrees with the previous report by Wu et al (39). The Slc27a1 has been shown to increase lipid accumulation in 3T3-L1 cells (40). Among 35 secreted proteins by SA, SE, VA and VE fraction 2, SPARC (Sparc), gelsolin and Fibulin-2 (Fbln2) were well-known adipokines (4,21,35,37,38). However, carboxylesterase 1D (Ces1d) secreted by SA, SE, VA and VE fraction 2 has so far not been described as secreted protein by adipocytes. The expression of Ces1d at mRNA by adipocytes has been reported previously (41). Fourteen secreted proteins by SA, SE, VA and VE fraction 3 were also identified.

Taking into account what has been reported previously (3,4,10,21,35-38) to be secreted by primary adipocytes and adipose tissue, 4 new proteins secreted by SA, SE, VA or VE secretion were identified. They are Carboxypeptidase Q (Cpq), aspartate aminotransferase, mitochondrial (Got2), Ces1d and Interleukin 1 receptor-like 1 (Il1rl1). Thus, the discovery of additional novel secreted proteins through this FPLC fractionation method significantly increased our understanding of differential secreted adipokines from different adipose depot and their positive and negative effects on the regulation of adipocyte formation.

Consistent with protein identification results by MS, we show the novel expression of Cpq, Got2, Il1rl1, Vim and Ces1d in 3T3-L1 cells. The expression of Vim, Cpq and

Got2 increased during late phase adipogenic differentiation of 3T3-L1 cells while Il1rl1 expressed during early phase differentiation time points. In agreement with previous data (42), we found that both undifferentiated and differentiated 3T3-L1 cells express SPARC. Slc27a1, Ces1d, Fbln2 Lgals3bp and Cp expression was found to be very low. Tf expression was up-regulated in undifferentiated 3T3-L1 cells while Ecm1 increased from 6 h up to 48 h during adipocyte differentiation. These data confirm the expression and secretion of these selected candidates by white adipocytes and adipose tissue explants.

A recent report identified Got2 as cell a surface protein from cancer cells (43), whereas previous studies considered this protein intracellular. However, Got2 identification as secreted proteins by SA, SE, VA and VE and its up-regulated expression in mature 3T3-L1 adipocytes and VAT verified Got2 is actively secreted protein in line with Karhemo et al. (43). This protein is known to be a cell surface fatty acid transporter protein (44). It is well known that proteins can shuttle between organelles leading to multiple localizations for a single protein (44). Our data for the first time reported the secretion and expression of Got2 by white adipose tissue and its inhibitory effect on adipogenesis via negative paracrine feedback loop mechanism.

Furthermore, we provide the first report that mouse SAT and VAT expresses high levels of Cpq and secrete greater amounts of bioactive Cpq and the expression and secretion increased in VAT. Consistent with these data, we report that differentiated 3T3-L1 cells express increasing amounts of Cpq. We also show that Cpq expressed in other metabolic organs including: liver, brain and brown adipose tissue. In fact, there is no literature available to describe the role of this newly identified secreted protein in energy metabolism. However, these data together with the negative effect of Cpq on adipocyte formation provide strong support for a crucial function of Cpq in adipocyte differentiation and energy homeostasis in adipose and non-adipose metabolic organ. Another protein that has previously not been known to be associated with adipose tissue is Ces1d, which was identified as a secreted protein by adipocytes and adipose tissue. To fully understand the molecular mechanism underlying the effect of Cpq, Got2 and Ces1d on adipogenesis, further *in vitro* and *in vivo* investigation is required.

Several adipokines act in a local autocrine/paracrine fashion to regulate adipocyte differentiation and metabolism (8,9,15,20). Many studies have indicated that the development of insulin resistance and type II diabetes in obesity begins with local adipokine responses (9,15,20). For example down regulation of adiponectin expression in obese subject is partly due to overexpressed TNF-α, MCP-1 and IL-6 (6). This in turn will affect the inflammatory response, since adiponectin attenuates inflammatory responses to multiple stimuli (7,8,15,20,45). Moreover, the presence of macrophages in obese adipose tissue and insulin resistant subjects (9) is characterized by increased expression and secretion of these inflammatory molecules, TNF-α, IL-6 and MCP-1 (7,8,15,45). Thus, TNF-α appears to play a pivotal role with respect to the production of several other adipokines and affect adipocyte development and energy metabolism (7,8,15,20,45).

In the current study, it was found that, recombinant Vim treatment induced adipogenic differentiation of 3T3-L1 cells and rescued Vim knockdown effect on adipogenesis. A previous study indicated that disruption of Vim during adipose conversion of 3T3-L1 cells affects differentiation (46). Vim with other intermediate filament proteins is also involved in stabilizing the architecture of the cytoplasm (47). It has been reported that Vim knockout mice under special conditions, such as injury showed phenotypic abnormalities (47). Our finding of much higher expression of Vim in brown and white adipose tissue compared to other organs of lean mice indicates the wide effects of Vim in the development and function of both white and brown adipocyte.

Although knockdown of Il1rl1 expression induced adipogenic differentiation, treatment of 3T3-L1 cells by recombinant IL-33 protein, ligand of Il1rl1, markedly reduced adipocyte differentiation. Recently, the expression of IL-33 in adipocytes has been reported (48). However, there are no reports on the secretion of Il1rl1 by murine adipocytes and its influence on adipogenesis. Therefore, the present study is the first to show the secretion and a potential relationship between Il1rl1 and adipogenesis *in vitro*. The expression of Il1rl1 early in 3T3-L1 adipocyte differentiation and its increased expression in SAT and VAT of mouse suggests the local actions of Il1rl1on adipocytes. Il1rl1 or ST2, is a member of the toll-like receptor superfamily (49) and sST2 a secreted soluble form of Il1rl1/ST2 which can serve as a decoy receptor for IL-33 (50). Interestingly, a soluble decoy form of ST2 limits the biological effect of IL-33 (sST2)

(51). Recent studies indicate a protective role for IL-33 and ST2L in atherosclerosis and cardiac remodeling (51). IL-33 treatment reduced hypertrophy and fibrosis following transverse aortic constriction (TAC) *in vivo* via a reduction in NFκB activation. In contrast, ST2−/− mice had more fibrosis, and impaired survival compared with WT littermates following TAC (51).

The observed data confirm and provide convincing evidence that Il1rl1 has critical function in regulating adipogenesis likely via autocrine and/or local action, indicating the involvement of Il1rl1 in the regulation of metabolic disorders, in addition to its protective role in cardio vascular disease (51).

In conclusion, we were able to identify differentially secreted factors from SA, SE, VA or VE secretion fractions that positively or negatively regulate adipogenesis. Both co-culture and FPLC fractionation followed by identification of secreted factors and their functional role on adipocytes has improved our understanding of the paracrine and/or autocrine function of adipocytes and adipose tissue. The current evidence indicate that of all the adipocytes and adipose tissue secreted factors only Slc27a1, Vim, Got2, Cpq, Il1rl1, SPARC, Ces1d, Fbln2, Cpq, Cp, Lgals3bp, Tf and Ecm1 regulates adipocyte differentiation via distinct patterns of adipokine secretion from different adipose depot. The findings demonstrate that mouse adipocytes and adipose tissue secretes several paracrine, autocrine and endocrine factors, which could affect whole body energy metabolism. The expression and secretion of new identified molecules (Cpq, Got2, Il1rl1 and Ces1d) and Vim from adipocytes and adipose tissue together with their negative or positive paracrine and/or autocrine feedback loop mechanisms on adipogenic regulation indicates their wide range of effects on energy homeostasis.

4.6. References

1. Zimmet, P., Alberti, K. G. M. M., and Shaw, J. (2001) *Nature* **414**, 782-787
2. Bays, H. E., Gonzalez-Campoy, J. M., Bray, G. A., Kitabchi, A. E., Bergman, D. A., Schorr, A. B., Rodbard, H. W., and Henry, R. R. (2008) *Expert Rev Cardiovasc Ther* **6**, 343-368
3. MacDougald, O. A., and Burant, C. F. (2007) *Cell Metab* **6**, 159-161
4. Hocking, S. L., Wu, L. E., Guilhaus, M., Chisholm, D. J., and James, D. E. (2010) *Diabetes* **59**, 3008-3016
5. Zhang, Y., Proenca, R., Maffei, M., Barone, M., Leopold, L., and Friedman, J. M. (1994) *Nature* **372**, 425-432
6. MacDougald, O. A., and Burant, C. F. (2007) *Cell Metab* **6**, 159-161
7. Trayhurn, P., and Beattie, J. H. (2001) *Proc Nutr Soc* **60**, 329-339
8. Vazquez-Vela, M. E., Torres, N., and Tovar, A. R. (2008) *Arch Med Res* **39**, 715-728
9. Goossens, G. H. (2008) *Physiol Behav* **94**, 206-218
10. Bozaoglu, K., Bolton, K., McMillan, J., Zimmet, P., Jowett, J., Collier, G., Walder, K., and Segal, D. (2007) *Endocrinology* **148**, 4687-4694
11. Trayhurn, P., Bing, C., and Wood, I. S. (2006) *J Nutr* **136**, 1935S-1939S
12. Goralski, K. B., McCarthy, T. C., Hanniman, E. A., Zabel, B. A., Butcher, E. C., Parlee, S. D., Muruganandan, S., and Sinal, C. J. (2007) *J Biol Chem* **282**, 28175-28188
13. Horowitz, J. F., Coppack, S. W., and Klein, S. (2001) *Am J Clin Nutr* **73**, 517-522
14. Yu, Y. H., and Ginsberg, H. N. (2005) *Circ Res* **96**, 1042-1052
15. Karastergiou, K., and Mohamed-Ali, V. (2010) *Mol Cell Endocrinol* **318**, 69-78
16. Hausman, D. B., DiGirolamo, M., Bartness, T. J., Hausman, G. J., and Martin, R. J. (2001) *Obes Rev* **2**, 239-254
17. Gustafson, B., Gogg, S., Hedjazifar, S., Jenndahl, L., Hammarstedt, A., and Smith, U. (2009) *Am J Physiol Endocrinol Metab* **297**, E999-E1003
18. Wolfrum, C., Shih, D. Q., Kuwajima, S., Norris, A. W., Kahn, C. R., and Stoffel, M. (2003) *J Clin Invest* **112**, 345-356
19. Meissburger, B., Ukropec, J., Roeder, E., Beaton, N., Geiger, M., Teupser, D., Civan, B., Langhans, W., Nawroth, P. P., Gasperikova, D., Rudofsky, G., and Wolfrum, C. (2011) *EMBO Mol Med* **3**, 637-651
20. Heilbronn, L., Smith, S. R., and Ravussin, E. (2004) *Int J Obes Relat Metab Disord* **28 Suppl 4**, S12-21
21. Alvarez-Llamas, G., Szalowska, E., de Vries, M. P., Weening, D., Landman, K., Hoek, A., Wolffenbuttel, B. H., Roelofsen, H., and Vonk, R. J. (2007) *Mol Cell Proteomics* **6**, 589-600
22. Feng, B., Zhang, T., and Xu, H. (2013) *Ann N Y Acad Sci* **1281**, 160-177
23. Macotela, Y., Emanuelli, B., Mori, M. A., Gesta, S., Schulz, T. J., Tseng, Y. H., and Kahn, C. R. (2012) *Diabetes* **61**, 1691-1699
24. Challa, T. D., Beaton, N., Arnold, M., Rudofsky, G., Langhans, W., and Wolfrum, C. (2012) *J Biol Chem* **287**, 6421-6430
25. Meissburger, B., Stachorski, L., Roder, E., Rudofsky, G., and Wolfrum, C. (2011) *Diabetologia* **54**, 1468-1479
26. Bendtsen, J. D., Jensen, L. J., Blom, N., Von Heijne, G., and Brunak, S. (2004) *Protein Eng Des Sel* **17**, 349-356

27. Kershaw, E. E., and Flier, J. S. (2004) *The Journal of clinical endocrinology and metabolism* **89**, 2548-2556
28. Janke, J., Engeli, S., Gorzelniak, K., Luft, F. C., and Sharma, A. M. (2002) *Diabetes* **51**, 1699-1707
29. Shillabeer, G., Forden, J. M., and Lau, D. C. (1989) *J Clin Invest* **84**, 381-387
30. Deng, Y., and Scherer, P. E. (2010) *Annals of the New York Academy of Sciences* **1212**, E1-E19
31. Hemmingsen, M., Vedel, S., Skafte-Pedersen, P., Sabourin, D., Collas, P., Bruus, H., and Dufva, M. (2013) *PLoS One* **8**, e63638
32. Hajer, G. R., van Haeften, T. W., and Visseren, F. L. (2008) *Eur Heart J* **29**, 2959-2971
33. Du, Z. Y., Ma, T., Lock, E. J., Hao, Q., Kristiansen, K., Froyland, L., and Madsen, L. (2011) *PLoS One* **6**, e20917
34. Lamounier-Zepter, V., Ehrhart-Bornstein, M., Karczewski, P., Haase, H., Bornstein, S. R., and Morano, I. (2006) *Faseb J* **20**, 1653-1659
35. Kratchmarova, I., Kalume, D. E., Blagoev, B., Scherer, P. E., Podtelejnikov, A. V., Molina, H., Bickel, P. E., Andersen, J. S., Fernandez, M. M., Bunkenborg, J., Roepstorff, P., Kristiansen, K., Lodish, H. F., Mann, M., and Pandey, A. (2002) *Mol Cell Proteomics* **1**, 213-222
36. Wang, P., Mariman, E., Keijer, J., Bouwman, F., Noben, J. P., Robben, J., and Renes, J. (2004) *Cell Mol Life Sci* **61**, 2405-2417
37. Rosenow, A., Arrey, T. N., Bouwman, F. G., Noben, J. P., Wabitsch, M., Mariman, E. C., Karas, M., and Renes, J. (2010) *J Proteome Res* **9**, 5389-5401
38. Chen, X., Cushman, S. W., Pannell, L. K., and Hess, S. (2005) *J Proteome Res* **4**, 570-577
39. Wu, Q., Ortegon, A. M., Tsang, B., Doege, H., Feingold, K. R., and Stahl, A. (2006) *Mol Cell Biol* **26**, 3455-3467
40. Choi, H., Kim, S. J., Park, S. S., Chang, C., and Kim, E. (2011) *FEBS Lett* **585**, 2763-2767
41. Friedrichsen, M., Poulsen, P., Wojtaszewski, J., Hansen, P. R., Vaag, A., and Rasmussen, H. B. (2013) *PLoS One* **8**, e56861
42. Chavey, C., Boucher, J., Monthouel-Kartmann, M. N., Sage, E. H., Castan-Laurell, I., Valet, P., Tartare-Deckert, S., and Van Obberghen, E. (2006) *Obesity (Silver Spring)* **14**, 1890-1897
43. Karhemo, P. R., Ravela, S., Laakso, M., Ritamo, I., Tatti, O., Makinen, S., Goodison, S., Stenman, U. H., Holtta, E., Hautaniemi, S., Valmu, L., Lehti, K., and Laakkonen, P. (2012) *Journal of proteomics* **77**, 87-100
44. Bradbury, M. W., and Berk, P. D. (2000) *Biochem J* **345 Pt 3**, 423-427
45. Gastaldelli, A., Natali, A., and Corradini, S. G. (2010) *Dig Liver Dis* **42**, 310-319
46. Lieber, J. G., and Evans, R. M. (1996) *J Cell Sci* **109 (Pt 13)**, 3047-3058
47. Mor-Vaknin, N., Punturieri, A., Sitwala, K., and Markovitz, D. M. (2003) *Nature cell biology* **5**, 59-63
48. Saidi, S., Bouri, F., Lencel, P., Duplomb, L., Baud'huin, M., Delplace, S., Leterme, D., Miellot, F., Heymann, D., Hardouin, P., Palmer, G., and Magne, D. (2011) *Cytokine* **53**, 347-354
49. Yagami, A., Orihara, K., Morita, H., Futamura, K., Hashimoto, N., Matsumoto, K., Saito, H., and Matsuda, A. (2010) *J Immunol* **185**, 5743-5750
50. Miller, A. M. (2011) *Journal of inflammation* **8**, 22
51. Miller, A. M., and Liew, F. Y. (2011) *Pharmacology & therapeutics* **131**, 179-186

Chapter 5

5. Summary and prospective ideas

Obesity, the excessive accumulation of adipose tissue, is strongly associated with the development of metabolic disorders (1-6). Understanding the molecular biology of adipose tissue may translate into potential therapeutic intervention for the epidemic of obesity and T2D across the globe. Adipose tissue development or adipogenesis has been shown to be highly regulated by nutrition in addition to other elements including genetic, hormone and environmental factors (7). Adipocytes express many receptors to respond to local and systemic signals to regulate adipogenesis and energy metabolism (8). The aim of this PhD thesis was to understand the cross talk between adipose tissue, intestinal wall, and the brain to regulate and modulate energy metabolism through adipokines and incretin hormones.

In Chapter 2, we investigate the cross-talk between gastrointestinal wall and adipose tissue to regulate energy homeostasis. GLP-1 and GIP, incretin hormones, are released from the gut in response to food intake and enhance insulin secretion (9). We show that, GLP-1 or its analog liraglutide act as the signal transduction between the intestinal wall and the adipocytes thereby inducing adipogenesis as confirmed both *in vitro* and *in vivo.* GLP-1 was found to mediate its adipogenic effect via GLP-1R through the regulation of early phase of adipogenic differentiation markers C/ebpβ, δ and PPARγ via activation of ERK, PKC, and AKT signaling pathways (Fig.1). Activation of ERK, PKC, and AKT signaling pathways results in GLP-1 mediated Ser-136 phosphorylation of Bad that lead to the inhibition of apoptosis and thereby increasing pre-adipocyte proliferation (Fig.1). Our data demonstrate the cross-talk between the intestinal wall and adipose tissue through GLP-1 signal transduction.

In Chapter 3, we studied gut brain communication in the regulation of energy metabolism through GIP receptor using a newly generated mouse model. In addition to its insulinotropic actions in maintaining glucose homeostasis (10), GIP is also involved in fat metabolism (11). It promotes adipogenesis (Fig.1). On the other hand, *Gipr*$^{-/-}$ and defective leptin (*Gipr*$^{-/-}$, *Lep*^{ob}/*Lep*^{ob}) mice are protected from diet induced obesity and its associated complications that occur with defective leptin signaling, including T2D

and fatty liver (12). This indicates that specific metabolic organs must play a major role in the diet-induced regulation of body weight by GIPr.

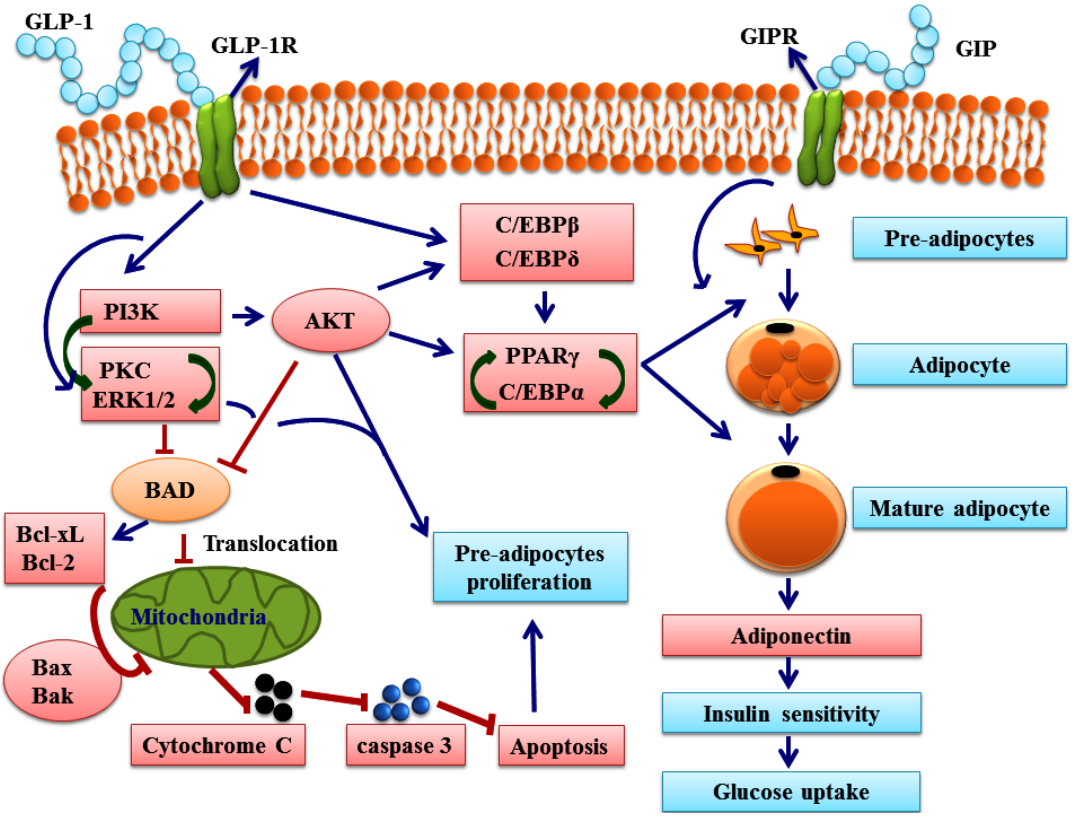

Figure 1. Summary of the molecular mechanisms underlying the adipogenic differentiation effect of GLP-1 and its receptor in 3T3-L1 cells. The involvement of GIP in adipocytes formation in 3T3-L1 cells.

The role of GIP action in the CNS on energy homeostasis has not been well studied, even though it is known that both GIP and the GIPr are expressed in the CNS (13,14). In the current study CNS-specific hGIPr deletion protects high fat diet induced obesity, insulin resistance and fatty liver, thereby improving insulin sensitivity and glucose tolerance. This effect is achieved in part via increased physical activity and suppression of caloric intake. In order to understand the molecular mechanisms underlying the central effect of GIP in the regulation of whole body energy metabolism further investigation will be necessary. In future studies, it will be of interest to identify signaling pathways or neuropeptides regulated by GIPr inactivation by using gene array methodologies. Moreover, it will be very interesting to dissect the GIP/GH/IGF signaling pathways to understand whether GIP signaling affects the pituitary-liver axis to control mouse development and metabolic status via IGF-1.

In Chapter 4, we investigated the role of novel adipokines, secreted by adipocytes or adipose tissue explants and their role on adipogenesis. There are several known active molecules secreted from adipocytes or adipose tissue explants. We specifically sought to identify novel adipokines and investigate their paracrine and autocrine role on adipogenesis.

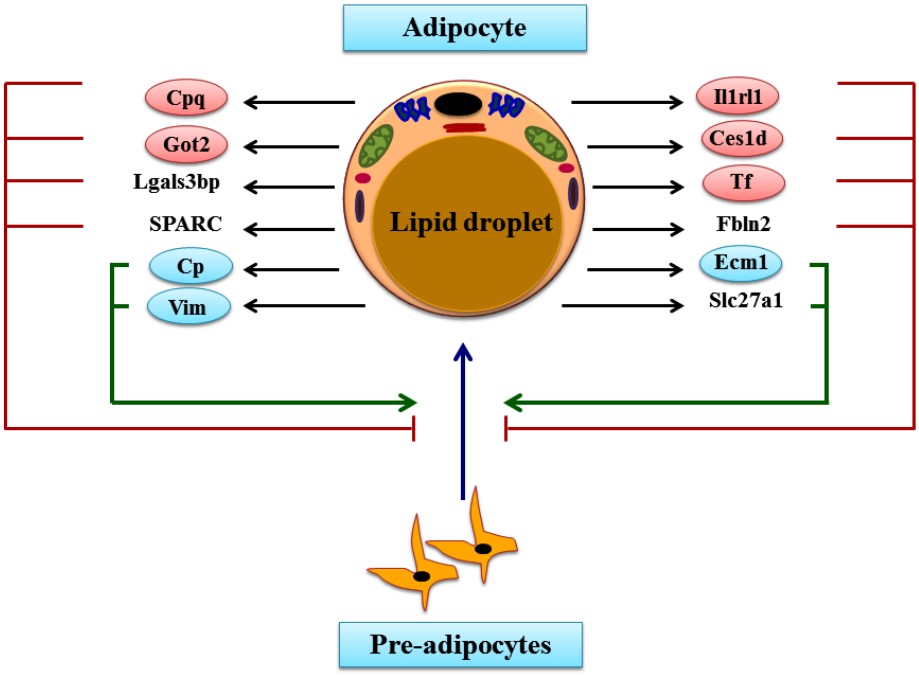

Figure 2. Some of the identified adipokines secreted by adipocytes and their role in adipocytes development.

We could show that fractions obtained from adipocyte or adipose tissue explants secretion using FPLC technique positively or negatively regulated adipogenesis through cross-talk mechanisms. Using a fractionation technique and proteomic approach, we found novel adipokines secreted by adipocyte or adipose tissue explants that induce or reduce adipocyte formation via paracrine/autocrine feedback loop mechanisms (Fig.2). Among other secreted adipokines, we identified Cpq, Got2, Il1rl1, Tf and Ces1d as novel secreted factors that reduce adipocyte formation, while Vim, Cp and Ecm1 promoted the formation of adipocytes from pre-adipocytes.

Our findings reveal that adipocyte and adipose tissue secrete several paracrine, autocrine and endocrine factors, which could affect whole body energy metabolism. The discovery of additional novel secreted proteins adds to our understanding of the

differential secreted adipokines from different adipose depot and their positive and negative effects on the regulation of adipocyte development. The studies reported in this thesis are representing a stepping-stone for future studies investigating the adipogenic differentiation markers underlying these novel adipokines.

5.1. References

1. Matsuzawa, Y., Fujioka, S., Tokunaga, K., and Tarui, S. (1992) *Proc Soc Exp Biol Med* **200**, 197-201
2. Montague, C. T., and O'Rahilly, S. (2000) *Diabetes* **49**, 883-888
3. Anderson, J. W., Hamilton, C. C., and Brinkman-Kaplan, V. (1992) *Am J Gastroenterol* **87**, 6-15
4. Dowling, H. J., and Pi-Sunyer, F. X. (1993) *Diabetes* **42**, 537-543
5. Pi-Sunyer, F. X. (1993) *Ann Intern Med* **119**, 655-660
6. Bays, H. E., Gonzalez-Campoy, J. M., Bray, G. A., Kitabchi, A. E., Bergman, D. A., Schorr, A. B., Rodbard, H. W., and Henry, R. R. (2008) *Expert Rev Cardiovasc Ther* **6**, 343-368
7. Lefterova, M. I., and Lazar, M. A. (2009) *Trends in endocrinology and metabolism: TEM* **20**, 107-114
8. Goossens, G. H. (2008) *Physiol Behav* **94**, 206-218
9. Brown, J. C., Dryburgh, J. R., Frost, J. L., Otte, S. C., and Pederson, R. A. (1978) *Adv Exp Med Biol* **106**, 169-171
10. Miyawaki, K., Yamada, Y., Yano, H., Niwa, H., Ban, N., Ihara, Y., Kubota, A., Fujimoto, S., Kajikawa, M., Kuroe, A., Tsuda, K., Hashimoto, H., Yamashita, T., Jomori, T., Tashiro, F., Miyazaki, J., and Seino, Y. (1999) *Proc Natl Acad Sci U S A* **96**, 14843-14847
11. Yabe, D., and Seino, Y. (2011) *Progress in biophysics and molecular biology* **107**, 248-256
12. Miyawaki, K., Yamada, Y., Ban, N., Ihara, Y., Tsukiyama, K., Zhou, H., Fujimoto, S., Oku, A., Tsuda, K., Toyokuni, S., Hiai, H., Mizunoya, W., Fushiki, T., Holst, J. J., Makino, M., Tashita, A., Kobara, Y., Tsubamoto, Y., Jinnouchi, T., Jomori, T., and Seino, Y. (2002) *Nat Med* **8**, 738-742
13. Nyberg, J., Anderson, M. F., Meister, B., Alborn, A. M., Strom, A. K., Brederlau, A., Illerskog, A. C., Nilsson, O., Kieffer, T. J., Hietala, M. A., Ricksten, A., and Eriksson, P. S. (2005) *J Neurosci* **25**, 1816-1825
14. Nyberg, J., Jacobsson, C., Anderson, M. F., and Eriksson, P. S. (2007) *J Neurosci Res* **85**, 2099-2119

Appendix – Chapter 2

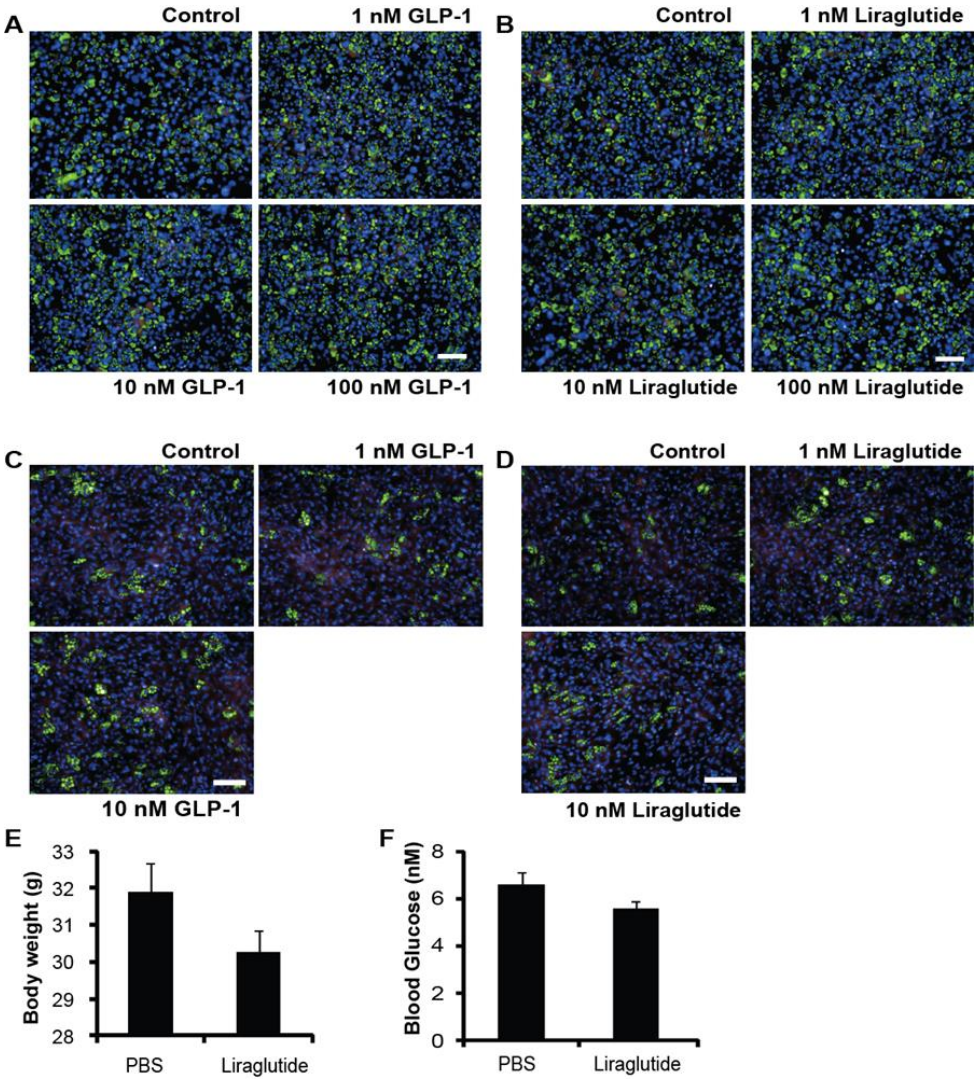

Supplemental Fig. 1. A and **B**) Cultured 3T3-L1 cells were incubated with indicated amounts of GLP-1 or liraglutide at onset of differentiation for 2 days; on day 8 differentiated 3T3-L1 cells were stained for lipid droplet formation (Bodipy 493/503, green), nuclei (Hoechst, blue), and cytosol (Syto60, red). Lipid droplet formation of differentiated adipocytes was quantified with high-throughput image analysis. Representative images of n=12 experiments. **C** and **D**) Primary pre-adipocytes were incubated with indicated amounts of GLP-1 or liraglutide at onset of differentiation for 2 days; on day 8 differentiated 3T3-L1 cells were stained for lipid droplet formation (Bodipy 493/503, green), nuclei (Hoechst, blue), and cytosol (Syto60, red). Lipid droplet formation of differentiated adipocytes was quantified with high-throughput image analysis. Representative images of n=4 experiments. **E**) Body weight from mice treated with twice daily s.c. injection of liraglutide (100µg/kg) for 17 days (n=12). **F**) Fasted blood glucose levels in mice treated with twice daily s.c. injection of liraglutide (100µg/kg) for 17 days (n=12). The graphs represents mean ± SEM (**p<0.01, ***p<0.001).

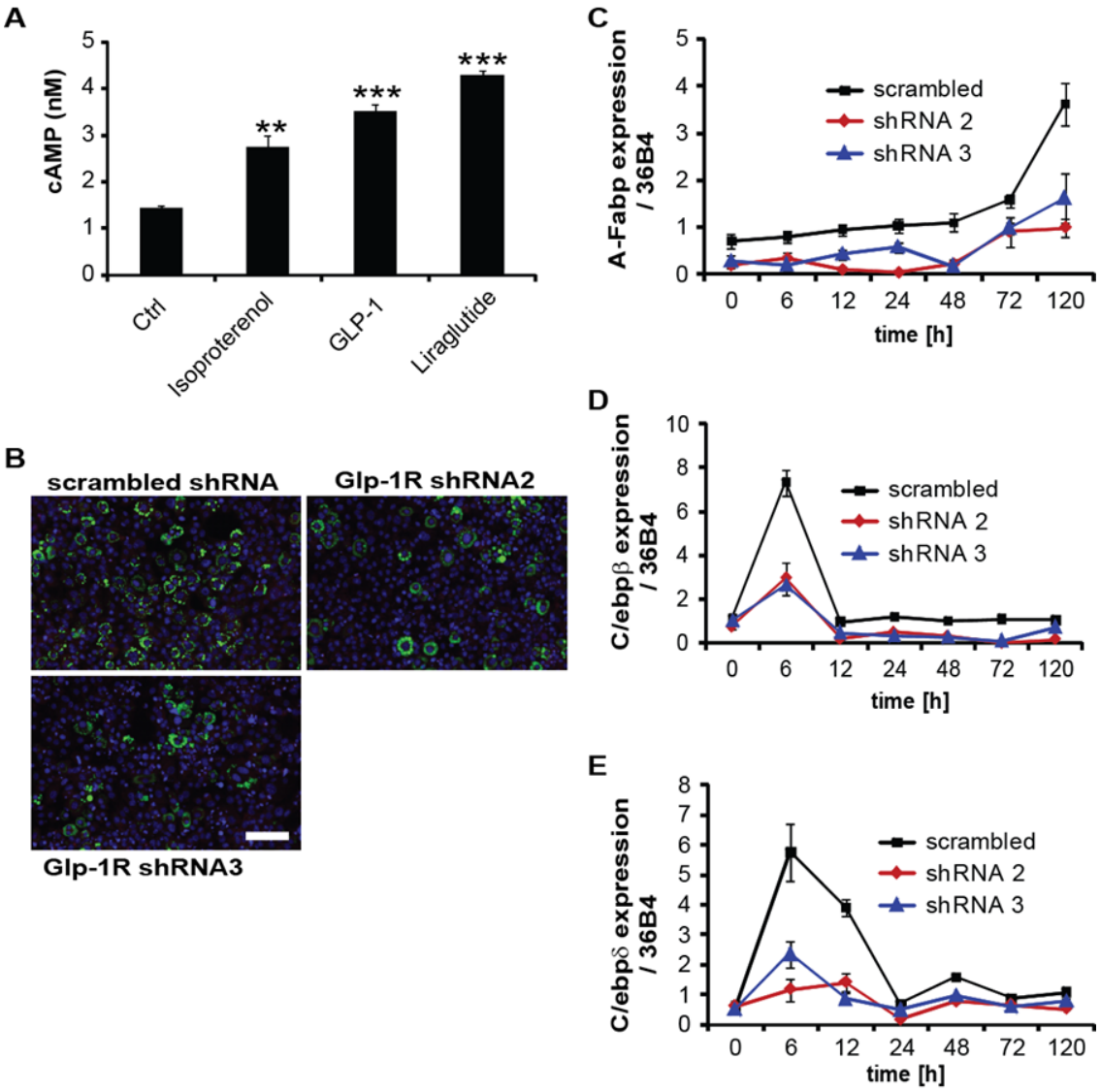

Supplemental Fig. 2. A) Intracellular cAMP levels in 3T3-L1 pre-adipocytes following treatment with 1, 10, and 100 nM GLP-1 or liraglutide for 30 min. 10 µM isoproterenol was used as positive control (n=4). **B**) Analysis of adipocyte differentiation using high-throughput image analysis in cells infected with GLP-1R shRNA expressing lentivirus or scrambled shRNA control and treated with 10 nM GLP-1 during induction of cell differentiation. Representative images shown are of n=12 experiments. **C, D** and **E**) Analysis of A-Fabp and C/ebpβ/δ mRNA expression in 3T3-L1 pre-adipocytes infected with GLP-1R shRNA expressing lentivirus (shRNA2 and shRNA3) or scrambled shRNA (n=4) and treated with 10 nM GLP-1 during induction of cell differentiation. The graphs represents mean ± SEM (**p<0.01, ***p<0.001).

Table 1. Primers used for relative quantification real-time PCR (all primers are suitable for mouse cDNA, F = forward, R = reverse)

Gene		Primer sequences
36B4	F	GCCGTGATGCCCAGGGAAGACA
	R	AACCCGCGGCCTTCTACGAG
GLP-1R	F	CGGAAATGCTGGGAGCGCTG
	R	GGACCACAGGAGGACCGGCA
C-Jun	F	ACCGCCGCGCCAAGACTCG
	R	AACTGGGTGGGGGGTCTGTGTAG
C/EBP β	F	GGTCGAGCGCAACAACATC
	R	CTCGGGCAGCTGCTTGAACAA
C/EBPδ	F	AACCCGCGGCCTTCTACGAG
	R	CACGGCGGCCATGGAGTCAA
PPAR γ	F	AGGCGAGGGCGATCTTGACAG
	R	AATTCGGATGGCCACCTCTTTG
A-FABP	F	ATGAAATCACCGCAGACGACAG
	R	GCCTTTCATAACACATTCCACCAC

Appendix – Chapter 3

Table 1. Genotyping primers used for PCR amplification (F= forward, R= reverse)

Gene		Primer sequences	Amplicon Size
hGIPr-flox	F	GAGACTCTGGCTACTCATCC	Internal Positive Control: 585 bp
	R	CCTTCAGCAAGAGCTGGGGAC	
	F	AGTCTCGCTTTGTTGCAAGG	Hetrozygous /homozygous humanized alleles: 343 bp
	R	CAAGACAGGTGGATCACAAGG	
	F	ACCTGTTCACGTCTTTCATGC	Hetrozygous /homozygous humanized alleles: 343 bp
	R	GTCGACGATGCATGCTAGC	
	F	CTTTCCCAGCTGAGCTTGC	wild type alleles: 282 bp
	R	ACCTCCTCTGCTACCTTCCAG	
	F	GGCAGAAGCACGCTTATCG	Flp transgene: 343 bp
	R	GACAAGCGTTAGTAGGCACAT	
NesCre-TG	F	GCGGTCTGGCAGTAAAAACTATC	Transgene: 100 bp
	R	GTGAAACAGCATTGCTGTCACTT	
	F	CTAGGCCACAGAATTGAAAGATCT	Internal Positive Control: 324 bp
	R	GTAGGTGGAAATTCTAGCATC	

Table 2. Primers used for relative quantification real-time PCR (all primers are suitable for mouse cDNA, F = forward, R = reverse, except hGIPr which is for human cDNA)

Gene		Primer sequences
36B4	F	GCCGTGATGCCCAGGGAAGACA
36B4	R	AACCCGCGGCCTTCTACGAG
hGIPr	F	TGTTTGCTCCCGTGACAGAG
hGIPr	R	CGACTGCACCTCCTTGTTGA
POMC	F	ACCCTCGTTTCTCTGCGCATC
POMC	R	AGGGCCCCTGAGCGACTGTA
PMCH	F	CCAATGCACTCTTGTTTGGC
PMCH	R	ATTGTTCCAGAGAAGGGGCG
AGRP	F	GCCATCTTCCACCTTTGCAG
AGRP	R	CCTGGTCAGGCCTTCTGATG
CART	F	CCTGCTGCTACTGCTACCTTT
CART	R	CGCTTCGATCAGCTCCTTCT
Npy	F	TGGACTGACCCTCGCTCTAT
Npy	R	GGGGCGTTTTCTGTGCTTTC
IGF1	F	ACCAAAATGACCGCACCTGC
IGF1	R	AACACTCATCCACAATGCCTGTC

Appendix – Chapter 4

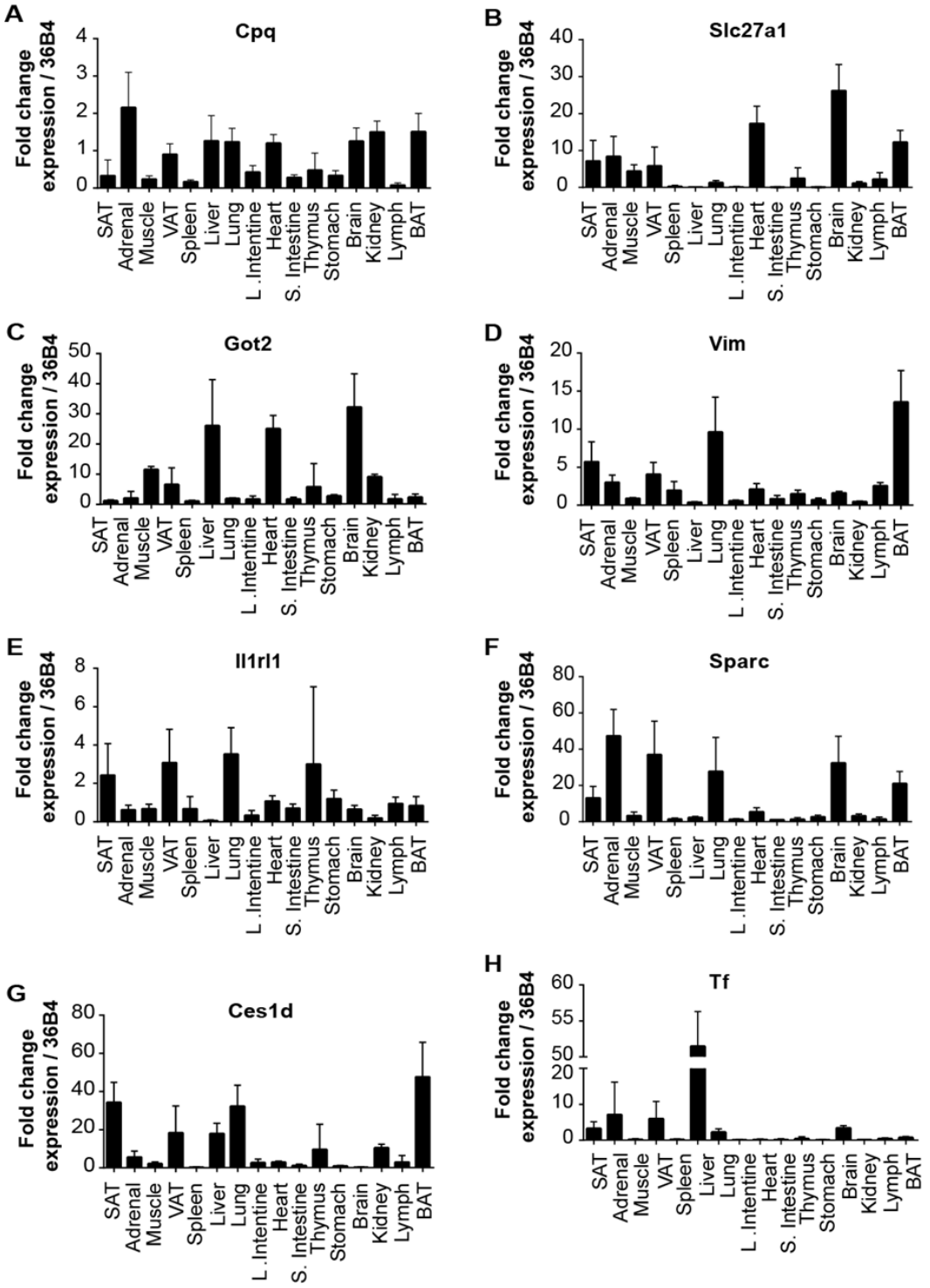

Supplemental Figure 1. A-H) Expression of Cpq, Slc27a1, Got2, Vim, Il1rl1, SPARC, Ces1d and Tf mRNA in fat tissue and different tissue of mice (n = 4). SAT = subcutaneous adipose tissue, VAT = visceral adipose tissue, BAT= brown adipose tissue.

Supplemental Table 1. Compression of secreted proteins identified from subcutaneous and visceral adipocytes and adipose tissue explants. Proteins secretion up-regulated, decreased, present or absent in SA1, SE1, VA1 and VE1 fractions.

Accession	Gene name	Description	Spectral count (QNTSC)				signal peptide NN score
			SA1	SE1	VA1	VE1	
P08226	Apoe	Apolipoprotein E	2.5	0.0	0.0	0.0	0.938
Q62000	Ogn	Mimecan	2.5	0.0	0.0	0.0	0.567
P28654	Dcn	Decorin	2.5	0.0	0.0	0.0	0.533
Q60714	Slc27a1	Long-chain fatty acid transport protein 1	2	0.0	6.5	0.0	0.846
Q8VCI0	Plbd1	Phospholipase B-like 1	2.5	0.0	3.5	0.0	0.789
Q3TCN2	Plbd2	Putative phospholipase B-like 2	2.5	0.0	3	0.0	0.757
Q08761	Pros1	Vitamin K-dependent protein S	4.5	0.0	1.0	1.0	0.65
A5A6H5	ATP5A1	ATP synthase subunit alpha, mitochondrial	2	0.0	2	0.0	0.574
Q61398	Pcolce	Procollagen C-endopeptidase enhancer 1	3	0.0	1.0	1.0	0.554
Q01730	Rsu1	Ras suppressor protein 1	3.5	0.0	3.5	0.0	0.52
P21460	Cst3	Cystatin-C	3.0	0.3	2.0	0.5	0.945
Q60994	Adipoq	Adiponectin	3.0	0.3	2.5	0.4	0.879
P11152	Lpl	Lipoprotein lipase	4.0	0.3	0.6	1.8	0.83
P08228	Sod1	Superoxide dismutase [Cu-Zn]	3.0	0.3	2.0	0.5	0.76
P18242	Ctsd	Cathepsin D	3.0	0.3	1.0	1.0	0.751
P07356	Anxa2	Annexin A2	6.0	0.2	4.0	0.3	0.739
P06797	Ctsl1	Cathepsin L1	3.0	0.3	0.8	1.3	0.686
P48759	Ptx3	Pentraxin-related protein PTX3	2.0	0.5	2.0	0.5	0.666
P35505	Fah	Fumarylacetoacetase	2.0	0.5	0.7	1.5	0.604
Q9WVJ3	Cpq	Carboxypeptidase Q	2.0	0.5	0.0	1.5	0.599
P06151	Ldha	L-lactate dehydrogenase A chain	2.1	0.5	0.8	1.3	0.568
P62962	Pfn1	Profilin-1	2.8	0.4	1.6	0.6	0.56
O88342	Wdr1	WD repeat-containing protein 1	2.0	0.5	2.0	0.5	0.518
P05202	Got2	Aspartate aminotransferase, mitochondrial	6.0	0.2	0.6	1.7	0.51
P10649	Gstm1	Glutathione S-transferase Mu 1	2.8	0.4	1.0	1.0	0.505
Q9DD06	Rarres2	Retinoic acid receptor responder protein 2	1.0	1.0	1.4	0.7	0.959
Q99P87	Retn	Resistin	0.1	7.0	0.6	1.7	0.914
P12032	Timp1	Metalloproteinase inhibitor 1	0.3	3.5	0.3	3.5	0.86
Q91VU0	Fam3c	Protein FAM3C	0.5	2.1	0.1	9.0	0.813
Q9D6Y7	Msra	Mitochondrial peptide methionine sulfoxide reductase	1.5	0.7	5.0	0.2	0.784
Q00724	Rbp4	Retinol-binding protein 4	0.8	1.3	1.1	0.9	0.76
Q8VCM7	Fgg	Fibrinogen gamma chain	0.3	3.3	0.1	14.0	0.654
P37804	Tagln	Transgelin	0.1	7.5	0.1	15.0	0.645

Supplemental Table 1 **(…continued)**

Accession	Gene name	Description	Spectral count (QNTSC)				signal peptide NN score
			SA1	SE1	VA1	VE1	
Q9DBP5	Cmpk1	UMP-CMP kinase	0.4	2.3	0.0	0.0	0.613
P21180	C2	Complement C2	0.5	2.0	0.3	4.0	0.596
P14719	Il1rl1	Interleukin-1 receptor-like 1	0.2	6.0	0.2	5.0	0.592
Q61581	Igfbp7	Insulin-like growth factor-binding	0.9	1.1	0.2	4.5	0.565
O88844	Idh1	Isocitrate dehydrogenase [NADP] cytoplasmic	0.5	2.0	0.2	5.0	0.563
P13020	Gsn	Gelsolin	0.9	1.1	0.3	3.0	0.55
Q9DBB8	Dhdh	Trans-1,2-dihydrobenzene-1,2-diol dehydrogenase	1.5	0.7	3.0	0.3	0.518
P20152	Vim	Vimentin	0.0	0.0	2.2	0.5	0.728
Q62426	Cstb	Cystatin-B	0.0	0.0	2.5	0.4	0.556
Q91V92	Acly	ATP-citrate synthase	0.0	0.0	1.5	0.0	0.532
P28798	Grn	Granulins	0.0	1.5	0.0	1.5	0.651
Q9WTR5	Cdh13	Cadherin-13	0.0	2	0.0	2.5	0.617
Q8K0E8	Fgb	Fibrinogen beta chain	0.0	1.5	0.0	1.5	0.564
P14106	C1qb	Complement C1q subcomponent subunit B	0.0	0.0	0.0	1	0.897
P33434	Mmp2	72 kDa type IV collagenase	0.0	0.0	0.0	2	0.589
P98086	C1qa	Complement C1q subcomponent subunit A	0.0	0.0	0.0	2	0.767

The proteins were identified after FPLC fractionation by mass spectrometry (MS). QNTSC = Quantitative normalized total spectral count used for the analysis. SA1 = subcutaneous adipocytes fraction 1, SE1 = subcutaneous adipose tissue explants fraction 1, VA1 = visceral adipocytes fraction 1, VE1 = visceral adipose tissue explants fraction 1.

Supplemental Table 2. Compression of secreted proteins identified from subcutaneous and visceral adipocytes and adipose tissue explants. Proteins secretion up-regulated, decreased, present or absent in SA2, SE2, VA2 and VE2 fractions.

Accession	Gene name	Description	Spectral count (QNTSC)				signal peptide NN score
			SA2	SE2	VA2	VE2	
P07214	Sparc	SPARC	2.0	0.8	0.5	1.3	0.921
O88668	Creg1	Protein CREG1	4.0	1.0	0.3	1.0	0.886
P02762	Mup6	Major urinary protein 6	3.5	0.2	0.0	0.0	0.864
P03953	Cfd	Complement factor D/ adipsin	2.5	1.0	0.4	1.0	0.858
Q8VCT4	Ces1d	Carboxylesterase 1D	4.4	0.8	0.2	1.2	0.757
O09131	Gsto1	Glutathione S-transferase omega-1	4.0	0.3	0.3	0.0	0.744
P97290	Serping1	Plasma protease C1 inhibitor	9.0	0.0	0.1	0.5	0.725
Q63918	Sdpr	Serum deprivation-response protein	2.0	1.4	0.5	0.7	0.654
Q9EQH2	Erap1	Endoplasmic reticulum aminopeptidase 1	2.0	1.0	0.5	1.0	0.637
P10923	Spp1	Osteopontin	2.0	0.8	0.5	1.3	0.627
P35700	Prdx1	Peroxiredoxin-1	2.4	1.0	0.4	1.0	0.542
Q91VI7	Rnh1	Ribonuclease inhibitor	6.0	0.5	0.2	0.0	0.526
P01887	B2m	Beta-2-microglobulin	2.0	1.5	0.5	0.7	0.523
P97807	Fh	Fumarate hydratase, mitochondrial	3.5	0.0	0.3	1.5	0.51
P07724	Alb	Serum albumin	1.7	2.3	0.6	0.4	0.553
P10605	Ctsb	Cathepsin B	1.3	0.3	0.8	3.3	0.852
O54724	Ptrf	Polymerase I and transcript release factor	0.4	0.4	2.5	2.3	0.722
Q61646	Hp	Haptoglobin	1.9	0.2	0.5	5.8	0.72
P09470	Ace	Angiotensin-converting enzyme	0.7	0.4	1.4	2.7	0.653
P28862	Mmp3	Stromelysin-1	0.5	0.6	2.0	1.7	0.629
Q9WVJ3	Cpq	Carboxypeptidase Q	0.2	0.7	5.0	1.5	0.599
P70663	Sparcl1	SPARC-like protein 1	0.3	0.7	3.5	1.4	0.594
P00920	Ca2	Carbonic anhydrase 2	0.5	0.4	2.0	2.5	0.579
Q9R045	Angptl2	Angiopoietin-related protein 2	0.5	0.7	2.0	1.5	0.568
Q61171	Prdx2	Peroxiredoxin-2	0.2	1.3	4.5	0.8	0.562
P13020	Gsn	Gelsolin	1.6	0.2	0.6	4.4	0.55
Q9JHI0	Mmp19	Matrix metalloproteinase-19	0.6	1.2	1.7	0.9	0.548
P01027	C3	Complement C3	0.8	0.5	1.3	2.1	0.536
P82198	Tgfbi	Transforming growth factor-beta-induced protein ig-h3	0.5	0.1	2.0	10.0	0.523
P02088	Hbb-b1	Hemoglobin subunit beta-1	1.7	0.2	0.6	6.3	0.508
Q61830	Mrc1	Macrophage mannose receptor 1	0.0	0.5	0.5	2.0	0.597
P32261	Serpinc1	Antithrombin-III	0.0	0.3	0.3	3.0	0.557
O88393	Tgfbr3	Transforming growth factor beta receptor type 3	0.0	2.0	0.0	0.0	0.674
Q9WTR5	Cdh13	Cadherin-13	0.0	2.0	0.0	0.0	0.617
P37889	Fbln 2	Fibulin-2	2.0	1.0	2.0	0.5	0.581

The proteins were identified after FPLC fractionation by mass spectrometry (MS). QNTSC = Quantitative normalized total spectral count used for the analysis. SA2 = subcutaneous adipocytes fraction 2, SE2 = subcutaneous adipose tissue explants fraction 2, VA2 = visceral adipocytes fraction 2, VE2 = visceral adipose tissue explants fraction 2.

Supplemental Table 3. Compression of secreted proteins identified from subcutaneous and visceral adipocytes and adipose tissue explants. Proteins secretion up-regulated, decreased, present or absent in SA3, SE3, VA3 and VE3 fractions.

Accession	Gene name	Description	Spectral count (QNTSC)				signal peptide NN score
			SA3	SE3	VA3	VE3	
P23953	Ces1c	Carboxylesterase 1C	2.0	0.5	0.6	1.8	0.877
Q61147	Cp	Ceruloplasmin	3.3	0.3	0.7	1.5	0.632
Q61233	Lcp1	Plastin-2	11.0	0.1	1.8	0.6	0.51
Q62356	Fstl1	Follistatin-related protein 1	4.0	0.3	0.5	2.0	0.507
Q07797	Lgals3bp	Galectin-3-binding protein	0.3	3.0	1.2	0.8	0.81
P51885	Lum	Lumican	0.4	2.7	0.0	3	0.556
P21812	Mcpt4	Mast cell protease 4	0.0	2	0.0	0.0	0.969
Q9QXP7	C1qtnf1	Complement C1q tumor necrosis factor-related protein 1	0.0	9.5	0.0	0.0	0.705
P06797	Ctsl1	Cathepsin L1	0.0	4	0.0	0.0	0.686
Q921I1	Tf	Serotransferrin	0.0	3.5	0.0	1	0.609
O88322	Nid2	Nidogen-2	1.1	0.9	0.4	2.3	0.712
P10810	Cd14	Monocyte differentiation antigen CD14	0.0	0.0	1	0.0	0.703
P21614	Gc	Vitamin D-binding protein	0.0	0.0	1	0.0	0.595
Q61508	Ecm1	Extracellular matrix protein 1	0.0	0.0	0.0	2.5	0.587

The proteins were identified after FPLC fractionation by mass spectrometry (MS). QNTSC = Quantitative normalized total spectral count used for the analysis. SA3 = subcutaneous adipocytes fraction 3, SE3 = subcutaneous adipose tissue explants fraction 3, VA3 = visceral adipocytes fraction 3, VE3 = visceral adipose tissue explants fraction 3.

Table 4. The sequence of SMARTpool siRNAs targeting genes

Gene	5' --> 3'	5' --> 3'
Apoe	GCGCCUAGCUGUGUACAAG	CCAGGAGAAUCAAUGAGUA
	GAACAGACCCAGCAAAUAC	CAGAUCAGCUCGAGUGGCA
Ogn	ACCAGAAAGUCUACGUGUA	GCUAAUGACACUCGUUACA
	CAUAAAAUGAUCAGCGUUU	GGAGCGAAUUGAAGAGAUU
Dcn	AGUAUAUCCAGGUCGUCUA	CUGUGAGUCUUUACGGCAA
	CCACUUAGUAAAGCGUUAA	GAUGAGGCUUCUGGCAUAA
Pros1	GUUUAAAUAUGACGUGGUA	GUGAAUGUCCCGACGGCUA
	GCAAAUACCUUGUUCGAAG	AGGGCAACCUUGAACGAGA
Pcolce	GGACAAUUACGGUGCCCGA	CCAACUGGCCUGAGUCGUA
	AUGUGGAGCCUGACACGUA	AGUCAAACCACCCACUAAA
Slc27a1	UGACGGUGGUACUGCGCAA	GGGCUUUGCACCAGGCGAU
	CCUCUCAGGUGACGUGCUA	GGGCAUGGAUGAUCGGCUG
Plbd1	UGUAGAAUACUCCGAUCAA	GGACUACUCUUAUGACUUA
	CAAGGGAACGUGACGGACA	GAUACUGGGCUUCCUAUAA
Plbd2	GAGACUGUAUUCAACGCUA	CAGCUAUGAAGGCCGUUUA
	UCGAAUACGAAGUCGGCUA	GUGCUGGAGUGGAUACGAA
Atp5a1	GGUUGACGCCCUCGGUAAU	ACGAUGGGACCGACGAGAA
	UGGUGAUGGUAUUGCGCGA	GCAGCCAAGAUGAACGAUU
Rsu1	UAUCUAAGCGACAACGAUU	GCCACCAAAUGUAGCGGAA
	GCAAAUGAAUACAGCGUGC	GCAGACACAUGCAAGCGAA
Ctsd	GCCCAGUACUAUGGCGAUA	CCAUGCAGUCAUCGCCUAA
	CAACAAUAGGGUCGGCUUU	ACCUGAACGUCACUCGAAA
Ctsl	GAAUUGAUGGGUAGCGGUA	GGACUGUUCUCACGCUCAA
	GGGAAUACAGCAACGGGCA	GUAAAUACAGAGCCGAGUU
Cpq	GCAGAAAUGAUGUCUCGAA	GAGGGAAGAUCAUUGUUUA
	GAAUGGUGUUUCUCAGCGA	CAACAUCCAUCGUCACAAA
Got2	GCUCCAAGGUUAUCGCUAC	ACAUGGGCCUGUACGGUGA
	GUGCAGACCAUUUCCGGGA	CAGAGCAGGUAGAGCGGCU
Gstm1	GGGUGACGCUCCCGACUUU	CGUCUACAAUAAAGUCUGA
	CUACAUCGCAACACCUAUA	AAGAUGGCCCACUGGAGUA
Lpl	GGAUGGACGGUAACGGGAA	CCACAAGUGUAGUCGUCAU
	GGAGGUGGACAUCGGAGAA	CAACCAGGCCUUCGAGAUU
Fah	GCAAGGAGAAUGCGCUGUU	GGAACAAAGGCCAUCGAUG
	CCAUAGGAGACUACACGGA	CAACCCAAAGCCACGGAUU
Ldha	CAACUGCAGGCUUCGAUUA	GUACGUCCAUGAUGCAUAU
	CAGCCUAGGCCGACGAGUU	GAACCAACCACCCAAGUGU
Pfn1	GCAAAGACCGGUCAAGUUU	UGGAACGCCUACAUCGACA
	GGGAAUUUACAAUGGAUCU	CUUCGUUAGCAUUACGCCA

Table 4 **(…continued)**

Gene	5' --> 3'	5' --> 3'
Cst3	GUGGAGAUGGGCCGAACUA	GUACCAAGUCCCAGACAAA
	GGUGAGAGCUCGUAAGCAG	GCGAGUACAACAAGGGCAG
Adipoq	CGAAGAUGACGUUACUACA	CUUCACAAUAUUCGCAUGA
	AGUAUUAUCCACACGUGUA	GCAGAUAACGUCAACGACU
Ptx3	UCCCAAUGCGUUCGAAGAA	GGGAUCGGGUUCUCAGCGA
	AUGUGAAUUUGGACAACGA	AAAUGUAGCUUACGUGUUA
Wdr1	UGGAUGACACAGUGCGGUA	CAACAGGGAGUGAUGAUAA
	CUACAGUGGACAAGGCGUU	GGAGCAUCUUCUAAAGUAU
Anxa2	GCUCAGUUAUUGACUACGA	CCAGUAUGAUGCUUCGGAA
	GGACAUUGCCUUCGCCUAU	GCAAAGGGCAGACGAGCAG
Sod1	UGAUUGGGAUUGCGCAGUA	GCAGGGAACCAUCCACUUC
	GGACAAAUUACAGGAUUAA	AAGAGAGGCAUGUUGGAGA
Rarres2	GAUAGUCCACUGCCCAAUU	GGACAGAGCCCGAACUCAG
	CAAAUAAGCCCUAGACAGG	CUUCCUACCUGGACAGUUU
Vim	CCAGAGAGAGGAAGCCGAA	GUCUUGACCUUGAACGGAA
	AGGAAGAGAUGGCUCGUCA	AAGCAGGAGUCAAACGAGU
Cstb	AGUCCCAGCUUGAAUCGAA	GAUAAAUGCGUGCACUUGA
	CAACAAAGAAAGGCACGAU	CAAGGUUGAUGUUGGUGGA
Retn	UUAAAUUGCUGGACAGUCU	GUGGGACAUUCGUGAAGAA
	GAUCAAACAAGACUUCAAC	UGAUGUCGGUCAGUUGAGA
Timp1	GCAGAUAUCCGGUACGCCU	CGGGAAAUUUCACAUCAAU
	GGGCUAAAUUCAUGGGUUC	GAUUCAAGGCUGUGGGAAA
Fam3c	GCUAAUGGCUACAUACGAU	CUUGAAGAGUCCCGAUUAU
	GGGAUGAGGCCACACGUAA	GAAGAAUAAUGUCGGAAGA
Msra	GGGACAAGUGUUCUACUAU	CGAAAGUCAUCUCCGCAGA
	GCAAGAACCCAGACGGCUA	CCUGAAGGUUCCAUCAACA
Rbp4	GGAUCGAACACAAUGGUUA	GAAUCUGGAUGGCACCUGU
	GUAGCAACGUCUAGGAUGU	CGAGAAGGGUCAUAUGAGC
Fgg	GGGACAACGACAACGAUAA	GGGAUGCCUUCGACGGCUA
	CGAGACAAGCAUUCGGUAU	GGAAAUGGUUGGACCGUAU
Tagln	CAUGACAGGCUAUGGGCGA	CGGCAGAUCAUCAGUUAGA
	CCACUGUCCUUGAUAUCGA	CUCUAUGAAGGUAAGGAUA
Cmpk1	CAAUAAAGUUUGAAGUCCA	GGGUAUCAGCUAAUUCUUG
	GCAGUAUAUUGGGAUUUGA	GAUAAAGCAAUCUAAUGGU
C2	GCUUUGAGUGUGACGAAGA	GUUCCAAGAAGGAUGGCGA
	UGAGGUAAAUGUCACGGUA	CAAUAUCACCGGUGGUAAU
Il1rl1	CCAAAGAGGACGCUCGACU	GUCCAACAAUUGACCUGUA
	UCAAGAAGAGGAAGGUCGA	AUGAUAAGGCACACCAUAA
Igfbp7	UCAGUUAUAACCUGCGAAU	GCUGUGAGGUCAUCGGGAU
	GAGUAUGAGUGCCACGCAU	AAGGACAUCUGGAACGUCA

Table 4 **(…continued)**

Gene	5' --> 3'	5' --> 3'
Igfbp7	UCAGUUAUAACCUGCGAAU	GCUGUGAGGUCAUCGGGAU
	GAGUAUGAGUGCCACGCAU	AAGGACAUCUGGAACGUCA
Idh1	GAUGAAAUGACACGAAUCA	CAGGAUAAGUCAAUUGAAG
	CAAAUUAGCUCAGGCCAAA	GAAGUAUGAUGGGCGUUUC
Gsn	CAACAGGAUCGGACGCUUU	GCGCGUACCUUUCGAUGCU
	GGUCAAAGGACGCCGUGUA	GAGUGGCCGUGCUCAAGUA
Dhdh	GCUUAAUUGCCAACGACUU	CCGAGGAGUUCGCACAGAA
	GUGAGAAACCCAUGGGCGU	CAGGAUAAACGCUGAUACA
Cdh13	CGAUAGCGACAGACCCGAA	ACGAGAAGCUGCACUACGA
	CUACAUCGAUCCCGAGAAA	UGAUUGACCAGAACGACAA
Mmp2	ACCAAGAACUUCCGAUUAU	GAACGCUGAUGGCGAGUAC
	CAUACAGGAUCAUUGGUUA	GACAAGUGGUCCGCGUAAA
C1qa	GGGACGAGGUGUGGAUCGA	CCGCAAAGGGUCGCAUUUA
	CCCAAGGACUGAAGGGCGU	GGAUGGGGCUCCAGGAAAU
Sparc	GCACCACACGUUUCUUUGA	UGAAGUUGCUGAGGAGAUA
	CUACAUCGGACCAUGCAAA	CCAGAACCAUCAUUGCAAA
Creg1	CAUAUAAUGAUGUCGGGAA	ACGCAGACACACACCGACA
	UUUAAUUGAGUGUGCGUAU	GAAAGGAACCGCAGGAAUU
Cfd	UACCGGAUGUGGAUCGAAA	UGGAUGGAGUGACGGAUGA
	CUGACAGCCUUGAGGACGA	CGUCUGUGGCAAUGGCAAA
Ces1d	GAGGGUCAGCUGUGCUUAA	AUGUCAAUUUGGAAGGAUU
	CUUGAUGGCUGAUGUGGUA	GGCAGUAAUAGGAGACCAU
Gsto1	CCUCUUGUGAGCAUCGAAA	AGAAUAAGCCCGAGUGGUU
	GCCAAGACCUACCGCGAGU	AGGAGGGCAUGGAUAAUUA
Serping1	UGGGUAAAGUAGCCAACGA	GAGCUUUGUGAUCGUGGUA
	CCCAUGAUGAGUAGCGUAA	GCUUCAGCUCCUCCGGUUA
Sdpr	UCGUCAGAACAUCGAGAAA	GAAGGAGUGAGGUGAAUAA
	UAAGAAAGUCCGAGAGGGA	UAGCAGUAAUGUAGUGAAU
Erap1	ACUGAAUAGUGAGGCAUAA	ACACAGUUAUCAUCGACUA
	GAUCAAAUUUAACGUGGGA	CAAGAUAAAUCAAGCCGAU
Spp1	CAGUCGGAUGUGAUCGAUA	CGGAUGAAUCUGACGAAUC
	CCACAUGGACGACGAUGAU	GAUCAGGACAACAACGGAA
Prdx1	GCGCUUCUGUGGAUUCUCA	GGGCAGACCAAUCUUCUAU
	GUAUAUGUGAGGCUAGUAA	AGAUCUACCUGCCUAUUUA
Rnh1	CCUCCAAAGCUUCGCUACA	GAGCUUUGGUUGGGAGACU
	CCAUGAACCUGGUGUCCGU	CAAUAAGCACUGUGGUCUU
B2m	AUACUGAACUGCUACGUAA	GCAAAGAGGCCUAAUUGAA
	CCGGAGAAUGGGAAGCCGA	CUAGAUAGCUGAGCAAUAA
Fh1	CUCCGAACGUCGCGCGAAU	AGGCCAACACAGAGCGGAU
	GGAGUAUGGUCUCGAUCCA	CAGGAUCGGUUUCGCAGAA

Table 4 **(…continued)**

Gene	5' --> 3'	5' --> 3'
Ctsb	CGGAUGACCUGAUUAACUA	UGAAGCCGGUGAUAUGAUG
	GAUAAGCACUUUGGGUACA	GACAUAAGCUAUCUGAAGA
Ptrf	GCGUCAACGUGAAGACCGU	GACAAGAGCGACAGCGACU
	AGAAGAUCCGCGAGGGCGA	CGAGCAACACCGUGAGCAA
Hp	GGUGUGUACGUGAGGGCGA	ACACCUUAAACGACGAGAA
	CGUGGUGGAUAUCGGGCUA	AGAGAUUGCAAACGGCUAU
Ace	GCACGGAGGUAUCCAAUCA	AAACACCGCUCGCGCAGAA
	UGAUAGCGCACCACGAAAU	AAGUGUUGUUGAACGAGUA
Mmp3	CUGCAUAUGAGGUUACUAA	AGUCUUGGCUCAUGCCUAU
	CGAUGAUGAACGAUGGACA	CAUCCUACCCAUUGCAUGA
Sparcl1	GAUCCUAACCAACGCGCAA	UCCCAAACAUGGCGGCUAU
	AAGUGUAGAUCCAACGGAA	GUGGCAAUCCCGACAAGUA
Car2	CUACAGAUUGAUCCAGUUU	CUCCUUUAACGUUGAGUUU
	CCGACUCGCAUCUGGUAUU	CAAAACAGGUAAACAGUCA
Angptl2	GGACUGGUCUGGCCGUAAA	ACGGAGGCAUCGUGAGCGA
	GGUCAUUGCUCAGCUCGAA	GGAUGGUGGUAUAACGCCU
Prdx2	GCAACGCGCAAAUCGGAAA	AGAAUUACGGCGUGUUGAA
	AAAUCAAGCUUUCGGACUA	GCGACCAUGCUGAGGACUU
Mmp19	GAAACAAGGUGUGGCGGUA	GGAGGGAAACUGUCAAUCA
	AAAGAGUAUUGGCGCCUUA	AAACCUAGAUGCUGCCGUU
C3	GGACAGCCUUCGUGAUUUU	CCUCUGGAGUAGAUAGAUA
	GUGAACAGCAGGAACUUAA	GCAGUGGGAUCCCGAUUGU
Tgfbi	GAGUCUUUGUUUAUCGAAA	CAACCGACCACAAGAACGA
	CAAACAGGCGUCAGCGUAU	GCUCAAUGCUCUCCGCUAC
Hbb-b1	GGGGAAAGGUGAACGCCGA	AAGUGAAGGCCCAUGGCAA
	GGGCAAUAUGAUCGUGAUU	CUUUAACGAUGGCCUGAAU
Mrc1	CAACUGGAUUUGUCAGAUA	GAAGUAGCCUAUCUUAUGA
	GAAAUGGGAGUGUAAGAAU	GGCUUUGGUUGAACGACAA
Serpinc1	CCGAGAAGACAUCCGACCA	CGUGAUUACUGGCCGGUCA
	CGACAUCUGCAUAGCGAAG	GGCUAAUCCUUGUGUGAAC
Tgfbr3	UCAAUUACCUUGCGGAGUA	GAAUGGUACCCACUUUGUA
	GAUGAGAGAUGAGGAAGUC	CCAUGACAGUGACCAAAUU
Ces1c	CAGGACCAGCGGAGCGAAA	GGUCAUAAAUACAAACGUG
	CUCUCAAGAUUUCGGAAGA	CAAGAUGCAGGUUGGGCAA
Cp	GAAAUAAAUUGGCGAUAAG	ACAAAGUGCUUCCCGGACA
	UUACAUUGCUGCCGAGGAA	GAGAAUCCAUCGUGUGGUA
Lcp1	GGGUACCGAGUGAGAGAAA	ACUCAACAAUGCAAAGUAU
	CUGCAUUAGUGAAAGGCUU	CGUGAAGGAAGGAUAUUAU
Fstl1	CUAUAGAACAAGACGGCAA	GGAUGGACGCUCAGGCUAU
	UCUUUGAGCCUCCGAAUAA	AAUGGUAGUUUGUGGUUUA

Table 4 **(…continued)**

Gene	5' --> 3'	5' --> 3'
Lgals3bp	GUGGUCUGCUCCAACGAUA	CAGGAAAGGGACCGAUCAU
	CCUUGGACCUUUAUGCGUA	GUGCAUGCCUGUCGUCAGA
Lum	GUGGCCAAUACUACGAUUA	AUGAGUACUUCAAGCGCUU
	GUAAGCAUUUGCCCGGUUA	GCAAAUGAAAUCACCGUUA
Mcpt4	GAAAGAAAAGAUCGGCAUA	AAACAAAUCGUUCACCCAA
	CUAUUGGCAUUAUGACUAU	CGAACUGGAGUGACAGAAC
C1qtnf1	GGAGCUCAAUGUACGUAUA	UCUUCAAGGGCGAGCGUGA
	CCCAAAGGAUGGUGCGAUC	GAAAUAAAGCUCCUACUAU
Trf	GCGCAGUGUCAGAGCACGA	AUGUUGUGGUCUCACGAAA
	ACAUGCAAUCUGUCGGUAA	CACCAAAUGUUUCGUUAAA
Nid2	GAUCAAGUCUUCACGUAUA	CGGAAGGACUUGCCAUCGA
	AGUCGAGGUUUUACGGAAA	UGUGAGCGUUGGCGGGAAA
Cd14	UAUCAAGUCUCUGUCCUUA	GACCCGAUCUCAACAUCUU
	GUCCAGCGCUUUCAAUUGU	GAUCGCCUCUUUGUUUAAG
Gc	CUAGAGAGAGGCCGAGACU	UCUAAGUGCUGCUCUAUAA
	UCAUAAAACUAGCCCAAAA	UAUGAGUAUUCCAGCAAUU
Ecm1	GCUUCAGACCAGCGAGAGA	CGAACACUCAUUACAAUAA
	GAAGAUAAGCAAAUCAACU	CCAUGAAGUAGGUUAUGCA
Ctsz	GUACUGGAUUGUCCGAAAU	GGGAGAAGAUGAUGGCCGA
	CCCGAGAGGAGACGGUAAA	GGAGAAAUGUGAACGGUGU
Emilin1	AGAAUAAGCCUGUGGCCGA	GAACAGGAUUCUCGGGUCA
	ACUACAAGGCCUACGUGAA	AGUGCUAAGUGGACGCAGA
Pdia4	CUAAUGAUGCUAAGCGGUA	CGACAUCACCAACGACCAA
	CGCCAUUGCUGACGAGGAA	CCGGAGAUGCACACGAAGA
Fn1	AGAACAAACACUAACGUAA	GGAGAGAGAUGCACCGAUU
	GGUCAUUUCAGAUGCGAUU	GGUUCAGACUCGAGGCGGA
Csf1	CCAUAUUGCGACACCGAAU	GAACAAGGCCUGUGUCCGA
	GAUGAGACCAUGCGCUUUA	GCAACUGCCUGUACCCUAA
Fbln2	CCAAUAGCCUGCCGGGAGA	GAGGAGGGCUACUUCGUCA
	GCUAUAUCCUCAACGCACA	GCGAAGGCUACCAGUACUA
Aebp1	UGGAAACGCUGGAUCGGUU	GCAAUGUGGACUACGAUAU
	GGCUCAAGAUCUACGCAAU	CACCAAUGGCUACGAGGAA
Col18a1	GGUCACAAGUGGCCAAUCA	GAGCUGAAGGUACGCAAAA
	GGGUCGACCUGGAACGAAU	GGUAGAGCUUCCUGGCGAA
Pfn1	GCAAAGACCGGUCAAGUUU	UGGAACGCCUACAUCGACA
	GGGAAUUUACAAUGGAUCU	CUUCGUUAGCAUUACGCCA
Non-Targeting Control siRNA		UAAGGCUAUGAAGAGAUAC

Table 5. Primers used for relative quantification real-time PCR (all primers are suitable for mouse cDNA, F = forward, R = reverse)

Gene	Primer	sequences
36B4	F	GCCGTGATGCCCAGGGAAGACA
36B4	R	AACCCGCGGCCTTCTACGAG
Cpq	F	CTGTGGCATCCCTCATCCAA
Cpq	R	CCACGAGAAGCCATTCGAGA
Slc27a1	F	GCCAGGGATCTCTCTCTCCA
Slc27a1	R	CACAGAGGCTGTTCCTGCTC
Got2	F	GTCTGCCTCTGCCAATCGTA
Got2	R	GGGTTGGAATACAGGGGACG
Vim	F	ATGTGCGCCAGCAGTATGAA
Vim	R	TCCGGTACTCGTTTGACTCC
Il1rl1	F	TGAGGTTGCTCTGTTCTGGAG
Il1rl1	R	TTTCAAGAACGTCGGGCAGA
Sparc	F	GTTGGCCCGAGACTTTGAGA
Sparc	R	AACGTGTGGTGCAATGTTCC
Ces1d	F	TGGCTTTCTCTTGCTGCGT
Ces1d	R	TCTCAAGGAGCCAAGAGGGG
Tf	F	GTGTGACGAGTGGAGCATCA
Tf	R	AGGCACTAGACCACACTGG

Acknowledgements

I would like to express my sincere gratitude to my supervisor Prof. Dr. Christian Wolfrum for allowing me to work on a highly interesting and promising topic. I am very grateful to him for his limitless and excellent guidance, trust and scientific freedom he provided. His encouragement and the moral support especially during the most difficult times when I was stacked with my experiments, has motivated and inspired me a lot to stay on the right track. His vast knowledge in science and dedication to the scientific work and his valuable comments on my thesis has been of great importance to me in completing my thesis. In general, I could not have imagined having a better supervisor for my PhD study. Without his support and understanding, my PhD journey would not have been easy and possible for me.

I am grateful to Prof. Dr. Wolfgang Langhans, for the opportunity, he has given me to be part of one of the highly collaborative project on GLP-1 and for his support and scientific input.

I would also like to thank my PhD thesis committee members, Prof. Dr. Wolfgang Langhans, Prof. Dr. Michael Detmar and Prof. Dr. Med. Gottfried Rudofsky for their support, guidance and helpful suggestions.

I would like to thank former members of the Wolfrum group, Bettina Meissburger who has always been very kind and taught me how to dissect animal models. I am deeply grateful to Hansjörg Möst for being smart and humbly, and for being so supportive from the first day of my arrival to Wolfrum lab. Whatever and whenever I had a question, he was willing to explain and help, never said wait or no.

I would also like to thank all the members of Wolfrum group: especially Eva Röder, Leon Gabriel Straub, Dr. Daria Peleg-Raibstein, Dr. Salvatore Modica, Elke Kiehlmann, Matthias Geiger, Elisabeth Weber, Marcel Morf, Mandy Sütö, Simone Läubli, Grether Daniela Nicole, McGrath Rory, Michele Nahvi-Djoo and Susanna for their great support.

I am deeply grateful to Eva, she has been so kind to me and I enjoyed a lot working with her in the lab. I am also very thankful for her friendship and great support all the time. Many of the experiments could not have been done without Leon and Daria supporting me and I owe them a lot. I would like to express my deep gratitude to Leon for creating a nice working environment and positive attitude toward my projects. I am grateful for his positive energy and great motivation. I enjoyed his challenging questions and great discussions.

Daria's advice especially during the hard time has been very helpful and encouraging and I am deeply grateful for all the support she has given me. Her scientific and practical support on the GIP project has been a core point of this project.

I would also like to thank Salvatore for being available in the lab every time and answering all my questions. I am grateful to Elke for being rational and looking at the situation from all the angles, I could not have done most of my experiments without her support. My further thanks go to Liz for her assistance with the staining.

The members of the Prof. Dr. Wolfgang Langhans group have contributed enormously to my projects through collaboration. I am especially grateful to Myrtha Arnold, her enthusiasm and dedication to science is inspirational. I am also grateful to Eugenia McAllister for the collaboration and great contribution to my project.

I am grateful to all my friends, Lemlem Ghrmay, Meselu Demisse, Sofia Abdi, Gebriel Fayissa, Abate Yimam, Yurdanos Alem and Atoma Gudissa for their unconditional love, support and encouragement.

I would also like to thank Dr. Byron Bitanihirwe, Dr. M.P. Jab and Bayissa Hatew for proof reading my thesis.

Finally, I owe very special thanks to my family and parents for their love and support.

Curriculum vitae

Personal information

Name	**Tenagne Delessa Challa**
Address	Guggachstrasse 25, 8057 Zürich, Switzerland
Phone:	+41 788 200 566
E-Mail:	tenagne-challa@ethz.ch / tenagnetd@gmail.com
Nationality	Ethiopian
Place of birth	Gindeberet, Ethiopia
Date of birth	20 May 1981

Education

12/2009 to present	**PhD student** in Molecular Life Sciences, Health Sciences and Technology. Swiss Federal Institute of Technology (ETH Zurich), Switzerland
10/2007 to 11/2009	**M.Sc.** in Nutritional Sciences (graduated with honor). The Hebrew University of Jerusalem, Israel
9/2000 to 7/2005	**B.Sc**. in Applied Biology (minor in Applied Chemistry). Addis Ababa University, Ethiopia

Professional experience

12/2009 to present	**PhD thesis** at Institute of Food, Nutrition and Health (IFNH), Laboratory of Translational Nutritional Biology. ETH Zurich, Switzerland Supervisor: Prof. Dr. Christian Wolfrum *"Regulation of adipogenesis and energy metabolism through the cross-talk between adipose tissue, gastrointestinal wall and the brain: Evidence from adipokines and incretin hormones*"
10/2008 to 11/2009	**M.Sc. thesis** at Institute of Biochemistry, Food Science and Nutrition. The Hebrew University of Jerusalem, Israel Supervisor: Prof. Dr. Efrat Monsonego Ornan *"The use of in vitro model to study the effect of adipocytokines on bone development"*

4/2007 to 9/2007 **Research assistance** at department of food microbiology, Agricultural Research Organization, Volcani Center, Israel

Scholarships and awards

10/2007 to 11/2009 **Recipient of Pears Foundation** Scholarship, London, UK

List of publications

Challa T.D., Beaton N., Arnold M., Rudofsky G., Langhans W., and Wolfrum C. 2012. Regulation of adipocyte formation by GLP-1/GLP-1R signalling. The Journal of Biological Chemistry. 287: 6421-6430.

Challa T.D., Rais Y., and Monsonego Ornan E. 2010. Effect of adiponectin on ATDC5 proliferation, differentiation and signalling pathways. Molecular and Cellular Endocrinology. 323: 282-291.

Winkler J.K., Woehning A., Schultz J., **Challa T.D.**, Minkova S., Roeder E., Nawroth P.P., Friederich, H., Wolfrum, C. and Rudofsky, G. 2012. The A1-allele of theTaq1A polymorphism in the Dopamine D2 Receptor gene complicates weight loss and maintenance in younger obese patients. Nutrition. 28 (10): 996-1001.

Bayissa Hatew, **Tenagne Delessa**, Vered Zakin, and Natan Gollop. 2011. Antagonistic intestinal microflora produces antimicrobial substance inhibitory to Pseudomonas species and other spoilage organisms. Journal of Food Science. 76: M522-M530.

Challa T.D., Straub L.G., Peleg-Raibstein D., Arnold M., McAllister E., Langhans W., Wolfrum C. CNS-specific GIP receptor ablation protects from diet induced obesity and insulin resistance (in preparation).

Challa T.D., Straub L.G., Wolfrum **C.** The regulation of adipogenesis through novel adipokines secreted by adipocytes and adipose tissue explants (in preparation).